AN INVESTIGATION INTO THE EFFECT OF INLINE COAGULATION AND AIR SCOURING TO MINIMIZE ULTRAFILTRATION MEMBRANE FOULING

by

Simon Muzi Sibiya

A thesis presented in partial fulfilment

of the requirements for the Degree

of

MASTER OF ENGINEERING

(CHEMICAL ENGINEERING)

in the Faculty of Engineering

at StellenboschUniversity

Supervisor

Professor V L Pillay

December 2020

DECLARATION

By submitting this thesis electronically, I declare that the entirety of the work contained therein is my own original work, that I am the sole author thereof (save to the extent explicitly otherwise stated), that reproduction and publication thereof by Stellenbosch University will not infringe any third party rights and that I have not previously in its entirety or part submitted it for obtaining any qualification.

Date: [14 September 2020]

PLAGIARISM DECLARATION

1. Plagiarism is the use of ideas, material and other intellectual property of another's work and to present it as my own.
2. I agree that plagiarism is a punishable offence because it constitutes theft.
3. I also understand that direct translations are plagiarism.
4. Accordingly, all quotations and contributions from any source whatsoever (including the internet) have been cited fully. I understand that the reproduction of text without quotation marks (even when the source is cited) is plagiarism.
5. I declare that the work contained in this assignment, except where otherwise stated, is my original work and that I have not previously (in its entirety or part) submitted it for grading in this module/assignment or another module/assignment.

Initials and surname: S.M. Sibiya

Date: 14September 2020

ABSTRACT

The quality of raw water is an essential factor that determines the treatment technologies and level of treatment required to attain specified treatment objectives. Water utilities such as Rand Water currently use conventional water treatment processes to purify water to drinking water standards. However raw water quality had been gradually deteriorating due to agricultural and industrial activities and poorly performing wastewater treatment plants.

Low-pressure membrane filtration processes such as microfiltration (MF) and ultrafiltration (UF) have become an attractive alternative treatment technology to replace or supplement conventional water treatment for surface waters, as they consistently produce drinking water of high quality. However, the major disadvantage of membrane filtration is membrane fouling.

The objective of this study was to determine the effect of coagulant dosage, air scouring rate and the frequency of air scouring on the rate of membrane fouling and final water quality, for Vaal Dam raw water.

The investigation into the effect of the polymeric coagulant dosage, air scouring rate and the frequency of air scouring on the rate of membrane fouling was conducted using a bench-scale outside-in hollow fibre PVDF submerged UF module. Firstly, ranges for polymeric coagulant dosage, air scouring rate, and the frequency of air scouring were selected and independently validated using an OFAT approach. These validated ranges were then used in a full factorial design of experiments (DoE). The purpose of conducting the DoE was to determine the combined effects of the factors and factors interactions on the rate of membrane fouling.

In the scanning and validation investigation, the rate of membrane fouling reduced by 60% when the polymeric coagulant dosage was in the range of 1 to 8 mg/l, relative to no polymeric coagulant dosage. Excessive polymeric coagulant dosage increased the rate of membrane fouling. The rate of membrane fouling decreased with increasing air scouring rates range of 1 to 5 $m^3/m^2.h$. Air scouring rates above 5 $m^3/m^2.h$ increased the rate of membrane fouling. The rate of membrane fouling reduced with increasing air scouring frequency from 0% to 100%. The air scouring frequency of 0% and 25% resulted in a similar rate of membrane fouling. Similarly, the air scouring frequency of 75% and 100% resulted in a similar rate of membrane fouling.

The results from the DoE were analysed with statistical software and a regression model was obtained. This showed that 0 mg/l polymeric coagulant dosage and 10 min off / 10 min on air scouring frequency, irrespective of the air scouring rates resulted in the highest rate of membrane fouling. The treatment combination of 1 mg/l polymeric coagulant dosage,

continuous air scouring resulted in the lowest rate of membrane fouling, irrespective of the air scouring rates.

A Pareto plot indicated that the polymeric coagulant dosage, followed by the air scouring rate were the most critical factors in reducing the rate of membrane fouling. The frequency of air scouring had a moderate effect on the rate of membrane fouling, while the interaction of the air scouring rate and frequency of air scouring had a marginal effect.

OPSOMMING

Die kwaliteit van rouwater is ’n essensiële faktor wat die behandelingstegnologieë en vlak van behandeling benodig bepaal om gespesifiseerde behandelingsdoelwitte te bereik. Waterutiliteite soos Rand Water gebruik tans konvensionele waterbehandelingsprosesse om water na drinkbare waterstandaarde te suiwer. Rouwaterkwaliteit het egter geleidelik agteruitgegaan as gevolg van landbou- en industriële aktiwiteite en afvalwaterbehandelingsaanlegte wat swak presteer.

Laedruk membraanfiltrasieprosesse soos mikrofiltrasie (MF) en ultrafiltrasie (UF) het ’n aantreklike alternatiewe behandelingstegnologie geword om konvensionele waterbehandeling vir oppervlakwater te vervang of aan te vul, omdat dit drinkwater van hoë kwaliteit konstant produseer. Die groot nadeel van membraanfiltrasie is egter membraanaanpakking.

Die doel van hierdie studie was om die effek van koagulantdosering, lugskuurtempo en die frekwensie van lugskuring op die membraanaanpakking en finale waterkwaliteit vir die Vaaldam rouwater te bepaal.

Die ondersoek om die effek van die polimeriese koagulantdosering, lugskuurtempo en die frekwensie van lugskuring op die tempo van membraanaanpakking is uitgevoer op ’n banktoetsskaal buitekant-binne hol vesel PVDF onderdompelde UF-module. Eerstens, die bestek vir polimeriese koagulantdosering, lugskuurtempo, en die frekwensie van lugskuring is gekies en onafhanklik gevalideer deur ’n OFAT-benadering te gebruik. Hierdie bestekke wat gevalideer is, is toe gebruik in ’n vol faktoriaalontwerp van eksperimente (DoE). Die doel van die uitvoering van die DoE was om die gekombineerde effekte van die faktore en faktorinteraksies op die tempo van membraanaanpakking te bepaal.

In die skandering en validasie ondersoek, het die tempo van membraanaanpakking afgeneem met 60% wanneer die polimeriese koagulantdosering in die bestek van 1 tot 8 mg/l was, relatief tot geen polimeriese koagulantdosering. Oormatige polimeriese koagulantdosering het die tempo van membraanaanpakking laat toeneem. Die tempo van membraanaanpakking het afgeneem met toenemende lugskuurtempo’s in die bestek van 1 tot 5 $m^3/m^2.h$. Lugskuurtempo’s bo 5 $m^3/m^2.h$ het die tempo van membraanaanpakking laat toeneem. Die tempo van membraanaanpakking het afgeneem met lugskuurfrekwensie wat toeneem van 0% tot 100%. Die lugskuurfrekwensie van 0% en 25% het ’n eenderse tempo van membraanaanpakking tot gevolg gehad. Op dieselfde manier het die lugskuurfrekwensie van 75% en 100% ’n eenderse tempo van membraanaanpakking tot gevolg gehad.

Die resultate van die DoE was geanaliseer met statistiese sagteware en ’n regressiemodel is verkry. Dit het getoon dat 0 mg/l polimeriese koagulantdosering en 10 min af/10 min aan

lugskuurfrekwensie, ongeag die lugskuurtempo's, die hoogste tempo van membraanaanpakking tot gevolg gehad het. Die behandelingkombinasie van 1 mg/l polimeriese koagulantdosering, ononderbroke lugskuring, het die laagste tempo van membraanaanpakking tot gevolg gehad, ongeag die lugskuurtempo's.

'n Pareto-plot het aangedui dat die polimeriese koagulantdosering, gevolg deur die lugskuurtempo die mees kritiese faktore was in die verlaging van die tempo van membraanaanpakking. Die frekwensie van lugskuring het 'n gematigde effek op die tempo van membraanaanpakking gehad, terwyl die interaksie tussen die lugskuurtempo en frekwensie van lugskuring 'n marginale effek gehad het.

ACKOWLEDGEMENTS

I would like to express my deepest gratitude to the following remarkable individuals and institutions:

i. Professor Visvanathan Lingamurthi Pillay, my supervisor for always making time and offering sound advice at all times.

ii. Dr Herman Franken for assisting with the design of the laboratory scale submerged ultrafiltration membrane plant.

iii. Mr Calvin Mokgaditse for assisting with the experiments.

iv. Ms Zandile Nonyana for assisting with the statistical analysis.

v. My employer (Rand Water)for providing financial support.

vi. Stellenbosch University, Process Engineering department for accepting my application.

vii. My wife Lerato Sibiya and five beautiful kids for not giving up on me in times where I could not spend time with them.

CONTENTS

TABLE OF FIGURES

TABLE OF TABLES

LIST OF ABBREVIATIONS

Abbreviation	Definition
AS-MBR	activated sludge membrane bioreactor
AWWA	American Water Works Association
AWWARF	American Water Works Research Foundation
ANOVA	analysis of variance
A	area
AOC	assimilable organic carbon
ATR	attenuated total reflection
BSA	bovine serum albumin
BET	brunauer, emmett and teller
CT	capillary tubes
CA	cellulose acetate
cm	centimetre
cP	centipoise
CIP	chemical cleaning in-place
CFU/100ml	Coliform Unit / hundred millilitre
CP	concentration polarization
CI	confidence interval
r^2	Correlation coefficient
m^3/h	cubic meters per hour
$m^3/m^2.h$	cubic metres per meter squared per hour
D	dalton
^{0}	Degrees
^0C	Degrees Celsius
DWS	Department of Water and Sanitation

DoE	design of experiment
Φ	Diameter
DBPs.	disinfection by-products
DAF	dissolved air flotation
DOM	Dissolved Organic Matter
EC	electrical conductivity
EDL	electrical double layer
ED	electrodialysis
EDR	electrodialysis reversal
EDS	energy Dispersive x-ray spectroscopy
EPA	Environmental Protection Agency
E.coli	Escherichia coli
EPS	extracellular polysaccharides
FS	flat sheet
Q	flow rate
FTIR	fourier-transform infrared spectroscopy
g/l	gram per litre
GAC	granular activated aarbon
HAA	haloecetonitriles
N_H	Head Number
H	height
HFCA	high flux cellulose acetate
HF	hollow fibre
HMI	human machine interface
N	impeller rotation speed
I/O	inside-out
R_m	intrinsic membrane resistance

IX	ion exchange
R_{ir}	irreversible membrane resistance
J/s	joules per second
KD	kilodalton
kg	kilograms
kg/m^3	kilograms per metre cubed
$kg.m^{-1}.s^{-2}$	kilograms per metre per seconds squared
kPa	kiloPascals
LMS	least mean square
l	litre
l/h	litres per hour
LHM	litres per hour-meter squared
$l/m^2.h$	litres per metre squared per hour
MIEX	magnetic ion exchange resin
m/v	mass per volume
MBR	membrane bioreactor
J	Membrane flux
K_w	Membrane permeability
m	metre
$m^3/m^2.h$	metre cubed per metre squared per hour
m^2	metre squared
10^{-6}	micro
MF	microfiltration membrane
µg	microgram
µg/l	microgram per litre
mPa	miliPoise
mg/m	milligram per gram

mg/l	milligrams per litre
ml	millilitre
ml/min	millilitre per minute
mm	millimetre
mS/m	millisiemens per metre
min	minute
MW	molecular weight
MWCO	molecular weight cut-off
MPN/ml	Most Probable Number per millilitre
MT	multi-tubular
10^{-9}	nano
NF	nanofiltration
nm	nanometers
NOM	natural organic matter
NTU	Nephelometric Turbidity Unit
OFAT	one factor at a time
O/I	outside-In
Pa	Pascal
cm^{-1}	per centimetre
$m^{-1}min^{-1}$	per metre per minute
s^{-1}	per second
%	Percentage
PAM	polyacrylamide
PAN	polyacrylonitrile
PACl	polyaluminium chloride
PES	polyethersulfone
PE	polyethylene

PP	polypropylene
PS	polysulfone
PVC	polyvinyl chloride
PVDF	polyvinylidene difluoride
PAC	powdered activated carbon
N_p	Power Number
P	pressure
P&ID	process and instrumentation diagram
PFD	process flow diagram
N_Q	Pumping Number
RLV	rate of log removal
R_{rmri}	Rate of Membrane Resistance Increase
C	regenerated cellulose
RSD	Relative Standard Deviation
RO	Reverse Osmosis
Rr	reversible membrane resistance
RPM	Revolutions Per Minute
R_e	Reynolds number
SEM	scanning electron microscopy
s	seconds
SANS	South African National Standard
SW	Spiral Wound
SOC	synthetic organic carbon
T	temperature
TDS	total dissolved solids
R_{tf}	total fouling membrane resistance
R_T	total membrane resistance

TMP	transmembrane pressure
ΔP	Transmembrane Pressure
THM	trihalomethanes
UF	ultrafiltration membrane
UV_{254}	Ultraviolet at 254 nm wavelength
Vg	Vereeniging
μ	Viscosity
V	volume
ρ	Water density
WRC	Water Research Commission
WTP	water treatment plant
W	watts
WHO	World Health Organization
Zb	Zuikerbosch

NOMENCLATURE

Nomenclature	Definition
$Al_2(SO_4)_3$	Aluminium sulphate
NH_4-N	Ammonia-Nitrogen
NH_4Cl	Ammonium chloride
$CaCO_3$	calcium carbonate
C	Carbon
Cl	Chloride
Cl_2	Chlorine
ClO_2	Chlorine Dioxide
$C_6H_8O_7$	Citric Acid
Co	cobalt
F	fluoride
HCl	hydrochloric acid
H_2O_2	hydrogen peroxide
HNO_3	nitric acid
O_3	Ozone
$C_2H_4O_3$	peroxyacetic acid
Pt	Platinum
Pt-Co	Platinum-Cobalt
NaOH	Sodium hydroxide
NaClO	Sodium hypochlorite
NaOCl	Sodium hypochlorite

CHAPTER 1 INTRODUCTION

1.1 Background to the project

Raw water quality is an essential factor that influences the treatment technologies and level of treatment required to attain specified treatment objectives. Rand Water abstracts raw water from the Vaal Dam and purifies it to drinking water standards. The Vaal Dam raw water quality is characterised by a relatively low salt content with a highly variable turbidity.Rand Water currently uses a conventional water treatment processes for the purification of Vaal Dam raw water, viz.coagulation, flocculation, sedimentation, sand filtration,and disinfection. In the recent past, the raw water quality from the Vaal Dam has gradually deteriorated due to an increase in agricultural and industrial activities, and poorly performing wastewater treatment plants,while drinking water quality standards have become more stringent. Accordingly, Rand Water is investigating alternative water treatment technologies that are resilient to changes in raw water quality, and will consistently produce an acceptable drinking water quality that meets the South African National Standard drinking water quality standard, referred to as SANS 241.

Globally, low-pressure membrane technologies are increasingly being favoured as alternative technologies to replace or supplement conventional water treatment processes. To investigate this option, Rand Water purchased a direct submerged hollow fibre ultrafiltration membrane (UF) pilot plant from a commercial vendor, to evaluate UF for the treatment of Vaal Damraw water to potable water quality standards.The pilot plant utilises coagulant addition as a pre-treatment to membrane filtration. Air scouring during permeation to reduce membrane fouling is a standard operating feature of the pilot plant.

The purpose of the submerged UFpilot plant was to evaluate the operability and economics of low-pressure membrane technologies to produce an acceptable drinking water quality from Vaal Dam raw water. This requires a determination of the sensitivity of the treatment process to variations in the operating parameters. However, the pilot plant was delivered fully automated with no flexibility to change operating parameters such as air scouring rate, air scouring frequency, filtration run time and membrane flux. According to Guo et al., 2018; Xing et al., 2018; Lok et al., 2017; Yu et al., 2013; Tian et al., 2010; Walsh et al., 2009 and Konieczny et al., 2006, the performance of UF is highly dependent on the air scouring regime and whether or not a pre-treatment step such as coagulation is employed.

Hence, this investigation was set up, to enable an experimental investigation of how coagulation and the air scouring regime affects membrane performance for the specific water considered.

1.2 Low-pressure membranes for potable water production

The replacement of conventional water treatment processes with low-pressure membrane systems has rapidly emerged as an alternative option in the potable water treatment industry internationally. Microfiltration (MF) and ultrafiltration (UF) have replaced or supplemented conventional solids-liquid separation processes such as sedimentation and rapid gravity sand filtration in water treatment (Ratnayaka, et al., 2006). Membrane filtration systems have been successfully employed in countries like Singapore to replace sedimentation and filtration processes(Arnal et al., 2009; Van Doesburg et al., 2009; Ratnayaka et al., 2009; Xia et al., 2004).

In membrane processes, there is no need to create large flocculated particles to achieve settling in sedimentation tanks, or for capture by granular media filters, as membranes are capable of removing pin floc due to the membrane surface pore sizes in the range of 0.1 to 0.001 micron (Guo et al., 2012; Nemeth et al., 2003).

UF membrane systems have become an attractive alternative treatment technology to replace or supplement conventional water treatment for surface waters as they consistently produce drinking water of high quality (Yu et al., 2016; Yu et al., 2013; Nakatsuka et al., 2010). UF results in a high level of removal of pathogens such as viruses, bacteria and protozoa cysts and oocysts (*Giardia* and *Cryptosporidium*) compared to the conventional water treatment process train (Guo et al., 2012). This trend has been attributed to the improved effectiveness of membrane systems as compared to conventional treatment technologies such as sedimentation and filtration and to progressively more stringent drinking water quality regulations (Ratnayaka et al., 2009).

Summarising the significant benefits of low-pressure membrane technologiessuch as UF for potable water treatment (Carollo 1997):

i. Membrane filtration produces a consistent,high-quality product water – membrane fibres have billions of microscopic pores on the surface. These pores form a barrier to particulate and colloidal impurities such as bacteria and viruses, while allowing pure water molecules to pass through the membrane system.

ii. The required facility footprint for installation is small compared to conventional granular media filtration processes – UF Membranes have a low filtration rate compared togranular media filtration systems. However, due to high membrane packing density, the footprint required by the membrane process to produce the same flowrate as filter media filtration is significantly less.

iii. Membrane plants require less personnel to manage the process – Due to the simplicity of the membrane process, less personnel are required to manage the process, compared to a multiple-unit conventional water treatment processof the same capacity.

iv. Membrane plants require less infrastructure for automation - The simplicity and compactness of the membrane process requires less infrastructure for automation compared to a conventional water treatment process of the same capacity.

The major disadvantage of membrane filtration is membrane fouling. Membrane fouling is the gradual accumulation of impurities on the membrane surface or within the pores of the membrane structure. This inhibits the passage of water, thus decreasing the productivity (Szymanska et al., 2014). The membrane flux is the flowrate of water produced per unit area of the membrane surface. The transmembrane pressure,TMP, is the net pressure drop across the membrane. Membrane fouling increases the resistance to product flow, and leads to a reduction in the membrane flux, an increase in the TMP, or both.

All membranes experience fouling. However, there are various methods employed to manage membrane fouling and these include pre-treatment of the raw water, chemical modification of the membrane material to improve the anti-fouling properties, optimisation of the operating conditions, and periodic membrane cleaning (Shei et al., 2014).The application of coagulants, in combination with air scouring, is one of the commonly reported membrane fouling management strategies for both UF and MF membrane processes.

Studies conducted by Walsh et al., 2009; Konieczny et al., 2007 and Konieczny et al., 2006, on the effect of pre-treatment by coagulation and flocculation on membrane performance and water quality demonstrated that coagulation was one of the factors that can be employed to manage membrane fouling and improve final water quality. The coagulant demand for the submerged membrane process was relatively low compared to conventional water treatment processes (Walsh et al., 2009). According to Akhondi et al., 2014; Li et al., 2014 and Yu et al., 2014, the application of air scouring during filtration greatly assists in managing membrane fouling,and has been demonstrated to be amongst the effective membrane fouling control strategies for UF. In another study conducted by Lok et al., 2017 on the effect of periodic and continuous air scouring on membrane fouling, it was demonstrated that continuous air scouring was more effective in managing membrane fouling compared to periodic air scouring.

However, the criteria used in the selection of the membrane fouling management strategy, such as the selection of the coagulant dose, the air scouring rate, and the frequency of air scouring,are not well documented. Also, there is very little information available on the effects of coagulant dosage with air scouring on UF membranes operated on South African raw waters.

Hence, there was a need for an experimental investigation into the effects of coagulant dosage as a pre-treatment, air scouring rate, and frequency of air scouring on membrane fouling and final water quality for the Vaal Dam raw water.

1.3 Objectives

The overall objective of this study was to determine the effect of coagulant dosage, air scouring rate, and the frequency of air scouring on membrane fouling and final water quality,in the ultrafiltration of Vaal Dam raw water. The specific objectives of the study were as follows:

i. To determine the optimal coagulant dosing range to manage membrane fouling effectively.

ii. To determine the optimal air scouring rate regime to manage membrane fouling effectively.

iii. To quantify the combined effect of coagulant dosage and air scouring on membrane fouling and final water quality.

1.4 Approach and Thesis Organisation

A literature review was conducted on the application of low-pressure membrane technologies for drinking water production. It also focused on the critical factors that affect membrane performance in terms of fouling and final water quality. Different membrane fouling management strategies were reviewed. This is reported in Chapter 2.

An experimental plan was then devised to address the objectives. It was decided that a One Factor at a Time (OFAT) approach would be used to select suitable ranges for coagulant dose, air scour flowrate, air scour frequency and sparger geometry. Thereafter a Design of Experiments (DoE) approach would be used to investigate the combined effects of coagulation and air scouring on fouling reduction. This is reported in Chapter 3.

A bench-scale submerged UF membrane system with air scouring and coagulant addition as a pre-treatment method was then designed and constructed. The bench-scale rig had a scaled down membrane module based on the same membranes used in the pilot plant. The rig enabled the coagulant dose, air scouring flowrate and frequency, filtration time and filtration flux to all be varied independently. This equipment and the methodology for the investigation is reported in Chapter 4.

The results of the investigation are presented and discussed in Chapter 5. Firstly a suitable geometry for the air sparger, and suitable ranges for coagulant dose, air scouring frequency and air scouring rate were decided via OFAT investigations. Thereafter a 3 factor 2 level full factorial investigation was conducted on the combined effects of these parameters.

The conclusions of this investigation are presented in Chapter 6.

CHAPTER 2 LITERATURE REVIEW

2.1 Water Characteristics and Quality Parameters

2.1.1 General water characteristics

The interactions of water with the environment alters the physical, chemical and the biological characteristics,resulting in water that may be harmful to human health and aquatic life (AWWA M57 2010; Schutte 2006).Contaminants in water include suspended (coarse) particles, colloidal material, and dissolved substances(Morrison 2006).The overall water quality characteristics can be classified in terms of physical, chemical and microbiological parameters.

Physical water quality parameters characterise the inherent properties such as temperature, viscosity,colour, taste and odour, and turbidity (Howe et al., 2012; Morrison 2006). The main contaminants contributing to turbidity are the hydrophobic colloidal and suspended solids in water, and have a particle size range of between 0.2µm to 10 µm(Crittenden et al., 2012; Cohn & Cox 1999). These hydrophobic colloidal substances include inorganic clay minerals and colloidal organic substances such as humic and fulvic acids (Crittenden et al., 2012; Schutte 2006; Cohn & Cox 1999).The common units for turbidity is ‘nephelometric turbidity units’, NTU (Howe et al., 2012;Schutte 2006).

Chemical water quality characteristics arise from inorganic or organic substances that easily dissolves in water(Crittenden et al., 2012; Schutte 2006). The dissolved organic substances may either be natural organic matter (NOM) caused by decaying plant materials, algae and carbohydrates, or synthetic organic matter (SOM) such as pesticides, herbicides as well as compounds formed during water treatment processes such as chlorination (trihalomethanes and halo-acetic acids) and chloramination (halo- acetonitrile) (Crittenden et al., 2012; Morrison 2006).

Dissolved inorganic substances such as sodium, calcium, chlorides, and sulfates arise as the result of the dissolution of rocks, or from industrial wastewater effluents(Crittenden et al., 2012; Schutte 2006; Cohn & Cox 1999).Electrical conductivity (EC) is the surrogate measurement of the total dissolved solids(TDS) (Crittenden et al., 2012; Morrison, 2006).

There are three groups of microbes that impact on microbial water quality parameters, namely, protozoans, bacteria and viruses(Proctor &Hammes 2015;Cabral 2010; Khan, 2004). Protozoans (Cryptosporidium oocyst and Giardia cyst) have an average particle size of 5µm, bacteria range from 2 µm to 5 µm, viruses have a diameter of around 0.03 µm(Proctor &Hammes 2015; Khan 2004; Schutte 2006). Not all water borne microbes are harmful. The harmful (disease-causing) microorganisms are called pathogenic microorganismsand are regardedas an acute health risk

(SANS-241_1, 2015). They cause diseases such as cholera, gastroenteritis, typhoid fever, salmonellosis, bacillary dysentery or shigellosis, and diarrhea(Cabral 2010).The presence of pathogenic microbes in water indicates that the water has been exposed to faeces of animals or humans.

The presence of bacteria in water is quantified in terms of 'total counts', or TC. TC is measured as 'Most Probable Number per 100 ml of water' (MPN/ 100 ml) or 'Colony Forming Units/ 100 ml) (CFU/100 ml) (Khan, 2004; Cabral, 2010). The difference between MPN and CFU arises from the analytical method used - the CFU method uses a solid medium to culture bacteria whereas the MPN method uses a liquid medium (Cabral 2010).

2.1.2 Drinking water quality regulations and standards

The regulation of drinking water quality provides the numerical values obtained from health-based target studies to manage and mitigate health risks, and ensure that the drinking water is suitable for safe consumption (WHO 2011). Global organizations such as the Environmental Protection Agency (EPA) and the World Health Organization (WHO) develop guidelines on the water quality parameters to be regulated, and provide maximum threshold values for each water quality parameter. Individual countries then customise these parameters for their local circumstances.

South Africa has its specific drinking water quality standards, called the South African National Standard for drinking water, number 241(SANS-241_1 2015). The latest SANS 241:2015 drinking water quality standard was adopted from the WHO 2011 report "Guidelines for Drinking-water Quality". Table 2-1 below shows the important water quality parameters regulated by the SANS 241 drinking water quality standard.

Table 2-1: Some of the SANS 241 Drinking Water Quality parameters(SANS-241_1, 2015).

Water quality characteristic	**Parameter**	**Risk**	**Units of measurement**	**Standard Limit**
Microbiological	E.coli	Acute health	MPN/100ml	Not detected
	Cryptosporidiumcyst	Acute health	Counts per 10L	Not detected
	Giardia oocyst	Acute health	Counts per 10L	Not detected
	Heterotrophic plate count	Operational	CFU /ml	≤ 1 000
Physical and aesthetic	Turbidity	Operational	NTU	≤ 1
	Total Dissolved solids	Aesthetic	mg/l	≤ 1 200
	pH at 25^0C	Operational	-	≥5 to ≤9.7
	Colour	Aesthetic	mg/l as Pt-Co	≤ 15
	Electrical Conductivity	Aesthetic	mS/m	≤ 170
Chemical (macro)	Sodium	Aesthetic	mg/l	≤ 200
	Nitrate	Acute health	mg/l	≤ 11 as N
	Nitrite	Acute health	mg/l	≤ 0.9 as N
	Chloride	Aesthetic	mg/l	≤ 300
	Sulphate	Aesthetic	mg/l	≤ 250
Chemical (micro)	Arsenic	Chronic health	µg/l	≤ 10
	Iron	Chronic health	µg/l	≤ 2 000
		Aesthetic	µg/l	≤ 300
	Manganese	Chronic	µg/l	≤ 400
		Aesthetic	µg/l	≤ 100
	Mercury	Chronic health	µg/l	≤ 6
Chemical (Organic)	Total Organic Carbon	Chronic health	mg/l as C	≤ 10

2.1.3 Vaal Dam raw water quality

The Vaal Dam is the primary water source for the Gauteng province. Rand Water abstracts and treats Vaal Dam raw water to drinking water standards using conventional water treatment processes,at the Zuikerbosch and Vereeniging Water Treatment Plants. A relatively low salt content with highly variable turbidity characterises the Vaal Dam raw water quality (Table 2-2).

Table 2-2: Vaal Dam raw water quality for the period 2010 to 2016 (DWS, 2019)

Water quality parameter	Units	Mean	Median	Minimum	Maximum	Target Water Quality (SANS 241)
Alkalinity	(mg/l as $CaCO_3$)	69	68	5.00	230	-
Colour	(mg/l as Pt-Co)	67	62	5.00	269.00	≤15
Conductivity	(mS/m)	19	19	1.60	145.00	≤170
pH	(pH units)	7.95	7.98	5.14	11.69	≥5 to ≤9.7
Turbidity	(NTU)	56	57	25	125	≤1
Total Dissolved Solids	(mg/l)	166.3	165.0	78.0	455.0	≤1200
Total Organic Carbon	(mg/l)	5.18	5.10	2.00	9.70	≤10
Heterotrophic plate count	CFU/ml	3294	560	203	36225	≤ 1 000
E.coli	MPN/100ml	784	411	25	2000	Not detected

From Table 2-2, it can be seen that the Vaal Dam raw water does not meet the SANS 241 drinking water quality standard, and is not safe for human consumption without treatment.

2.2 The conventional water treatment process for drinking water production

The purpose of water purification is to treat and produce water that is safe for human health (Wang 2016; Cohn & Cox 1999). For water to be safe and acceptable for public use, the following criteria must be met(WHO 2011):

i. Aesthetically appealing to customers,
ii. Chemically stable, neither corrosive nor scale forming, and
iii. Complies to drinking water quality guidelines and prescribed regulations by relevant authorities.

The conventional water treatment process for drinking water production consists of the following unit processes/operations (Wang 2016; Kawamura 2000; van Duuren 1997):

i. **Trash Rack:**a unit operation that is installed at the raw water abstraction point to remove large floating debris.

ii. **Coarse screen:** a unit operation that is installed at the head of work to sieve coarse debris.

iii. **Coagulation**: a unit process where by the chemical coagulant is rapidly dispersed to ensure the homogeneous mixing of the chemical coagulant and the raw water. During this process, the raw water particle destabilisation occurs, resulting in the formation of pin-flocs.

iv. **Flocculation**: a unit operation where the pin flocs formed during coagulation are promoted to larger aggregates by gentle mixing of the coagulated water. The pin flocs formed during coagulation agglomerate to form micro and macroflocs that are eventually removed from water by clarification processes.

v. **Clarification** (Sedimentation or Dissolved Air Flotation)

   a) Sedimentation: a solid-liquid separation process whereby the macroflocs formed during coagulation/flocculation processes are allowed to settle by gravity into the bottom of a largequiescentbasin.

   b) Dissolved Air Flotation: a solid-liquid separation process whereby the macroflocs formed during coagulation/flocculation processes are separated from water by dissolving air in water under pressure and then release air at atmospheric pressure in a quiescent basin.The released air forms tiny bubbles which adhere to the macroflocs causing the macroflocs to float to the top surface of the basin where they are scraped off.

vi. **Rapid filtration:** the unit operation that removes suspended and colloidal particles from water by filtering water using a thick bed of granular media such as silica sand and anthracite.

vii. **Disinfection**: the final unit process, where disinfectant such as chlorine, chlorine dioxide, ultraviolet (UV) or ozone are added into the water to inactivate or sterilize all residual disease-causing (pathogenic) microorganisms

Figure 2-1 shows the process flow diagram of Rand Water's water treatment process train.

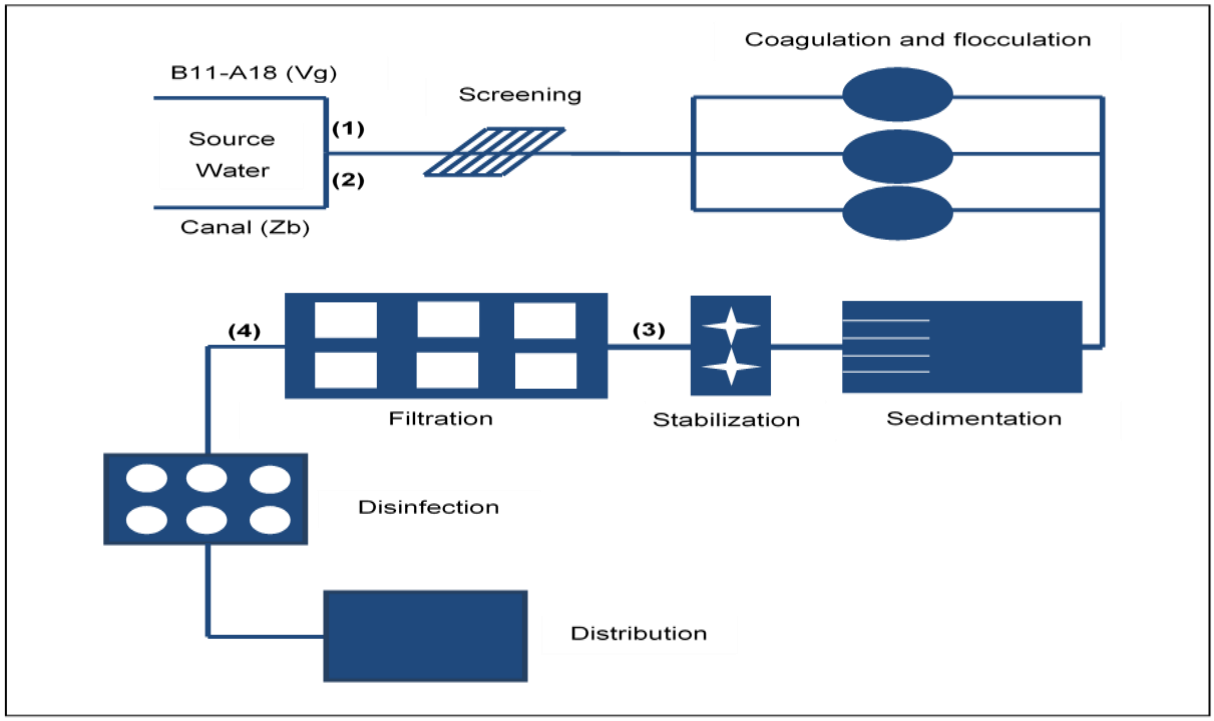

Figure 2-1: Rand Water's water treatment process flow diagram (PFD)

Table 2-3 indicates the advantages and the disadvantages of the conventional water treatment process train.

Table 2-3: Advantages and disadvantages of the conventional water treatment process(Tuan 2008)

Advantages	**Disadvantages**
• Simple and easy to operate • Low capital cost due to cheap material of construction • Suitable for relatively clean surface water • Low operation and maintenance cost	• High chemical usage • Marginal disinfection by-products pre-cursors removal. • Low microbiological removal rate • Low total organic matter removal rate • Requires a large footprint for installation • Low removal of dissolved organic carbon. Dissolved organic carbon causes drinking water to be unpalatable • Not suitable for producing high-quality drinking water.

This investigation includes the application of coagulation as a pre-treatment process to the submerged UF membrane process, hence coagulation is the only unit process that will be discussed further.

2.3 The coagulation process

2.3.1 Overview of coagulation

Coagulation is the addition of a compound, the coagulant, into water causing suspended and colloidal particle to agglomerate together into larger flocs that would separate easily from water (Davis & Marc 2014; Howe et al., 2012). The suspended and colloidal particles in raw water usually carry a negative electrical charge(Bradby 2006;Letterman 1999). Particles of the same charge repel each other, and this applies to suspended and colloidal particles in water. In water treatment, this natural repelling electrical force is called the *zeta potential* (Bradby 2006). Figure 2-2 indicates the two opposing forces acting on particles in suspension.

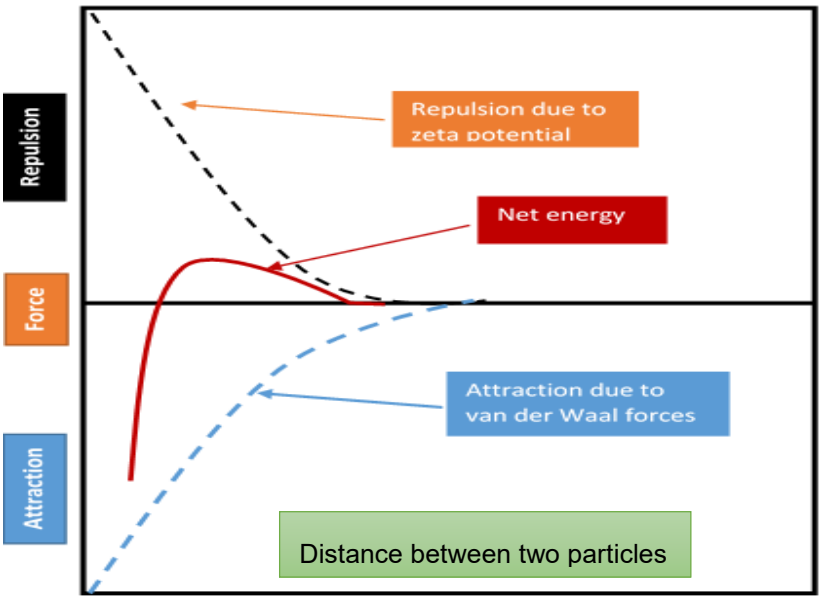

Figure 2-2: Colloidal inter-particulate potential energy versus Distance between two particles (redrawn from Morrison 2006; Letterman et al., 1999)

Electrostatic *stabilisation* is the mechanism whereby colloidal and suspended particles in the water remain as individual entities,since they carry the same electric charge (usually negative) causing repulsion between particles when they approach each other. (Howe et al., 2012; Bratby 2006; Letterman 1999;Kolarik & Booker 1995).

Destabilisation occurs when the addition of a positively charged compound into the water with the negatively charged colloidal and suspended particles decreases the repulsive energy between particles. The net energy acting between the particles approaches zero and the overall electrical charge of each particle becomes neutral. Particles can then approach each other leading to

agglomeration (Davis & Marc 2014; Crittenden et al., 2012). Particle agglomeration commences as pin-flocs during coagulation, and continues to micro and macroflocs during the flocculation process. Particle destabilisation mechanisms during coagulation vary depending on the type of coagulant used(Crittenden et al., 2012). The following section discusses the different particle destabilisation mechanisms that can occur in the coagulation process.

2.3.2 Mechanisms of coagulation

The mechanisms involved in particle destabilisation during coagulation include(Singh 2015; van Duuren 1997):

i. Compression of the double-layer
ii. Charge neutralization
iii. Inter-particle bridging
iv. Enmeshment in a precipitate (sweep floc)

2.3.2.1 Double-layer compression

Double-layer compression arises from the addition of metal salts as a coagulant, causing a reduction in the net energy of the particles (Morrison 2006).The addition of metal salts ions compresses the thickness of the diffuse charge layer surrounding the particles, thus reducing the repulsive forces. This promotes particle agglomeration as a result of Brownian motion and Van der Waals forces of attraction(Letterman et al., 1999). The amount of metal salt required to achieve coagulation by double-layer compression is independent of the concentration of colloids in water (Davis & Marc 2014; Leopold & Freese 2009).

Destabilisation by double-layer compression is not practical in a large-scale conventional water treatment process because the required salt concentration (ionic strength) will almost approach that of the seawater(Crittenden et al., 2012; Letterman et al., 1999).

2.3.2.2 Particle surface charge neutralisation

Particle surface charge neutralisation occurs by the addition of positively charged coagulant. This can be hydrolysed metals salts, prehydrolysed metal salts, and cationic organic polymers. The positive charge added causes the net particle charge to approach zero, and the destruction of the electrical double layer. Van der Waal forces subsequently cause the particles to stick together (Crittenden et al., 2012; Morrison 2006; van Duuren 1997). However, excess positively charged coagulant may adsorb onto the surface of the particles to a point that the net surface particle charge reverses and, in some cases, the net particle charge increases to a point of particle restabilisation (Morrison, 2006).

2.3.2.3 Adsorption and inter-particle bridging

Particle destabilisation by adsorption mechanisms occurs specifically when polymeric coagulant addition causes inter-particle bridging in two ways (van Duuren 1997):

i. Coulombic attraction - if the polymeric coagulant and particle are of opposite charges;
ii. Dipole interaction (ion-exchange) - if the polymeric coagulant and particles are of similarcharges.

The “tail” of the polymeric coagulant spreads out into the raw water and adsorb on available sites of other particles, thus form a chemical bridge between particles, and resulting in large particles that can settle more efficiently (Bradby 2006; Letterman et al., 1999). Polymer bridging is an adsorption phenomenon. Consequently, the optimum dosage will generally be proportional to the concentration of the particles present (Bradby 2006; Letterman et al., 1999).

2.3.2.4 Sweep floc mechanism

The sweep floc mechanism occurs when specifically inorganic salt coagulants such as iron oraluminium salts are used as the coagulant (Bradby 2006; Letterman et al., 1999;van Duuren, 1997).The sweep floc coagulation mechanism occurs in one of the following ways:

i. The hydrolysis and polymerization of metal ions,
ii. The adsorption of hydrolysis products at the particle surface interface,
iii. Charge neutralization.

The sweep floc coagulation mechanism requires high dosages of inorganic salts. At high concentrations of the iron and aluminium salts, the nucleation of a precipitate occurs on the surface of the particles, leading to the growth of an amorphous precipitate with the entrapment of particles in this amorphous structure (Crittenden et al., 2012). This type of destabilisation has been described as precipitation and enmeshment or sweep floc (Bradby 2006; Letterman et al., 1999; van Duuren 1997). This mechanism is predominant in water treatment applications where pH values are between pH 6 and 8, and aluminium or iron salts concentrations exceeding the solubility point for the amorphous metal hydroxide solid that form (Howe et al., 2012; Kawamura 2000; van Duuren 1997). Colloidal particles are electrostatically attached to the sweep flocs(Rattanakawin et al.,2005). At low colloid concentrations, an excessive amount of coagulant is required to produce a sufficiently large amount of precipitate that will enmesh the relatively few colloidal particles as it settles(Bratby 2006). At high colloids concentrations, the coagulation will occur at a lower chemical dosage because the colloids serve as the nuclei to enhance precipitate formation (Bradby 2006; Letterman et al., 1999; van Duuren1997).

2.3.3 The Jar test method

The 'Jar Test' is the method commonly used by water practitioners to simulate coagulation, flocculation and clarification in a conventional water treatment process (Kawamura 2000). The jar test is used in conventional water treatment plants to determine the optimal coagulant type, the required dosage of the coagulant,and the optimum mixing conditions for the coagulation (rapid or flash mixing), flocculation (slow mixing) and the clarification step (Crittenden et al., 2012;AWWA 2011;Kawamura 2000; Kolarik & Booker 1995).

The jar test method allows for the rapid testing of the coagulant type and the dosing range using a four or six paddle mixers. The method consists of batch addition of the coagulant followed by rapid mixing, simulating the coagulation step, and then slow mixing, simulating flocculation. The flocs formed in each jar are allowed to settle, and supernatant samples are taken for analysis of residual turbidity.

Figures 2-3 and 2.4 are examples of the jar test apparatus used for rapid assessment of the coagulant type and the dosing range.

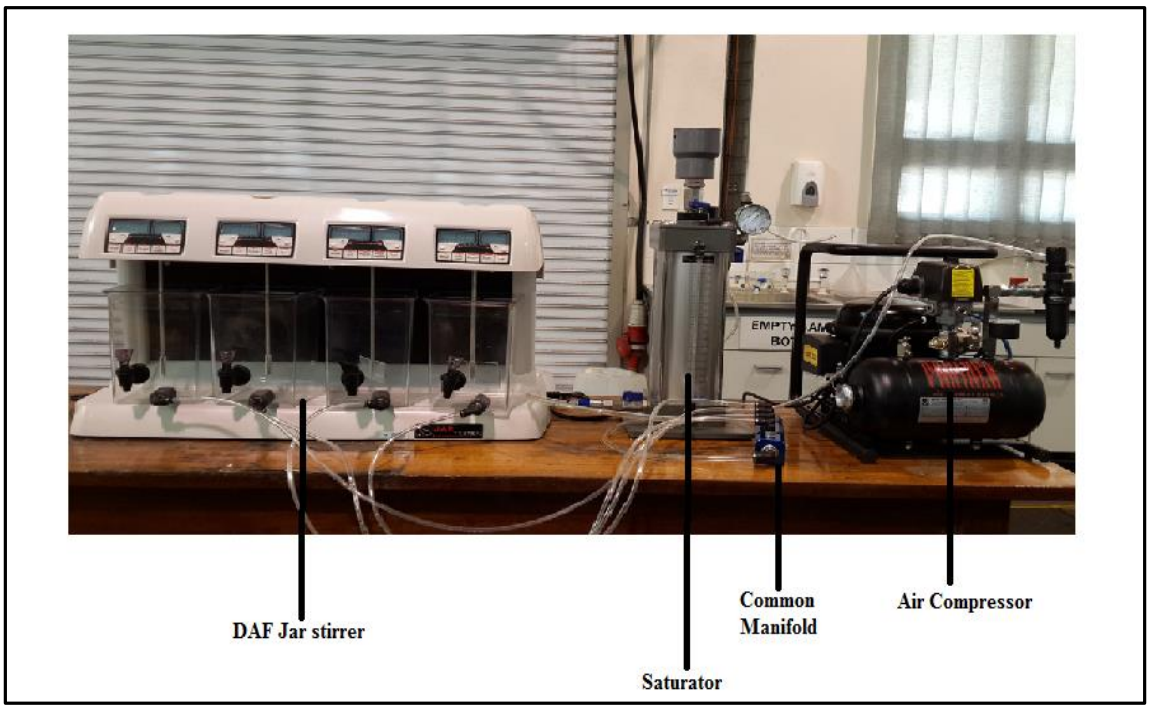

Figure 2-3: The jar test apparatus used to simulate coagulation, flocculation and DAF - Rand Water.

Figure 2-4: The jar test apparatus used to simulate coagulation, flocculation and sedimentation - Rand Water.

2.3.4 Mixing intensity

A parameter of great importance in coagulation is the 'mixing intensity'. The mixing intensity (also known as velocity gradient, $\bar{G}$) is the rate at which the energy is dissipated in water, measured in per sec (s^{-1}). The mixing energy varies with water temperature irrespective of the mixing device and the rotation speed. (Crittenden et al., 2012; AWWA 2011). The water velocity during mixing varies in both space and time inside the coagulation chamber under the turbulent conditions and calculated as follows (Crittenden et al., 2012; Howe et al., 2012; Kawamura 2000).

$$\frac{P}{V} = \mu \left(\frac{dv}{dz}\right)^2 \qquad \text{Equation 2-1}$$

The velocity gradient ($\bar{G}$) is, $\bar{G} = \frac{dv}{dz}$, rearrange the equation 2-1 and making $\bar{G}$ the subject of the formula

$$\frac{P}{V} = \mu \bar{G}^2$$

$$\bar{G}^2 = \frac{P}{\mu V}$$

$$\bar{G} = \sqrt{\frac{P}{\mu V}} \qquad \text{Equation 2-2}$$

Where $\bar{G}$ = Velocity gradient, s^{-1}

μ = water viscosity, mPa

V = Volume of the coagulation basin, m^3

P = Power, W, J/s or $kg.m^2.\ s^{-3}$

The parameters of importance in the design of the mixing devices are power number (N_p), the pumping number (N_Q) and the head number (N_H). The N_p is determined by the torque meter on the mixer shaft and the tachometer to measure the rate of mixer rotation. The N_p is calculated as follows.

$$N_p = \frac{P}{\rho N^3 D^5} \qquad \text{Equation 2-3}$$

where N_p = Power number, dimensionless

P = Power required, J/s (W)

D = diameter of impeller, m

N = Impeller's rotations, speed, s^{-1}

ρ = water density, kg/m3

Rearranging equation 2-3 to make P the subject of the equation yields:

$$P = N_p \rho N^3 D^5 \qquad \text{Equation 2-4}$$

Substituting equation 2-4 into equation 2-2, $\bar{G}$ becomes:

$$\bar{G} = \sqrt{\frac{N_p\ \rho N^3 D^5}{\mu V}} \qquad \text{Equation 2-5}$$

The recommended $\bar{G}$ value for the coagulation process ranges between 600 and $5000 s^{-1}$, with the contact time of between10 to 30 sec(Howe et al., 2012; Kawamura 2000).

2.4 Membranes processes

2.4.1 Overview

A membrane is a semi-permeable material that separates entities from water using the difference in permeability of the impurities (Laîné, et al., 2003). In water treatment, membrane filtration processescan remove particulate, colloidal and dissolved impurities from water, using pressure as a driving force (Koyuncu, et al., 2015; Fan, et al., 2014). A membrane process consists of three streams:-the rawor feed stream;the permeate containing material that has passed through the membrane; and the retentate containing non-permeating material (Zirehpour& Rahimpour, 2016; Hugo, 2015). These streams are shown in Figure 2-5.

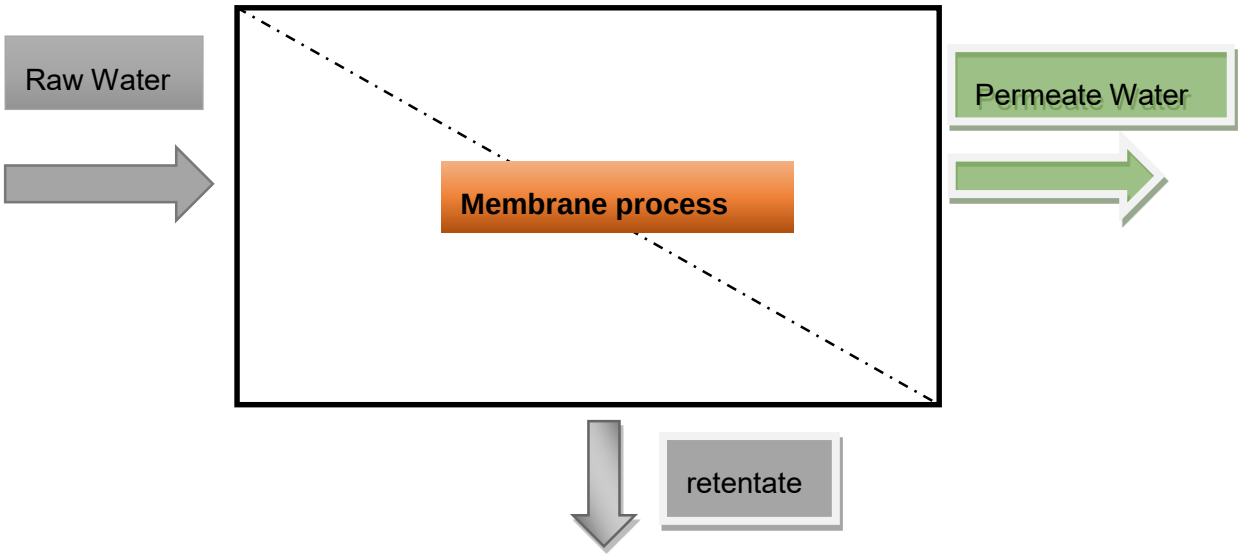

Figure 2-5: Schematic of the membrane filtration process(redrawn from Zirehpour & Rahimpour, 2016)

The membrane can either be asymmetric or symmetric (Zirehpour& Rahimpour, 2016; Hugo, 2015; Howe, et al., 2012; Judd et al., 2011). *Symmetric membranes* are membranes that have a homogeneous structure across the membrane thickness, i.e. the membrane uses the same material both for the active and the support layers. *Asymmetric membranes* are membrane where the top layer and the porous supporting layer originates from two or more materials cast on top of one another.

Membrane classification generally follows the criteria below (Hugo, 2015; Crittenden, et al., 2012):

i. Molecular weight cut-off (MWCO),
ii. Membrane pore size,
iii. Membrane material and geometry,
iv. Targeted materials.

The molecular weight cut-off (MWCO) is the capability of a membrane to reject greater than 90% of spherical macromolecules such as polyethylene glycol, dextran, or proteinby the membrane's pores (AWWA, 2016; Hugo, 2015; Crittenden, et al., 2012; Kawamura, 2000). The unit of MWCO is Dalton (1 Dalton is the mass of one hydrogen atom = 1.66 $x10^{-27}$kg). The main limitation with the MWCO is the adsorption of proteins on the surface and inside the pores due to membrane–protein interaction resulting in (a) a reduced pore size, and (b) a secondary film forming on the membrane surface (AWWA, 2016).

2.4.2 Membrane types

There are four groups of membrane filtration processes commonly used in water treatment, viz., Microfiltration (MF), Ultrafiltration (UF), Nanofiltration (NF) and Reverse Osmosis (RO) (AWWA, 2016; Twain, 2015; Vigneswaran, et al., 2012; Kawamura, 2000; Smith, 1995).The pore size of the active skin and the impurities removed from water differentiate the membrane processes (Meier-Haacka, et al., 2003). MF membranes have a relative pore size of between 0.1 – 10 micrometre (µm) and designed to remove suspended matter, colloidal particles and some bacteria (Koyuncu, et al., 2015; Shon, et al., 2012; Lebeau, et al., 1998). UF membranes have a relative pore size of between 0.01 – 0.1 µmand remove suspended matter, colloids, bacteria and some viruses (Koyuncu, et al., 2015; Arnal, et al., 2009). NF has a relative pore size of between 0.001 – 0.1 µm and removes divalent dissolved ions and organics (Koyuncu, et al., 2015). RO has a relative pore size of between 0.0001 – 0.001 µm and designed to remove monovalent dissolved ions and low-molecular organic matter(AWWA, 2016;Crittenden, et al., 2012; Vigneswaran, et al., 2012; Howe et al., 2012; Kawamura, 2000; Kolarik & Booker, 1995).

Membrane systems for water treatment are broadly categorised into two groups, namely;(AWWA, 2016; Ang & Mohamma, 2015).

i. Low-pressure membranes (MF and UF): submerged and pressurised membranes for the removal of the suspended material, colloidal material, bacteria and viruses.
ii. High-pressure membranes (NF and RO): for the removal of dissolved inorganic and organic impurities from water.

Figure 2-6 below shows a schematic representation of the membrane filtration processes and the contaminants rejected.

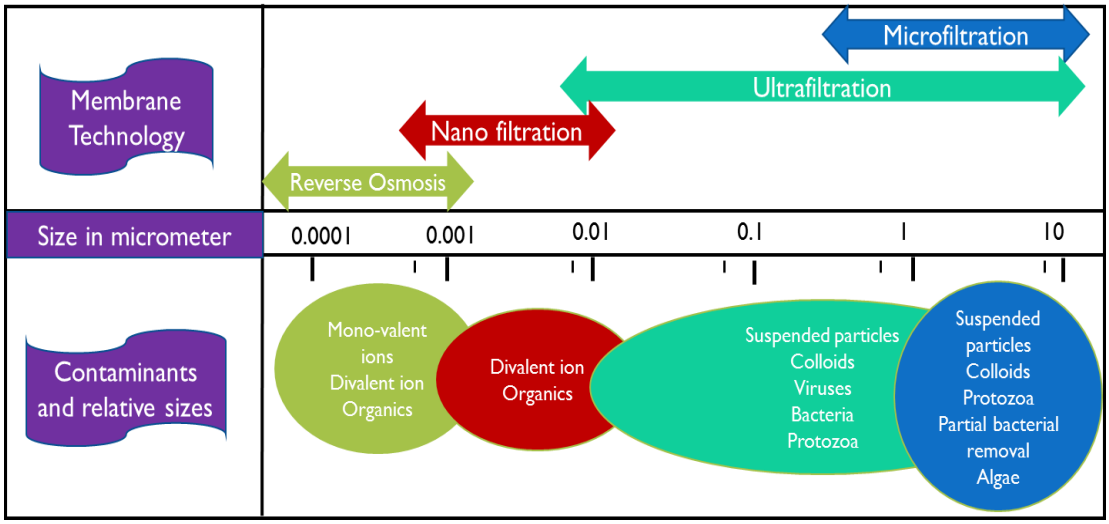

Figure 2-6: Membrane filtration technologies and rejected contaminants (redrawn from AWWA, 2016; Vigneswaran, et al., 2012)

2.4.3 Membrane materials

There are two types of materials used in membrane manufacturing, i.e. organic and inorganic materials (Zirehpour & Rahimpour, 2016). Inorganic membranes such as metals and ceramics (CE) are not commonly used in drinking water treatment due to the high capital and operating costs (Singh et al., 2015). Regenerated cellulose(C), cellulose acetate (CA), polyamides (PA), polyacrylonitrile (PAN), polycarbonate (PC), polyethylene (PE), polyolefins (POF), polypropylene (PP), polysulphone (PS), polytetra fluoroethylene (PTFE), polyvinyl chloride (PVC) polyvinylidene fluoride (PVDF) and thin-film composite (TFC) are the available membrane materials for water treatment processes (Chang et al., 2017; Zhang et al., 2012). Table 2-4 shows the different type of membrane materials, and Figure 2-7 shows the membranes that are commonly used in water treatment.

PVDF, PS,and PES are most commonly employed materials in low-pressure membranes due to high resistance to harsh chemical cleaning, chlorine, and moderately high temperature tolerance and operate at pH range of 2 to 12 (Sing et al., 2015).

Table 2-4: Membrane material types and application in water treatment (Chang, et al., 2017; Singh, 2015;Zhang, et al., 2015).

Membrane filtration process	**MF**	**UF**	**NF**	**RO**
Membrane structure	Macropores	Mesopores	Micropores	Dense
Materials	CA, CE, PAN, PC, PE, POF, PP, PS, PTFE, PVDF	C, CA, CE, PA, PAN, TFC, PS, PVDF	CA, PA, TFC	CA, PA, PS, TFC

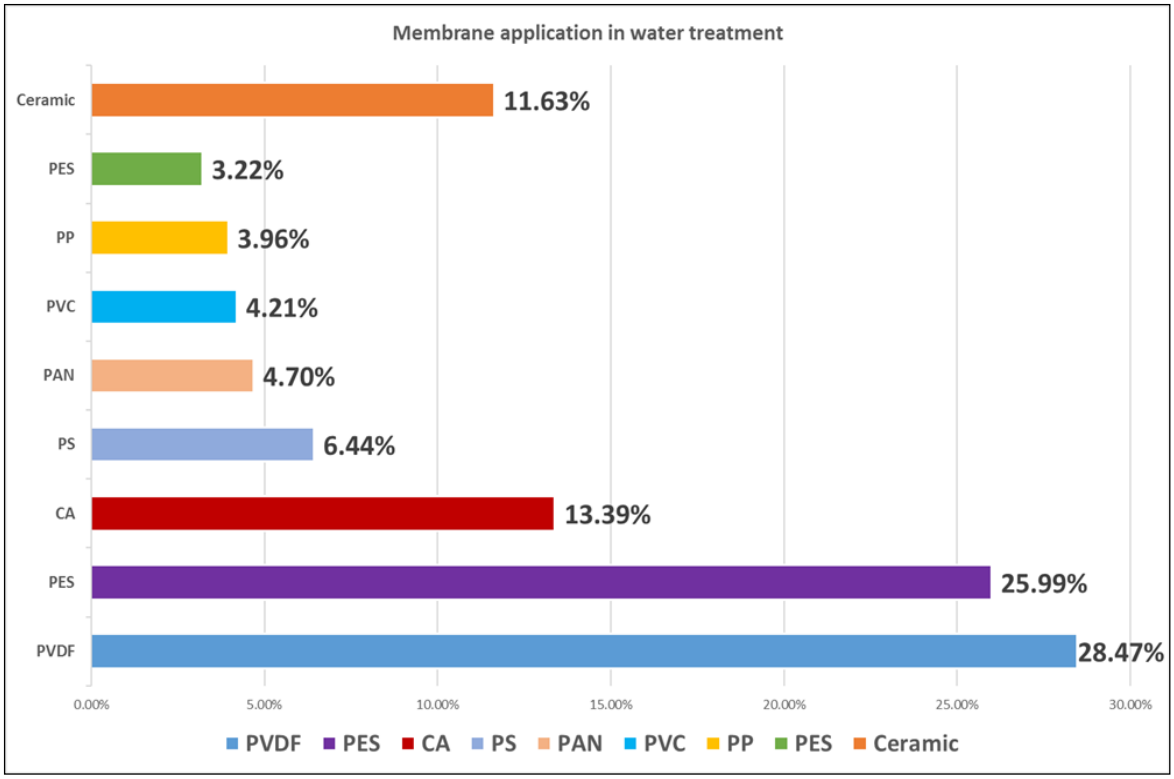

Figure 2-7: Membrane materials commonly used in water treatment (redrawn from Chang, et al., 2017)

The most dominant membrane filtration processes used for non-saline surface waters are MF and UF.

2.4.4 Membrane module configurations

The membrane module configuration refers to the membrane orientation relative to the water flow (AWWA, 2016). Membranes maybe planar or cylindrical in geometry (Pearce, et al., 2011). Different types of configurations include (AWWA, 2016).:

i. Plate and Frame / Flat sheet (FS)
ii. Hollow fibre (HF)
iii. Multi-tubular (MT)
iv. Capillary tubes (CT)
v. Plate filter cartridges (PC)
vi. Spiral wound (SW)

Raw water flow in the different membrane orientations can either be outside-in or inside-out.The location of the membrane skins defines the water flow direction(Hugo, 2015). Figure 2-8 shows the water flow directions of different membrane geometries.

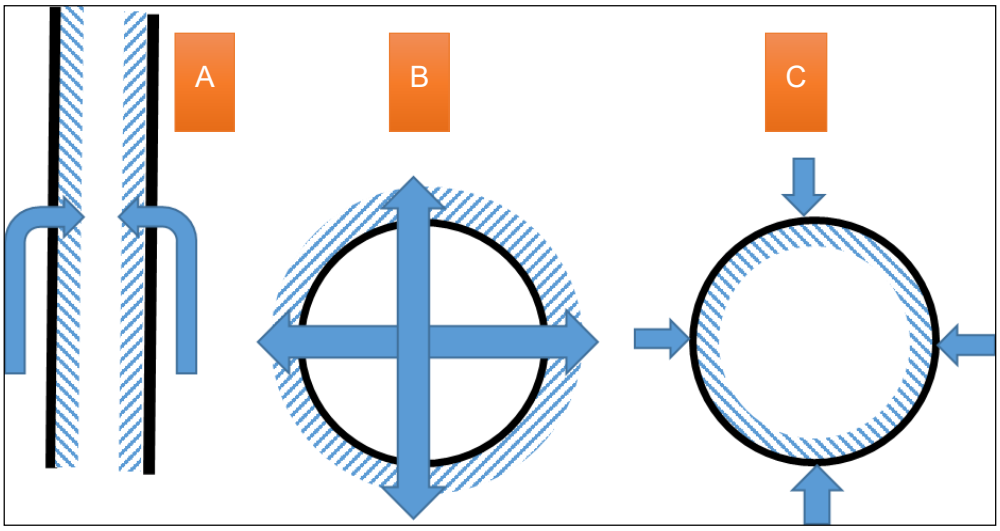

Figure 2-8: Water flows through the membrane orientation (a) Flat sheet, (b) Capillary tube or Multi Tubular and (c) Hollow fibre(redrawn from Hugo, 2015)

In Figure 2-8, the solid black line indicates the membrane skin, the blue shaded lines indicate the supporting layer and the arrows show the water flow direction(Chang et al., 2017; Hugo, 2015).Figure 2-9 below indicates the application of the thedifferent membrane configurations in water treatment.

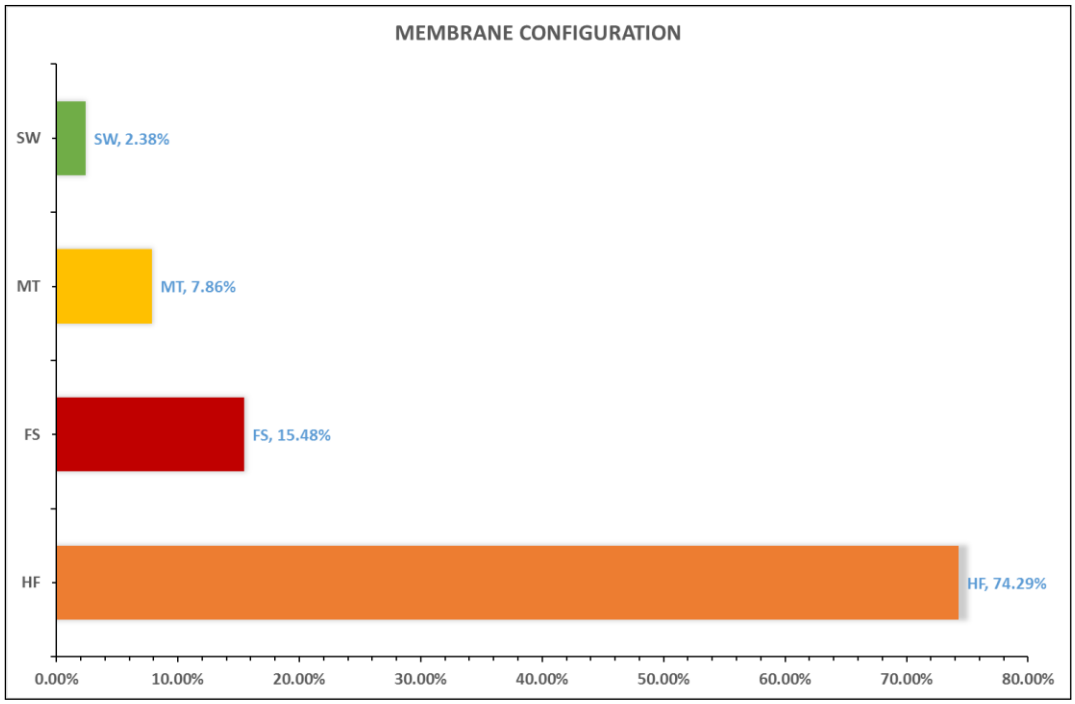

Figure 2-9: Application of the different configuration in water treatment (redrawn from Chang, et al., 2017)

From 2-9, HF is the most popular membrane configuration (74.3%) followed by the FS.

2.4.5 Membrane Filtration modes

2.4.5.1 Dead end and cross-flow operation

Membranes may operate in one of two modes, viz., a dead-end mode, or a cross-flow mode.In the cross-flow filtration mode, the raw water flows parallel to the membrane surface thus creating shear forces that reduce the development of the cake on the membrane surface(Galvañ, et al., 2014). In the cross-flow regime, the solids pass the membrane surface with the retentate instead of accumulating on the membrane surface (Nguyen, 2012;Pearce, et al., 2011). Figure 2-10 shows the operation of the cross-flow mode.

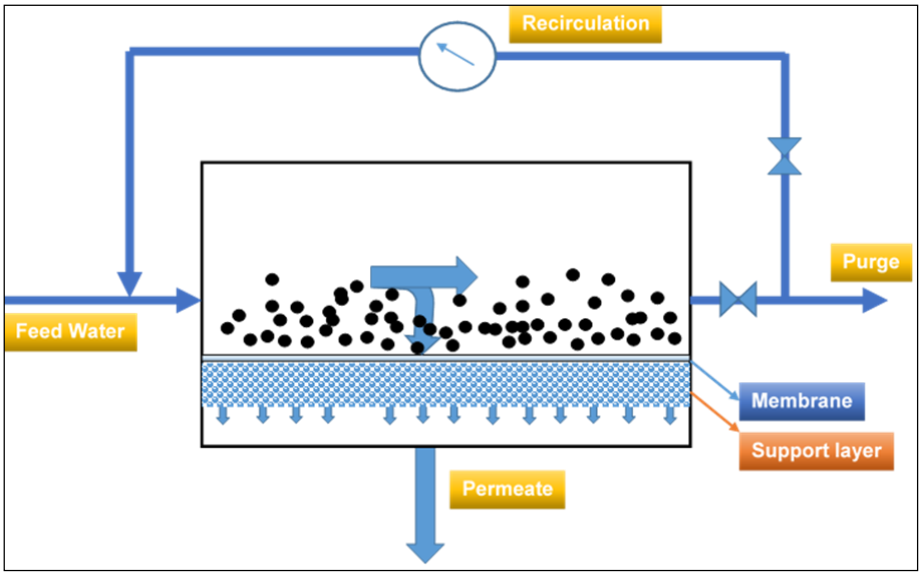

Figure 2-10: Schematic presentation of cross-flow filtration regime (redrawn from Nguyen, 2012)

In the dead-end filtration mode, the rawwater passes directly into the membrane, and there is no retentate flow. All the solids accumulated on the membrane surface are removed during backwashing (Nguyen,2012; Pearce, et al., 2011). Figure 2-11 shows the dead-end membrane filtration mode.

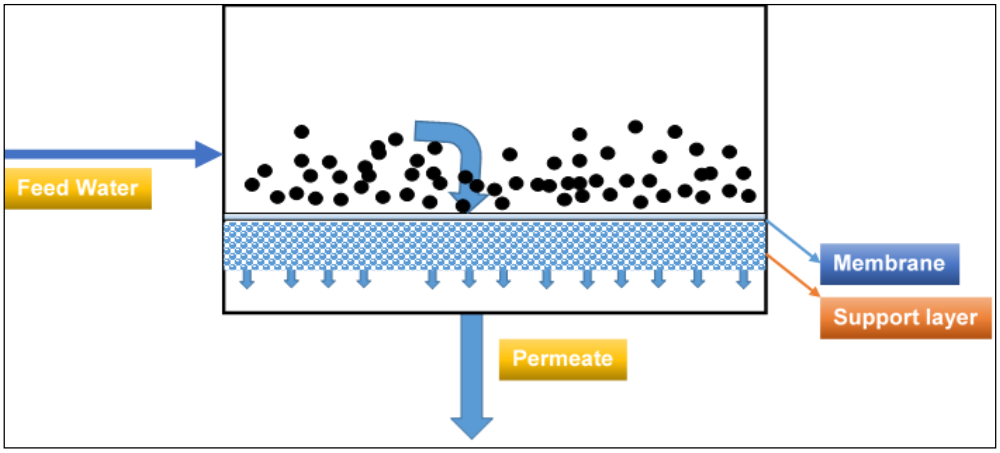

Figure 2-11: Schematic presentation of the dead-end filtration regime (redrawn from Nguyen, 2012)

2.4.5.2 Constant Flux vs Constant Pressure operation

In the constant flux operating regime, the membrane flux remains constant while the trans-membrane pressure (TMP) increases during filtration. In the constant TMP regime, the TMP remains constant while the membrane flux declines for the filtration period (Dick, 2015 and Singh et al., 2015). Figure 2-12 shows the membrane filtration operating modes for the period of filtration.

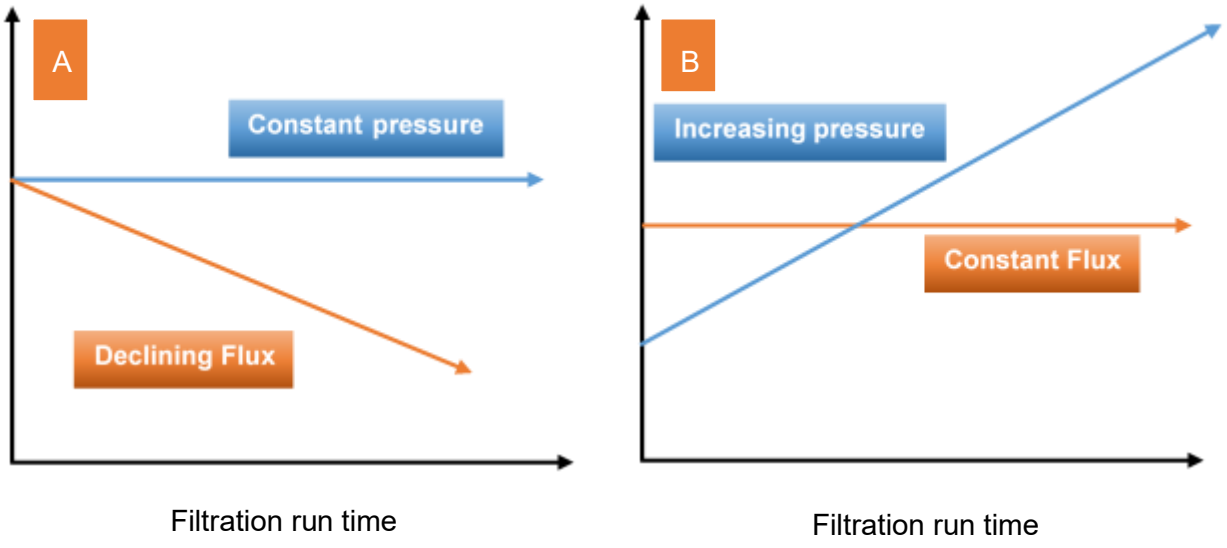

Figure 2-12: Membrane filtration operating modes: (A) Constant TMP and (B) constant membrane flux.

2.5 Limitations to membrane performance

The major limitations to membrane performance are concentration polarisation, fouling and membrane ageing.

2.5.1 Concentration polarization

Concentration polarization is the accumulation of sieved impurities near the membrane surface causing higher impuritity concentrations near the surface than that of the raw water (AWWA, 2016; Ang & Mohamma, 2015; Guo, et al., 2012).

Figure 2-13 is a schematic presentation of concentration polarization in membrane systems.

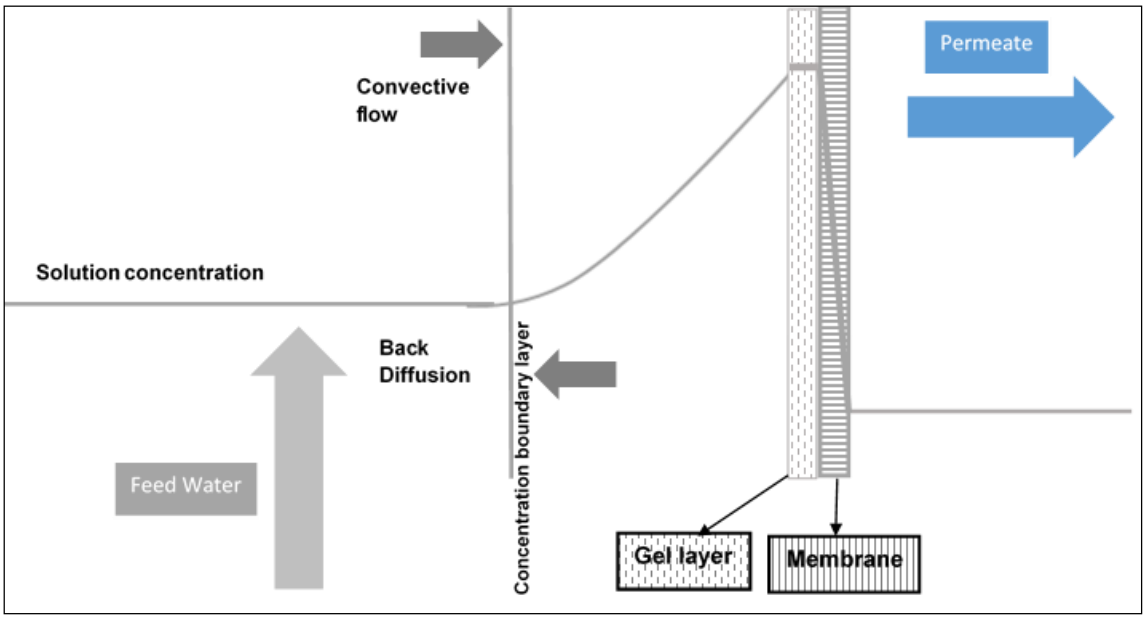

Figure 2-13: Schematic representation of concentration polarisation near the surface of the membrane **(**redrawn from Zirehpour & Rahimpour, 2016**;**Hugo, 2015;Pearce, et al., 2011)

The accumulation of the impurities near the membrane surface creates a concentration gradient, and, as a result, the impurities diffuse back into the water. Under steady-state conditions, the convection flow of solute to the membrane surface is equal to the solute that retained by the membrane surface, with the diffusion of solute back to the bulk feed solution (Ang & Mohamma, 2015; Pearce, et al., 2011).

Concentration polarization limits the operation of membrane processes due to the following(Pearce, et al., 2011 and Taylor & Wiesner, 1999):

i. The accumulation of sieved impurities near the membrane surface restricts the flow of water through the membrane, thus increasing the membrane resistance.

ii. The precipitation of sparingly soluble macromolecular polymeric and inorganic (gel layer formation and scaling, respectively) at the membrane surface may cause irreversible membrane fouling.

iii. The accumulated cake near the membrane surface causes the membrane pore blocking, reduces membrane permeability, and ultimately shortening the membrane system lifespan.

iv. Changing the membrane separation characteristics.

2.5.2 Membrane fouling

2.5.2.1 Overview of fouling

Membrane filtration of raw water results in complex physical, chemical, and biological reactions amongst the impurities,or between the impurities and the membrane surface (Gao, et al., 2012; Guo, et al., 2011). In membrane filtration, the membrane permeability gradually reduces due to the accumulation of impurities on the surface of, or within the membrane. This is referred to as fouling (Porcelli& Judd, 2010; Huang, et al., 200).

Raw water characteristics determine the method by which impurities are rejected at the membrane surface. The three different impurities rejection methods are defined as follows: (Kao, et al., 2012; Gao, et al., 2011; Guo, et al., 2012; Porcelli & Judd, 2010; Huang, et al., 2009; Mosqueda-Jimenez, et al., 2008):

i. **Physical rejection**:the removal of the suspended matter and colloidal particles such as clay and silt. These impurities have a particle size diameter that is greater than the average diameter of the membrane pores.

ii. **Chemical rejection**: the removal of impurities that are hydrophobic, polarised, and specific functional groups.

iii. **Biological rejection**: the removal of biodegradable impurities by the addition of specific media to the membrane filtration vessel for microbial organism growth.

The physical rejection method is the most prevalent in low-pressure membranes (Huang, et al., 2009; Mosqueda-Jimenez, et al., 2008).

Other factors that influence membrane fouling includethe membrane material, the membrane pre-treatment method, the operating conditions, and the raw water quality (Guigui, et al., 2001; Nakatsuka et al., 1996).

There are three main fouling characteristics/mechanisms in a low-pressure membrane (Guo, et al., 2012;Howe et al., 2012;.Kao, et al., 2012; Gao, et al., 2011):

i. Particulate fouling is a pore-blocking mechanism that occurs through a series of steps. Firstly, the larger particles accumulate on the membrane surface with smaller particles inside the membrane pores. Secondly, the cake layer formed due to particles precipitate onto the particles that have already deposited onto the membrane, thus creating resistance of membrane flux. This surface cake formation acts as a filtration medium, providing another

mechanism for rejection. The dynamic membrane filtration mechanism varies with time due to the development of the cake thickness during filtration.

ii. Organic fouling occurs when the natural organic matter (NOM) from the raw water accumulates on the membrane surface. The NOM is ever-present in natural waters and is known to be the primary precursor for the formation of disinfection by-products ifnot removed from the raw water (Zhang, et al., 2015). Molecular Weight (MW) and Specific Ultra Violet Absorption (SUVA) are the parameters used to categorise NOM fractions(Nkambule, et al., 2012). The SUVA is the quotient of the ultraviolet absorption at 254 nm wavelength (UV_{254}) and dissolved organic carbon (DOC) concentration, ($SUVA = \frac{UV_{254}}{DOC}$)(Nkambule, et al., 2012;Gora, et al., 2011). Table 2-5 shows SUVA values and the corresponding NOM fractions.

Table 2-5: NOM fractions and related SUVA values(Nkambule, et al., 2012)

SUVA (l/mg-m)	Composition	MW range, Da
>4	- A high fraction of aquatic humic matter - High aromatic and hydrophobicfraction - High molecular weight (MW)	> 10 000
(2-4)	-A mixture of aquatic humic and non-humic matter -A mixture of aliphatic and aromatic character -A mixture of low to high MW – transphilic fraction	1000 to 10 000
< 2	- A high fraction of non-humic matter - A high aliphatic and hydrophilic character - A low MW –Hydrophilic fraction	< 1000

The high MW weight NOM fraction accumulates on the membrane surface causing adsorptive fouling and cake layer deposition(Xing, et al., 2018)

iii. Microbial adhesion/ bio-fouling is as the result of the multiplication of the bacteria attached to the membrane surface which form colonies and cause bio-fouling. Their production of extracellular polymeric substances leads to the formation of biofilms. The severity of the bio-fouling is said to be significantly related to raw water characteristics such as the abundance of microbes, nutrients availability, and microorganisms present (Singh, 2015; Guo, et al., 2012; Watanabe, et al., 2009).

2.5.2.2 Physical rejectionfouling mechanisms

The physical rejection of particulates at a membrane surface occurs via three mechanisms (Singh, 2015; Howe, et al., 2012):

i. Straining (pore blocking) is the physical sieving due to difference between particulate size and membrane pore size.

ii. Adsorption occurs when the particles are small enough to enter the membrane pores and get adsorbed into the walls of the membrane pores.

iii. Cake filtration occurs due to particles precipitating onto the particles that have already deposited onto the membrane surface, thus creating resistance of membrane flux. This surface cake formation acts as a filtration medium, providing another mechanism for rejection

Pore blocking

Straining (also called sieving or steric exclusion) is the dominant filtration mechanism in low-pressure membrane filtration (AWWA, 2016). Particles greater than the membrane pore size are retained and collect on the membrane surface water, and smaller particles pass through the membrane (Kao, et al., 2012).

Adsorption

Adsorption occurs when the diameter of the particle is smaller than the membrane pore. Particles adhere to the membrane surface, or enter and adhere to the wall of the pore, resulting in anincreased hydraulic resistance (Guo, et al., 2012). NOM removal by low-pressure membrane systems is predominantly an adsorption mechanism onto the membrane surfaces (Van Doesburg, et al., 2009; Lebeau, et al., 1998). The adsorption mechanismis the prevelantrejection mechanism during the early stages of filtration with a clean membrane. Adsorbed material reduces the size of voids throughout the membrane hence increasing the ability of the membrane to retain smaller material by straining (Kao, et al., 2012).

Cake formation

Cake filtration occurs when particles that are small enough to pass through the membrane attach on the material that has already collected at the membrane surface (Hugo, 2015; Howe et al., 2012).

Figure 2-14 below shows the different fouling mechanisms.

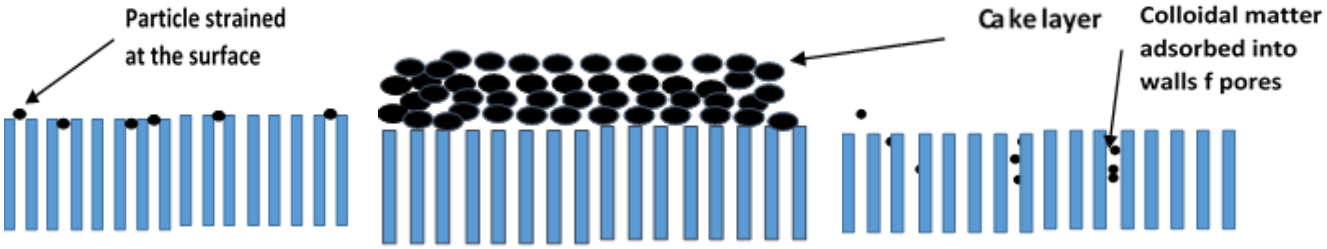

Figure 2-14: Particulate fouling mechanisms of low-pressure membrane filtration (redrawn from Howe et al., 2012 and Zhang et al., 2012).

2.5.3 Membrane ageing and failure

A membrane lifespan is mainly determined by the irreversible deposition of the impurities on the membrane surface,causing the deterioration of the membrane skin and the supporting layer. The physical damage to the membrane by foreign material causes membrane failure resulting in the loss of membrane mechanical integrity (Tng, et al., 2015). The following actions cause the membranes to be fragile to ageing and failure (Chang, et al., 2017;Tng, et al., 2015; Zsirai, et al., 2012):

i. The use of a high concentrations of the chemical cleaning agent during chemical cleaning in place (CIP).
ii. The application of high-pressure backwashes.
iii. Membrane puncture due to the presence of foreign objects.
iv. Inadequate pre-treatment processes.

To manage membrane ageing and failureandto improve lifespan, a better understanding of the specific fouling mechanism, selection of an appropriate operating strategy, and use of the relevant chemical cleaning protocol depending on the fouling agent are essential (Lazarova, et al., 2007)

2.6 Membrane fouling control

2.6.1 Approaches to membrane fouling control

All membranes are subject to fouling. However, the membrane fouling rate can be managed by various methods to maintain membrane lifespan.The following are the membrane fouling control mitigating methods, depending on the fouling agent: (Li, et al., 2014; Peiris, et al., 2013; Zsirai, et al., 2012; Guo, et al., 2012):

i. The conditioning of the raw water by chemical pre-treatment.
ii. The membrane filtration system operating protocol (permeate flux, membrane relaxation, backwash frequency,and constant pressure or constant flux operation).
iii. Periodic rinsing (backwashing or forward flushing).

iv. Chemical cleaning in place (CIP) by soaking the membrane in chemical agents such as acid solution, alkali solution or biocide solution.

v. Air scouring to induce shear forces on the membrane surfaces. This method enhances the back-transport of impurities from the membrane surface tothe water,thus preventing the excessive accumulation of impurities in the membrane surface.

Chemical pre-treatment, CIP, and air scouring were employed in this investigation and are discussed further in the following sections.

2.6.2 Chemical pre-treatment

Raw water pre-treatment refers to the unit processes or operations upstream to the membrane filtration process. The purpose of the pre-treatment is to modify the raw water characteristics to improve membrane performance and reduce membrane fouling (Huang et al., 2009). The effectiveness of the pre-treatment process in membrane fouling control is dependent on the membrane characteristics and the raw water characteristics. The pre-treatment processes alter the physical, chemical, and biological characteristics of the raw water to improve the performance of low-pressure membrane filtration.

The methods involved in pre-treatment include (Huang et al., 2009):

i. Physical methods – these increase the size of impurities in the raw water to a size that is separable by the membrane surface. The increased particulate size of impurities in the raw water shifts the membrane fouling mechanism from adsorption and pore constriction (blocking) to cake filtration that is usually less severe and more reversible.

ii. Chemical methods – its the addition of chemicals into the raw water (e.g., coagulants, oxidants, and adsorbents) to alter the water chemistry and reduce the affinity of the impurities to attach to the membrane surface thereby alleviating irreversible membrane fouling.

iii. Biological methods – this is aimed at reducing biofilm formation on or near the membrane surface.

The commonly employed pre-treatment options include coagulation, adsorption, magnetic ion exchange resin (MIEX), biological treatment and integrated pre-treatment (Yu et al., 2017; Huang et al., 2009). Factors that affect chemical pre-treatment include (Gao et al., 2011):

i. The chemical dosing rate, dosing point, dosing mode (stop-start or continuous)

ii. The chemical mixing energy and contact time

iii. The raw water characteristics (particulate, colloidal and dissolved organic and inorganic, temperature pH and ionic strength).

iv. The membrane characteristics (membrane charge, hydrophobicity, and surface morphology)

The selection of a chemical pretreatment process is mainly determined by the membrane and raw water quality characteristics (Huang et al., 2009)

2.6.2.1 Pre-treatment by coagulation

There are two categories of pre-coagulation (Gao et al., 201; Huang et al., 2009).

i. Standard coagulation: processes such as sedimentation and sometimes media filtration are included as pre-treatment processes
ii. Inline coagulation: pre-coagulation without flocculation and sedimentation, the coagulated water is directly fed into the membrane filtration process.

The conventional water treatment process employs a jar testing method to determine the optimum coagulant dosage for the formation of large macro flocs that can be removed by sedimentation or flotation (Kawamura, 2000 and Duuren, 1997).

However, this requirement does not apply to low-pressure membrane system such as UF. The fine membrane pores physically sieve the suspended, and colloidal particles (Vigneswaran, et al., 2012). Hence the objective of coagulation as a pretreatment to UF is simply to form micro flocs that are larger than the membrane pore size (Fan, et al., 2014; Arnal, et al., 2009 and Botes, et al., 1998).

There are two types of coagulants used in water treatment, inorganic and polymeric coagulants (Crittenden, et al., 2012; Howe, et al., 2012 and Bratby, 2006). The application of inorganic coagulants in water treatment is dependent on the water alkalinity, pH and carbonate chemistry (Davis & Marc, 2014; Bradby, 2006 and van Duuren 1997). The use of inorganic coagulants may require the addition of a chemical additive to adjust pH and alkalinity before the addition of an inorganic coagulant. However, polymeric coagulants are less sensitive to pH and alkalinity (Morrison, 2006; Letterman, et al., 1999; van Duuren, 1997).

The advantages of using polymeric coagulant include the following; less amount of coagulant dosage, the floc settles readily andis less sensitive to pH and alkalinity (Vigneswaran, et al., 2012; Leopold & Freese, 2009 and Bradby 2006).

2.6.2.2 Adsorption

The pre-treatment of raw water with adsorbents occurs before the membrane, and involves fixed adsorbant contactors or the addition of a suspended powder (Huang et al., 2009). The most commonly used adsorbent in membrane processs is powdered activated carbon, or PAC (Gao et al., 2011; Huang et al., 2009). In an integrated PAC/UF process, the PAC dosage is conducted in two ways, (1) the PAC is added directly into the membrane tank at a constant rate and (2) the PAC is added before the membrane tank (Gao et al., 2011).

2.6.2.3 Oxidation

The commonly employed oxidants in conventional water processes are ozone, chlorine, potassium permanganate, chlorine dioxide, and aeration (Atkinson, et al., 2010). The application of an oxidant as a pre-treatment process suppresses microbiological growth and changes the structure and properties of the natural organic carbon to assimilable organic carbon (AOC) (Lebeau, et al., 1998). Of the oxidants indicted above, ozone is not compatible with the polymeric membrane filtration (Gao et al., 2011 and Huang et al., 2009). The removal of undesirable dissolved ions in raw water may be achieved by pre-oxidation with an appropriate oxidant that is compatible with the low-pressure membrane and oxidises ions from soluble to insoluble state to be easily sieved out by membrane filtration. (AWWA, 2016).

2.6.2.4 Other pre-treatment methods

The other pre-treatment processesused include dissolved air flotation (DAF), magnetic ion exchange resin (MIEX), biological filter media, granular activated carbon (GAC), and green sand (Gao et al., 2011 and Huang et al., 2009). Appendix 20 is a summary of the pre-treatment methods used in membrane filtration processes.

2.6.3 Membrane chemical cleaning in place (CIP)

The foulants' properties determine the CIP method to be used (Lazarova, et al., 2007). Table 2-6 below indicates common chemicals used for CIP methods.

Table 2-6: Membrane CIP methods based on the membrane foulant and/or scalant (Zhang, et al., 2015; Shi et al., 2014; Vigneswaran, et al., 2012;Zsirai et al., 2012; and Lin et al., 2010)

Foulant or scalant	**Typical chemicals used for CIP**	**Category**	**Major function**
Natural organic matter	Sodium hydroxide (NaOH)	Caustic	Hydrolysis, solubilisation
Microbial; NOM; Synthetic polymers	NaOH, Hydrogen Peroxide (H_2O_2), Sodium hypochlorite (NaOCl) and peroxyacetic acid ($C_2H_4O_3$)	Oxidants/ Disinfectant	Oxidation, disinfection
Inorganic deposits	Citric acid ($C_6H_8O_7$), nitric acid (HNO_3) and hydrochloric acid (HCl)	Acids	Solubilisation

2.6.4 Air Scouring

2.6.4.1 Air scouring mechanisms

Air scouring is widely employed for fouling reduction in membrane systems. In tubular membranes air is introduced into the membrane tubes. Bubbles scour the membrane surface reducing foulant buildup and removing foulants.

In capillary and hollow fibre systems air is introduced on the outside of the membranes. The mechanism by which air scouring reduces fouling is more complex. Air scouring during permeation provides hydraulic surface shearing, causing membrane lateral motion/movement, and reduces the ability of foulants to stick to and accumulate on the membrane surface (Gao, et al., 2011). A buoyancy force moves the bubble upwards causing a secondary movement behind the bubble, referred to as fluid generated wake, which enhances the reduction of fouling (Cui, et al., 2003).

The effectiveness of air scouring is heavily dependent on the frequency of air scouring (i.e. continuous versus intermittent), the air scouring rate, and the size and direction of the bubbles. (Tian, et al., 2011). The shape and size of the bubble formed depends on the air scouring rate and the sparger pore size (Lu, et al., 2008). A lower rate of membrane fouling is achieved by more fibre movement, and the membrane movement is influenced by fibre looseness, higher gas velocity, raw water viscosity and raw water solids concentration (Lu, et al., 2008).

Air scouring is a major contributor to the energy costs of membrane systems. Hence it is desirable to operate at low air flowrates, and preferably with intermittent rather than continuous air scouring, to reduce operating costs. Accordingly, much research has been undertaken into ‘air scouring regimes’, i.e. how the the combination of air scouring flowrate, air scouring frequency, and sparger geometry affects the fouling rate.

In low-pressure membrane systems for drinking water production, air scouring is usually combined with coagulation as a chemical pretreatment (Singh, 2015). Various studies reported in the literature are discussed in the next section.

2.6.4.2 Low-pressure membrane fouling control using air scouring and chemical pre-treatment

Lu et al., 2008 investigated the effects of air scouring rate, bubble sizes and bubble flow characteristics on fouling using a PVDF submerged hollow fibreMF membrane. The membrane flux remained constant at 36 LMH. The investigated air scouring rateswere 50 ml/min, 80 ml/min, 110 ml/min and 150 ml/min. Spargers with orifice sizes of 1mm, 3mm, and 12mm controlled the bubble sizes and flow characteristics. The experiments used two synthetic raw waters prepared from yeast, with concentrations of 3 g/l and 5 g/l respectively.

The study concluded that the effectiveness of membrane fouling control does not depend only on the air scouring rate andthe bubble size and flow characteristics, but that the raw water quality influences the air scouring rate and bubble size required for the membrane fouling mitigation.

Lok et al., 2017 investigated the effect of air scouring during permeation and pre-treatment by coagulant addition on membrane fouling and NOM removal ata pilot-scale level using asubmerged hollow fibreUF membrane (ZW1000, GE Water and Process Technology). The study was conducted in Canada using Barrie surface water. The pilot plant was fully automated and operated at a constant flux between 37 and 49 LMH with 4 mg/l polyaluminiumchloride (PACl) as the coagulant and two hours (hr) filtration run time. The air scouring regime was varied as follows:

i. No air scouring for the first 60 min of each filtration run time, and air scouring applied for the last 60 min of the filtrationrun time.

ii. No air scouring for the first 10 min of filtration run time,and air scouring applied for the last 110 min of the filtration run time.

iii. Intermittent air scouring with 10 s on followed by 10 s off for the duration of filtration

iv. PACl applied for the first 60 min of the filtration run time,and no PACl in the last 60 min of the filtration run time.

v. PACl applied for the first 10 min of the filtration run time, andno PACl applied for the last 110 min of the filtration run time.

The outcomes of the investigation indicated that:

i. There was no significant difference on membrane fouling rate when the pilot plant operated at the intermittent air scouring frequencies of 60 minand 10 min.

ii. The intermittent air scouring of 10 s followed by 10 s off, and the air scouring rates of 5 and 20 l/min had similar membrane fouling rate.

iii. The addition of PACl for the first 60 min of the filtrationcycle did not affect the rate of membrane fouling when compared to thecontinuous PACl addition.

iv. The NOM removal at different PACl addition and periodic air scouring was similar to the continuous air scouring and PACl addition.

Park & Kim, 2014investigated the effect of pre-treatment by coagulant addition on the rate of membrane fouling using Han River supplying KW water treatment plant, Hanam in South Korea. The raw water turbidity ranged between 10 NTU and 46 NTU. The submerged PVDF hollow fibre membrane module SB module supplied by Cheil Industries Inc., South Korea was used for the experiments. The fixed PACl dosage of 2.5 mg/l was applied in all experiments. The outcome of the investigation indicated that the rate of membrane fouling was higher at no coagulation addition as

compared to 2.5 mg/l PACl addition. Therefore, the PACl addition minimised the rate of membrane fouling.

Tian et al., 2010 investigated the effect of air scouring rate and sparger pore size on the rate of membrane fouling, measured as the rate of TMP increase, using river and sand filter effluent. The river water and sand filter effluent had average turbidities of 10 NTU and 2 NTU respectively. The membrane plant used PVDF hollow fibre membranes supplied by Suzhou Litree ultrafiltration membrane Technology Co. Ltd. The continuous air scouring was compared with 1min on / 9 min off periodic air scouring frequency. The air scouring rates investigated were 1, 2.5, 5.0 and 7.5 $m^3/m^2.h$ The air scouring rate was calculated based on the bottom surface area of the raw water tank, not the membrane surface area. The sparger pore sizes investigated were 3.5mm, 5mm, 6.5mm, and 8mm. The TMP increase was used as the rate of membrane fouling.

The outcomes of the investigation were as follows:

i. Continuous air scouring resulted in a slower rate of the TMP increase compared to the 1 min on and 9 min off periodic air scouring at the same air scouring rates of $1.0m^3/m^2$. h., $2.5m^3/m^2$. h., $5.0m^3/m^2$. h. and 7.5 m^3/m^2. h.

ii. The lowest rate of TMP increase was at 5 $m^3/m^2.h$ air scouring rate. The selection of optimum air scouring rate took into consideration both the rate of TMP increase and the energy consumption.

iii. The 3.5 mm sparger pore resulted in the lowest rate of TMP increase compared with the 5 mm, 6.5 mm and 8 mm sparger pore sizes.

Liu, et al., 2014 evaluated the effect of air scouring rates on membrane fouling and on the flocs formed using UF hollow fibre membranes supplied by Litree Purifying Technology Co., Ltd in China, using Mingyuan lake raw water with aluminium sulfate($Al_2(SO_4)_3$) as a coagulant. The rate of TMP increase was taken as the measure of the membrane fouling. The rawwater turbidity ranged between 1.08NTU – 2.27 NTU. A jar test method was used to determine the dosage of $Al_2(SO_4)_3$ required.Three air scouring rates were investigated, 20 ml/min, 40 ml/min and 60 ml/min. The bench-scale unit operated at a constant flux of 20 LMH with filtration run time of 60 min.

The findings of the investigation indicated the following:

i. At the air scouring rate of 20 ml/min, the rate of TMP increase was slower compared to 40 ml/min and 60 ml/min. The rapid rate of TMP increase was observed at the air scour rate of 60 ml/min.

ii. The higher air scouring rate broke the formed flocs into tiny particles, and these tiny particles plugged the membrane pores through adsorption and pore blocking.

Walsh, et al., 2009 investigated, at bench scale level, the effect of pre-treatment by coagulation and flocculation on NOM removal using a submerged hollow fibre outside-in UF module (ZeeWeedTM 500) from GE Zenon Water and Process Technologies on three raw water sources namely, Lake Major in Dartmouth, Hantsport water treatment plant raw water and Bridgewater water treatment plant raw water in Canada.The parameters varied in the experiments were flocculation hydraulic retention time,amount of coagulant added and frequency of air scouring.

The membrane module had a total surface area of 0.047 m^2 with a nominal pore size of 0.04 µm and a 0.1 µm absolute pore size. The bench-scale membrane unit operated at the constant flux of 38 LMH with the air scouring rate of 10 l/h (equivalent to 0.213 $m^3/m^2.h$) at periodic air scouring of 15 s off 10 min on for the duration of the filtration run. The jar test method determined the amount of required $Al_2(SO_4)_3$ coagulant using DOC and UV_{254} percentage removal. The addition of NaOHadjusted the pH between 6 and 6.2 after the addition of a required amount of $Al_2(SO_4)_3$. The $Al_2(SO_4)_3$ dosages for the Bridgewater source water ranged between 0 mg/l to 30 mg/l, 0 mg/l to 25 mg/l for the Lake Major source water and 0 mg/l to 15 mg/l for Hantsport WTP raw water.The flocculation hydraulic retention times investigated were 0 min, 3 min, 10 min, and 25 min.

The outcome of the study indicated that in all three raw water sources:

i. The addition of different amounts of the aluminium sulphate did not improve the NOM removal irrespective of the flocculation hydraulic retention time.
ii. The periodic air scouring did not improve NOM removal.
iii. The flocculation step had no impact on NOM removal.

Guo, et al., 2018 investigated the effect of inclined plates and cylindrical floc separators installed in the outside-in (O/I) PVDF hollow fibre submerged UF membrane supplied by Litree Purifying Technology Co., Ltd, Hainan in China on final water quality and rate of membrane fouling. The membrane unit operated at constant flux, continuous air scouring with $Al_2(SO_4)_3$ as the coagulant. The quality of the raw water was as follows: temperature, 23.4 °C - 29.9 °C; pH, 8.21-8.95; turbidity, 3.22 NTU–6.98 NTU; UV_{254}, 0.098–0.118 cm^{-1}. After coagulation, turbidity and UV_{254}reduced to 1.47–2.39 NTU and 0.059– 0.068 cm^{-1}, respectively.

The outcomes of this investigation were as follows:

i. The permeate quality was relatively similar for the experiments conducted with inclined plates, cylindrical floc separators and membrane module configuration with no floc separator devices installed.

ii. The membrane configuration without floc separation devices showed a relatively low rate of TMP increase compared to inclined plates and cylindrical floc separation devices.The highest

rate of TMP increase was observed when the cylindrical device was installed as the floc separator.

Xing et al., 2018 evaluated the effects of coagulation, adsorption and sedimentation on the disinfectant demand and fouling rate of the submerged hollow-fibre UF fabricated with the PVC material, supplied by Litree Membrane Technology Co., Ltd. PCl was used as the coagulant. The groundwater located near the Zhujiang River in South China was used as the raw water. The membrane unit operated at a constant flux of 15 LMH with 8 hr filtration run time. The mechanical membrane backwashing was conducted after every filtration run time at 30 LMH flux for 5 min. The investigation compared the following configurations:

i. Pre-treatment with adsorption, coagulation and sedimentation.
ii. Pre-treatment with coagulation and sedimentation.
iii. No pre-treatment.
iv. The disinfectant decay and disinfection by-products formation determined the efficacy of the monochloramine disinfection process.

The characteristics of the ground water were as follows: turbidity, 4.5–33.2 NTU; UV_{254}, 0.025–0.033 cm^{-1}; DOC, 2.9–3.4 mg/L; pH, 6.95–7.54; NH_4-N, 0.15–0.50 mg/L; and temperature, 23.9–28.3 °C. Hongsheng PAC Co., Ltd. In Dongguan, China supplied PAC with the following characteristics: iodine value, 800 mg/g; methylene blue value, 146 mg/g; average particle size, 52.0 μm; average pore size, 1.18 nm; and Brunauer, Emmett, and Teller (BET) surface area, 576.4 m^2/g.

The outcomes of the study were as follows:

i. The rate of TMP increasedrapidly for the PACl and PAC pre-treatment.
ii. The pre-treatment with coagulation and sedimentation resulted in a lower rate of TMP increase compared to the PAC PCland sedimentation.
iii. The highest disinfectant demand was observed when the raw water was not pre-treated prior to the UF membrane system.
iv. Adsorption, coagulation and sedimentation pre-treatment process resulted in the lowest disinfectant demand.

Yu et al., 2013 investigated the effects of the application of the non-ionic polyacrylamide (PAM) as the coagulant aid to $Al_2(SO_4)_3$ on the rate of membrane fouling. Submerged hollow-fibre UF frabricated from the PVDF material was used for the study. The membrane module was supplied by Tianjin Motimo Membrane Technology Co., Ltd. The rate of the TMP increase was used to measure of the rate of membrane fouling. The jar testing method determined the dosages of $Al_2(SO_4)_3$and

PAM employed on the membrane. The membrane unit operated at continuous$Al_2(SO_4)_3$ dosage with 0 mg/l, 0.2 mg/l and 1 mg/l PAM dosage at a delayed time of 0 min, 1 min, 6 min, and 11 after $Al_2(SO_4)_3$ addition. The Malvern Mastersizer 200 laser diffraction instrument measured the size of flocs formed at different dosages.The bench UF unit operated at the constant flux of 20 LMH and the filtration run time 30 min.The UF membrane was backwashed at 40 LMH for 1 min after every filtration cycle.

The outcomes of the investigation were as follows:

i. The addition of PAM before UF reduced the rate of membrane fouling. The PAM promoted agglomeration of the flocs from pin flocs to macroflocs that were easily sieved by the UF membrane.

ii. The 0.2 mg/l of PAM dosage and 6 min dosage delay resulted in a steady increase in the rate of TMP increase.

iii. Higher dosage of PAM (1 mg/l) rapidly increased the rate of TMP increase. The excess PAM blinded the membrane pores resulting in the rapid increase of the TMP

2.6.4.3 Summary

Air scouring in combination with pre-coagulation can be very effective in reducing the rate of fouling. However, there are no general guidelines regarding the optimal coagulant dose and air scouring regime. These are very dependant on the membrane type, the membrane module construction, the sparger design, and the specific characteristics of the raw water investigated.

2.7 Membrane equations

In low-pressure membrane processes, the membrane skin acts as the physical barrier to suspended and colloidal impurities and these impurities remain on the raw water side of the membrane (AWWA, 2016). The membrane skin retains all particles greater than the membrane pore sizes and some smaller particles (Ang & Mohamma, 2015). The permeability (K) and driving force (pressure, ΔP(TMP)) of the membrane determine the permeate flow through the membrane (Zirehpour & Rahimpour, 2016).

The permeate flowing through a membrane (Q, m^3/h or L/h) is directly proportional to (Lee et al., 2012; Guigui et al., 2001 and Glucina et al., 1998):

i. The difference in raw water and permeate pressure (TMP) ΔP

(1 bar = 100kPa = 1kg. $m^{-1}.s^{-2}$)

i. The membrane surface area A

ii. The permeability of the membrane K

The relationship is shown in equation 2-6

$$\mathbf{Q = AK\Delta P} \qquad \text{Equation (2-6)}$$

The membrane flux (J) is the quantity of water passing through a unit area of membrane per time (Liu et al., 2014 and Judd et al., 2011) The SI unit for membrane flux is $m^3/m^2.h$ or $L/m^2.h$ (referred to as LMH).

$$J = \frac{Q}{A} \qquad \text{Equation (2-7)}$$

Substituting Q in equation 2-6 into equation 2-7

$$J = \frac{Q}{A} = K\Delta P \qquad \text{Equation (2-8)}$$

The membrane resistance (R) is a more frequently used term in the membrane terminology compared to the membrane permeability(K). The R is the reciprocal of the K.

$$K = \frac{1}{\mu x R}$$

$$J = K\Delta P = \frac{\Delta P}{\mu R} \qquad \text{Equation (2-9)}$$

Where μ is the dynamic viscosity ($kg.m^{-1}.\ s^{-1}$)

R is the total resistance (m^{-1})

The membrane resistance comprises:

i. The resistance of the membrane (R_m)

ii. The resistance due to particle deposited inside the pore or blocking the pore entry causing irreversible adsorption and pore blocking (R_{ir})

iii. The membrane resistance due to particles forming a cake(R_r), reversible

The total resistance in an operating membrane is the sum of the hydraulic resistance of the membrane itself and all resistances that cause flux decline due to pore blocking, pore adsorption, cake layer formation and concentration polarisation (Xing et al., 2018; Ao et al., 2016; Nguyen, 2012 and Guigui et al., 2001).

$$R = R_m + R_{ir} + R_r \qquad \text{Equation (2-10)}$$

The total resistance (R) was in equation 2-9 was substituted with equation 2-10.

$$J = \frac{\Delta P}{\mu(Rm + Rir + Rr)} \qquad \text{Equation (2-11)}$$

The measured flux is inversely related to the viscosity, and viscosity is a strong function of temperature (Table 2-7). A normalised membrane flux can be calculated using equation 2-12 (Zirehpour & Rahimpour, 2016):

$$J_T = J_t \ 1.024^{T-t}$$ Equation (2-12)

Where T = correction temperature (°C)

t = environmental temperature (°C)

Table 2-7 shows water viscocity at different temperatures.

Table 2-7: Water viscosity at temperature for the atmospheric pressure (AWWA, 2011)

Temperature, T (°C)	**Viscosity, centipoise (cP)** *(1cP = 1.00 x 10^{-3} $kg.m^{-1}.\ s^{-1}$)*
0	1.793
5	1.521
10	1.307
15	1.135
20	1.002
25	0.890
30	0.798
35	0.719

In all experiments conducted in this study, the membrane flux was corrected to 20^0C. In this regards, the viscosity (μ) used was 1.002*cP*:

Equation 2-11 was rearranged and R made the subject of the equation:

$$R = (R_m + R_{ir} + R_r) = \frac{\Delta P}{1.002 \times J_T}$$ Equation (2-13)

To determine the total resistance (R), flux was calculated and transmembrane pressure were recorded for the duration of the filtration period. The normalised flux was calculated using equation 2-12. The instantaneous total resistance was calculated using equation 2-13 at specific intervals. Graph of filtration time versus instantaneous membrane resistance was developed. The slope of the graph represented the "rate of membrane resistance increase'. The rate of membrane resistance increase (slope) was used as the measure of the rate of membrane fouling. Figure 2-15 indicates the interpretation of the filtration time versus instantaneous membrane resistance graph.

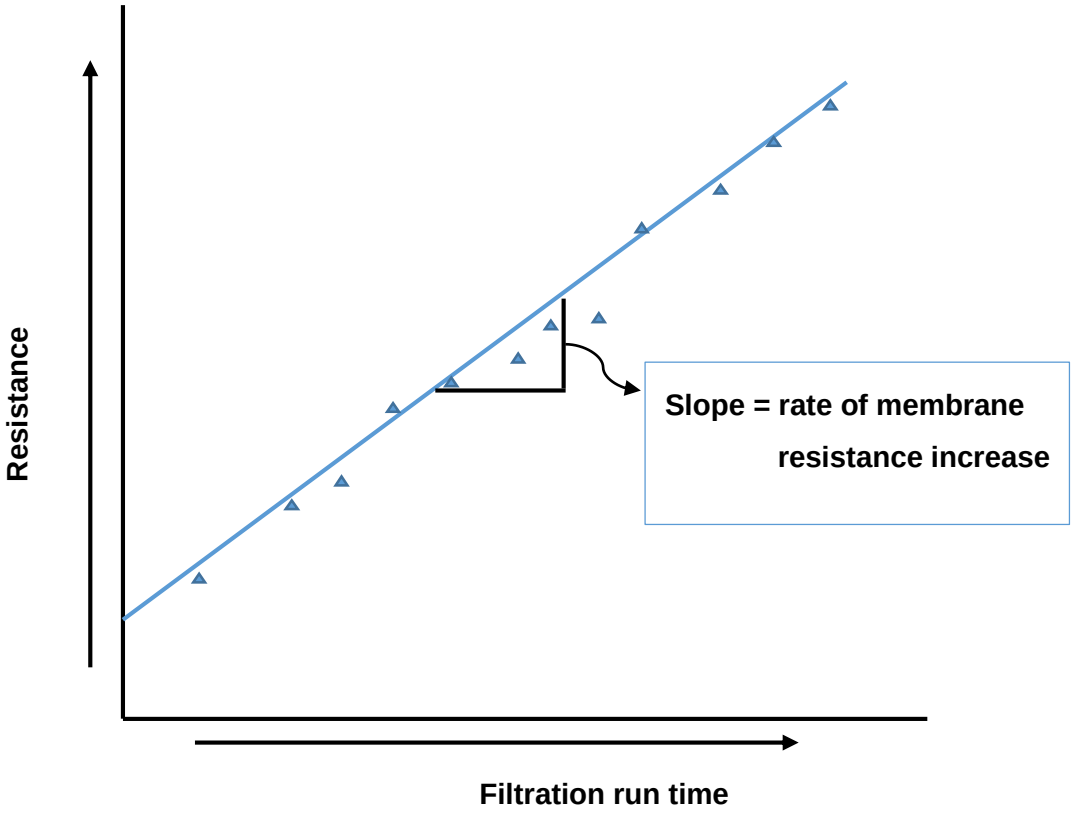

Figure 2-15: Determination of the rate of fouling from resistance plots

2.8 Findings and conclusions of the literature review

- Some of the reported studies used synthetic water to measure the membrane performance on final water quality and the rate of membrane fouling. The use of the synthetic water to measure membrane performance may produce results that may be misleading and practically not implementable.
- The raw water with turbidity of less 10 NTU was used in most of the reviewed literature on the low pressure membrane performance. The performance of the membrane on raw waters with turbidty greater than 20 NTU was not well documented.
- The mostly reported membrane fouling mitigating strategy was the use of coagulants as pre-treatment. However, there was limited information on the criterion for the selection of the appropriate coagulant dosages employed to minimise membrane fouling. The inorganic or organic coagulant used as a pre-treatment had similar effects on the rate of membrane fouling. The inorganic or organic coagulant pre-treatment had different effects on final water quality, especially on the removal of the NOM. The inorganic coagulant had superiority in removing NOM compared to the organic coagulant.

- Literature showed that application of oxidants such as PAC as pre-treatment improved permeate quality especially in NOM removal, however, the application of such oxidants increased the rate of membrane fouling.
- Air scouring during permeation was also a frequently used membrane fouling mitigating method. However, in most of the reported studies, water practioners used manufacturers' recommended air scouring rates. The validity of the recommended air scouring was never assessed. Only one study found in literature investigated different air scouring rates. The study concluded that higher air scouring rates increased the rate of membrane fouling.
- The continuous air scouring was reported to be the most effective air scouring frequency method in minimising the rate of membrane fouling. There was limited information on balancing the rate of membrane fouling and energy consumption due to continuous air scouring.
- The one factor at a time (OFAT) was the commonly applied experimental strategy. The OFAT experimentation is not able to study the combined effect of parameters simultaneously and analyse their interrelationship.
- Eventhough submerged and pressurised membrane configurations are available for low-pressure membranes, most of the studies used the submerged membranes configuration and pressurised membranes were rarely investigated.
- The use of PVDF material was observed in most studies followed by the PES.
- The increase in TMP or flux decline was used a the measure of the membrane fouling.

The Vaal Dam raw water had an average turdidty of 56 NTU with minmum and maximum turbidity of 25 NTU and 125 NTU respectively (DWS, 2019). None of the reviewed literature reported raw water with such high turbidity values. The study thus enable the assessment of the effects of raw water with higher turbidity on the rate of membrane fouling and final water quality. The study used design of experment (DoE) strategy on assessing the effects of coagulant dosage, air scouring rate and frequency of air scouring on the rate of membrane fouling and final water quality as opposed to just OFAT. The rate of membrane fouling was assessed using membrane resistance as opposed to either membrane flux or TMP. The membrane resistance takes into consideration both the membrane flux and the TMP as shown in equation 2-13.

CHAPTER 3 EXPERIMENTAL DESIGN

The rate of membrane fouling in a submerged UF system that utilises pre-coagulation and air scouring for fouling control isaffected by various factors, namely:

i. Equipment parameters:- the type of membrane material used, the module design and packing, the air sparger design,

ii. Operating conditions:- the operating flux, the filtration run time, the coagulant used and the coagulant dose, the air scouring rate,the frequency of air scouring, and the backwash regime.

The ultimate aim of this investigation was to identify which operating parameters would reduce membrane fouling and improve the performance of the membrane plant at Rand Water.

While the operating flux of the plant could be varied, it is constrained. The membrane supplier specified a membrane flux operating range which, if exceeded, would invalidate the membrane performance guarantee and warranty of the membrane plant. However, changing the coagulant dosage, air scouring rate and air scouring frequency would not invalidate the membrane performance guarantee and warranty.

On a laboratory scale rig it is feasible to vary the flux. However the effect of flux on fouling is well known and predictable. The rate of deposition of material onto the membrane is given by (flux **x** bulk concentration). Hence as the flux is increased, the rate of fouling increases linearly. However, from the literature survey, the effects of coagulant dosage, air scouring rate and air scouring frequency are very dependant on the raw water type, the particular membrane, and the module and sparger construction, and their effects cannot be easily predicted.

Hence it was decided that this investigation would focus on these parameters, viz. coagulant dose, air scouring rate and air scouring frequency. As these parameters were expected to be highly interactive, it was decided that they should be investigated in a Design of Experiments (DOE) approach. However, and firstly, suitable ranges for these parameters needed to be identified. A One Factor At a Time (OFAT) approach was employed in determining the ranges at which the coagulant addition, air scouring rate and air scouring frequency reduced the rate of membrane fouling.

3.1 Membrane material and geometry

For this investigation, a bench-scale PVDF hollow fibre outside-in submerged UF membrane module (MEMCOR®B40N) supplied by Evoqua Water Technologies, the suppliers of the Rand Water membrane pilot plant, was used. This was specially constructed for this investigation using identical membranes to that of the Rand Water plant.

3.2 Determination of initial ranges/choices for operating parameters

3.2.1 Operating mode – constant flux or constant pressure

The membrane process is generally operated by either keeping the membrane flux or TMPconstant. These operating regimes are only feasible in a fully automated process.

On a laboratory scale rig, it is challenging to operate at a fixed TMP or membrane flux. This would require expensive automation. Continuous manual adjust is not practical, and may result in inconsistent results. In this investigation, it was planned to use a peristaltic pump. Whilst a peristaltic pump is a positive displacement pump, the flowrate tends to decrease as pressure increases. Hence in the laboratory scale rig both the membrane flux and the TMP were allowed to vary with time, and the fouling resistance was calculated from the TMP and flux profiles.

3.2.2 Membrane flux

Whilst the effect of membrane flux on fouling is easily predictable, and was hence not a variable in the investigation, a flux had to be chosen such that significant fouling could be observed in a short period of time.

A flux for the investigations was decided via an OFAT approach, with the starting flux being the operating flux suggested by the suppliers of the Rand Water pilot plant.

3.2.3 Coagulant type and dose

Vaal Dam raw water had average turbidity of 25 NTU, with the minimum and maximum of 23NTU and 35NTU, respectively. The pH ranged between 6.9 and 8.1, with an average of 7.8 and the temperature range between 8 ˚C and 17 ˚C. Previous investigations indicated that a polymeric coagulant was a suitable coagulant than an inorganic coagulant, hence the polymeric coagulant was used as pre-treatment chemical in this study. The appropriate polymeric coagulant dosing range to be used was determined by the jar test method.

3.2.4 Air scouring rate

Submerged hollow fibre UF membranes operate with air scouring during permeation and membrane backwashing. However, the air scouring rate and frequency of air scouring vary from one membrane supplier to another. Water treatment practitioners employing air scouring rates are advised by the membrane manufacturers. Lu, et al., 2008 study showed that the selection of air scouring rate and frequency is also influenced by amongst other parameters, the raw water quality. Therefore, the “one-size-fits-all” approach is not realistic.

The rate of air scouring in low-pressure membrane filtration is influenced by, amongst other parameters, the raw water quality (Koyuncu et al., 2015; Mosqueda-Jimenez, et al., 2008 and Guigui, et al., 2001). The membrane supplier (EVOQUA water technologies) recommended an air scouring

rate between 0.4 -0.6 $m^3/m^2.h$ (Memcor® CS modules). Tian, et al., 2010 investigated the air scouring rates between 1 and 12 $m^3/m^2.h$ on membrane fouling, and the optimum air scouring rate was 5 $m^3/m^2.h$.

Based on the above, the air scouring range selected for this investigation was 0.4 $m^3/m^2.h$ to 12 $m^3/m^2.h$. This range was subsequently investigated and validated.

3.2.5 Air scouring frequency

Air scouring can be applied continuously or intermittently, the latter resulting in a significant saving in energy. Once again, the optimal frequency is highly dependant on the raw water. In this investigation the effect of air scouring frequency was firstly established using a OFAT method, and based on this an air scouring frequency was decided for subsequent investigations.

The appropriate range for the the frequency of air scouring on the rate of membrane fouling was investigated via an OFAT approach, with the following frequency options:- no air scouring (0% air scouring); 15 min off / 5 min on (25% air scouring); 10 min off / 10 min on (50% air scouring); 5 min off / 15 min on (75% air scouring); and continuous air scouring (100% air scouring) for the duration of the filtration run time. The initial membrane flux was 120 LMH and allowed to decline over time, polymeric coagulant dose and air scour rate were kept constant.

3.2.6 Filtration time

The manufacturers recommended the filtration run time of between 60 min and 90 min. Longer filtration run times may cause the soft deposits accumulated within the membrane pores and on the membrane surface to consolidate into hard deposits resulting in the irreversible membrane fouling.Due to the limited available membrane modules and to avoid the possible permanent membrane fouling and failure, the filtration run time was fixed at 60 min run time for all experiments.

3.2.7 Mechanical backwash regime (pressure and time)

Mechanical membrane backwashing entails reversing the permeate flow to clean membranes from the inside out. The membrane material and configuration influences the backwashing regime. For the membrane used in this study, the manufacturer recommended the maximum backwash pressure of 1 bar for 30 s. Higher backwashing pressures may affect membrane integrity and result in the membrane failure. Due to the limited available membrane modules and to avoid the membrane failure, the membrane backwashing was performed at 1 bar pressure.

3.2.8 Maintenance Clean

To resore membrane module originality, Chemical Enhanced Backwashing (CEBW) was performed by soaking the membrane module in 100 mg/l chlorines soltion for 24 hours every seven days to

provide interim disinfection. Prior to the subsequent experiments, the chlorinated was was drained from the membrane tank and membrane backwashed with permeate water.

Chemical Cleaning in place (CIP) was performed every twenty days by first soaking the membrane module in 2000 mg/l citric solution for 45 min followed by 200 mg/l solutionof chlorine solution for 45 min. The chlorine was used to remove residual residual polymeric coagulant and NOM that may have accumulated on the membrane surface, and citric acid removed inorganic deposits on the membrane surface, refer to Table 2-6. The pure water flux was conducted to determine the membrane restoration

3.3 Combined effects of coagulant addition, air scouring rate and air scouring frequency on membrane performance.

The investigation into the combined effects of the coagulant addition, air scouring rate and the air scouring frequency on the membrane fouling employed a design of experiments (DoE) method. The DoE was employed in order to determine the effect of each factor (coagulant addition, air scouring rate, and air scouring frequency) and the interactions of the factors on the rate of membrane fouling and final water quality.

3.3.1.1 Three-factor – two-levels factorial designof experiment

A three-factors, two-levels DoE method was used to assess the effect of the polymeric coagulant addition, air scouring rate and frequency of scouring on the rate of membrane fouling and final water quality.The two levels (high and low) of each factor were selected from the OFAT validation experiments. These parameters were labelled as follows:

i. Air scouring frequency (A)
ii. Air scour rate (Factor B)
iii. Coagulant addition (C)

The filtration run time was kept constant while the TMP and flux varied.The effect of each factor and the interactions of the factors on the rate of membrane fouling was determined by the rate of membrane resistance increase, as shown in Figure 2-15. Table 3-1 indicates the experimental design of the three factors-two levels DoE. Table 3-2 shows the high and low levels of each factor investigated. The (+) and (-) representing highest and lowest values respectively, notation used in the factorial design DoEreferred to as effect coding (Montgomery, 2013).

Table 3-1: Three factors – two levels (2^3) factorial design and the levels.

Design Run	Parameters			Labels
	Air scour frequency (A)	Air scour rate (B)	Coagulant dose (C)	
1	-	-	-	1
2	+	-	-	a
3	-	+	-	b
4	+	+	-	ab
5	-	-	+	c
6	+	-	+	ac
7	-	+	+	bc
8	+	+	+	abc

Table 3-2: Full factorial DoE and ranges of each parameter.

Factor	Full factorial design with two levels (high(+) and low (-)		
	Factor details	Level	Level values
A	The frequency of air scouring (min)	-	10 min off / 10 min on
		+	Continuous air scouring
B	Air scour rate ($m^3/m^2.h$)	-	1
		+	5
C	Coagulant dosage (mg/l)	-	No coagulant dosage (0)
		+	1

The effect of each factor and factors interactionswere calculated using the rate of membrane resistance increase corresponding to the labels, as shown in Table 3-3.

Table 3-3: Design run for 2^3 full factorial analysis

Design run	Labels	A (Air scour frequency)	B (Air scour rate)	C (Coagulant dose)
1	1	Periodic	1	0
2	A	Continuous	1	0
3	B	Periodic	5	0
4	Ab	Continuous	5	0
5	C	Periodic	1	1
6	Ac	Continuous	1	1
7	Bc	Periodic	5	1
8	abc	Continuous	5	1

The experiments were randomized to avoid nuisance factors.

Astatistical analysiswas used to calculate themain effects of coagulant dosage (C), air scouring rate (B), the frequency of air scouring (A), and theinteractions of the factors on the rate of membrane fouling (Appendix 16).

CHAPTER 4 EXPERIMENTAL EQUIPMENT AND METHODOLOGY

4.1 Process and Instrumentation diagram (P&ID) of equipment

Following the literature survey, and in view of the Objectives of this project, the main criteria for the laboratory scale experimental rig were was follows:

i. The rig should have pre-coagulation followed by membrane filtration;
ii. The permeate flux, filtration time, coagulant dose, air scouring rate, and air scouring frequency should be varied independently.

The bench-scale submerged UF membrane unit was designed and constructed such that the coagulant dosing, air scouring rate and the frequency of air scouring could be independently varied. Figure 4-1 shows the process and instrumentation diagram (P&ID) of the bench-scale submerged UF membrane unit,and Figure 4-2 is the labelled image of the bench-scale submerged UF plant.

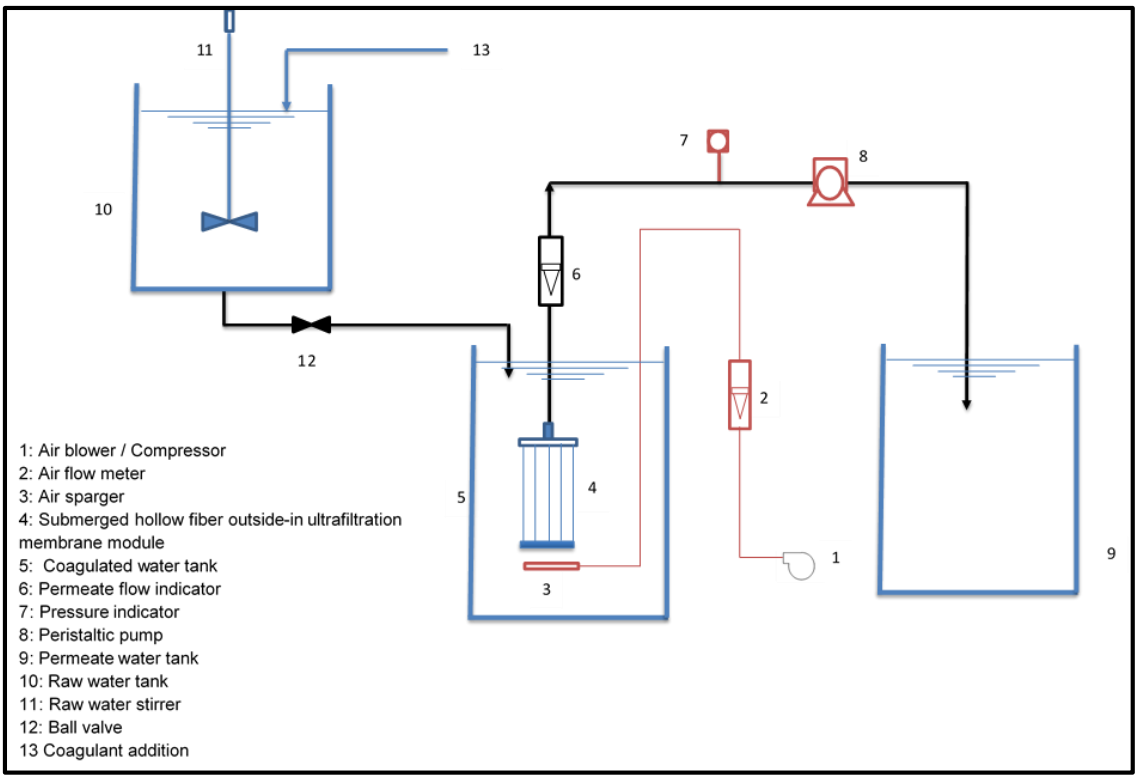

Figure 4-1: P&IDof the bench-scale submerged hollow fibreUF membrane unit

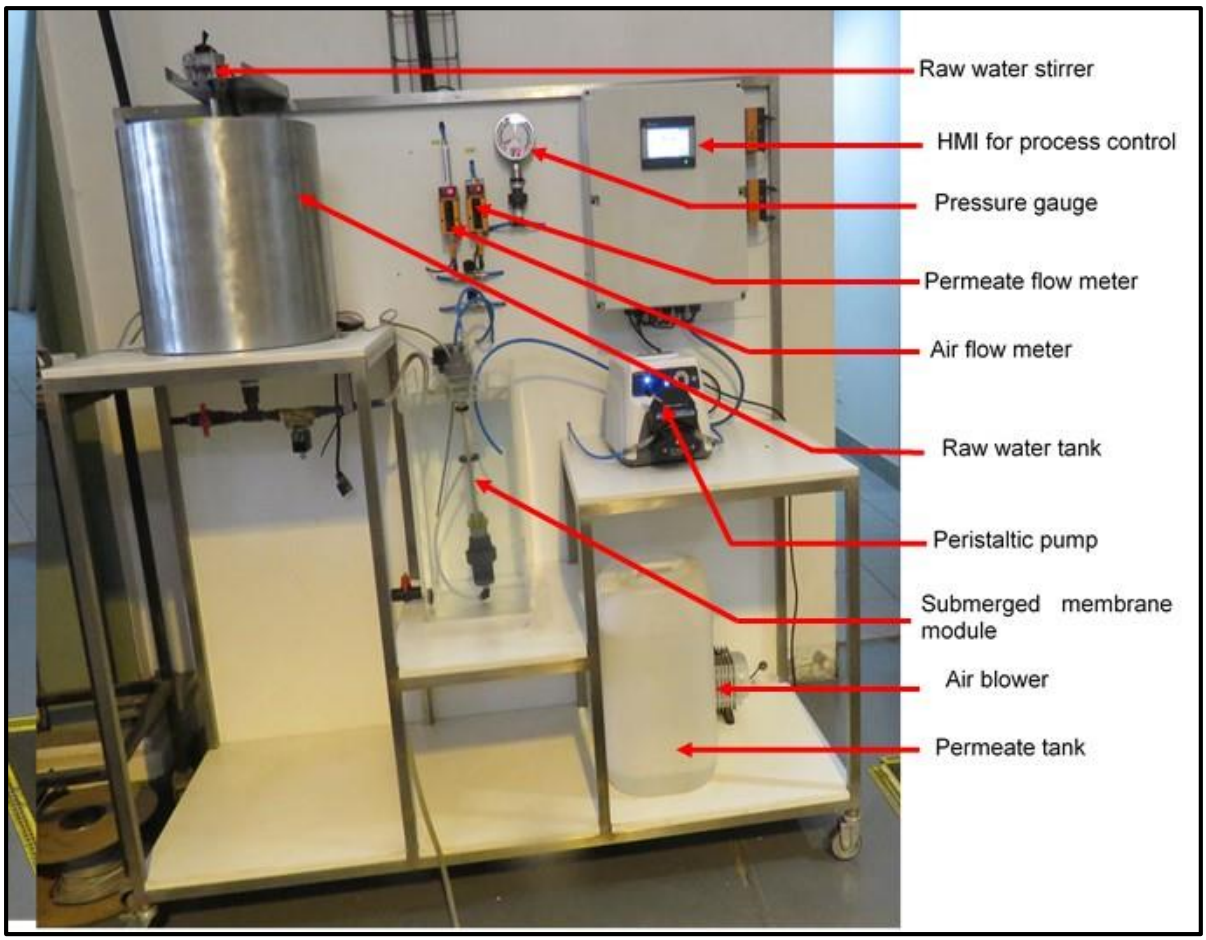

Figure 4-2: Image of the bench-scalesubmerged PVDF hollow fibre outside-inUF membrane unit.

4.2 Equipment List

4.2.1 Raw water tank mixing system and feed water

The cylindrical raw water tank was made of stainless steel with an internal diameter of 40 cm and a height of 40 cm. The total tank volume was 50 l. The raw water tank was fitted with a fixed speed mechanical stirrer for mixing the raw water with the polymeric coagulant. The stirrer was connected to the Delta DOP 4.3-inch Human Machine Interface (HMI) touch screen to control the bench-scale UF unit. The stirrer was synchronized with an actuated ball valve situated at the bottom of the raw water tank to allow coagulated water to gravitate into the membrane tank.

4.2.2 Membrane tank

The membrane tank was made of transparent acrylic perspex material with a length, breadth, and the height of 35 cm, 35 cm, and 50 cm respectively. The total volume of the membrane tank was 60 l. The membrane module support was glued at the height of 45 cm from the bottom of the tank on opposite sides of the tank to keep the module in position and upright. The active membrane tank volume was 55 l. A drain tap was installed at the bottom of the membrane tank.

4.2.3 Membrane module

EVOQUA Water Technologies supplied the membrane module. The membrane module consisted of 50 PVDF hollow UF fibres. Each fibre had an inner and outer diameter: 0.65mm and 1.3 mm respectively with a height of 250mm. As per the membrane supplier information, the pore size range was 0.04 µm to 0.1 µm. The filtration direction was outside-in. Each fibre had the surface area of 0.00102 m^2, and the membrane module had the total surface area of 0.051 m^2. The end blocks of the membrane module were made up of polyurethane material.The membrane module specification, as provided by the manufacturer, is shown in Table 4-1. Figure 4-3 is the image of the membrane module.

Table 4-1: Hollow fibre PVDF outside-in submerged ultrafiltration membrane manufacturer's design specification

Design flux range (LMH)	25 – 45
Operating temperature (°C)	5 – 35
pH range	2 – 10

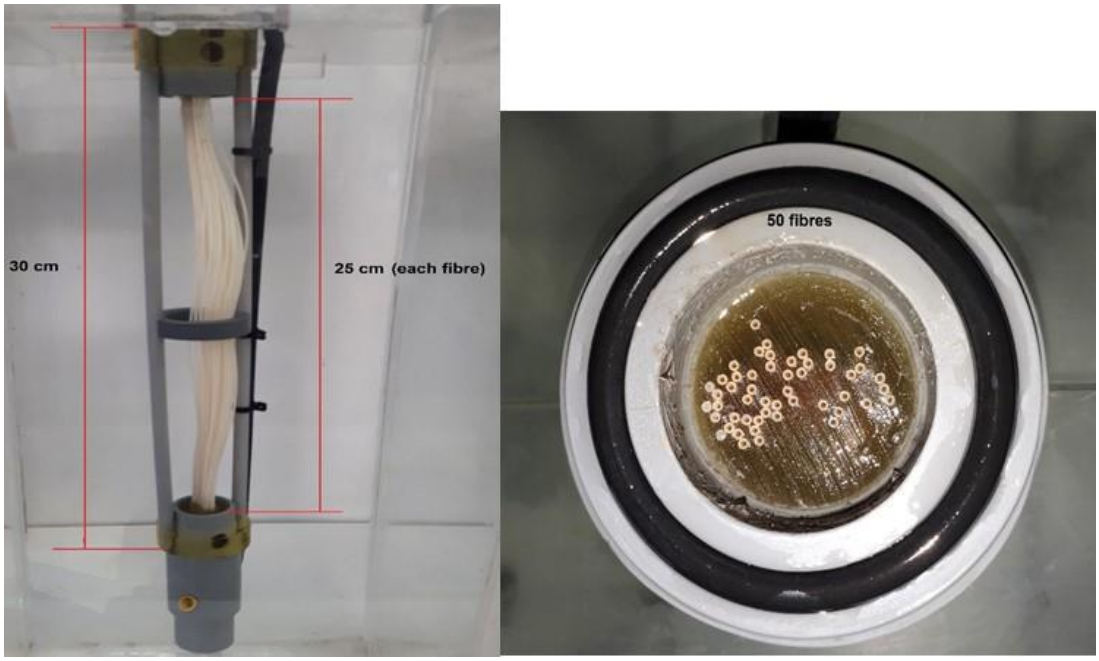

Figure 4-3: Left: Membrane module, Right: membrane fibrespotted into an end block using polyurethane material

4.2.4 Permeate suction pump

The Cole Parmer MasterFlex peristaltic pump with Easy Bond II head was used to pull the permeate from the membrane module gently. The Easy Bond II head takes 15 mm,24 mm,35 mm, and 36mm tubing. The speed of the Easy Bond II head ranged from 0 to 600 revolutions per minute (RPM). For

the experiments, the 15 mm diameter Tygontube was used to pull the permeate out of the membrane module gently.The peristaltic pump operating range was 1l/h to 65 l/h.

4.2.5 Permeate tank

The permeate tank wasa25 l clear plastic container.

4.2.6 Piping

Flexible PVC blue piping was used on the bench scale submerged UF unit. The quick-release couplings and associated fittings were used to connect the flexible PVC pipes where required. The flexible PVC pipe had internal and external diameters of 5 mm and 10 mm, respectively.

4.3 Process monitoring equipment

4.3.1 Air scour rate

The air flow rate was measured with a IFM SD 5000 gas flow meter. The operating rangewas 1 l/min to 250 l/min with 1% uncetrainity.

4.3.2 Permeate flow rate

The permeate flow rate was measured witha IFM SQ 0500 water flow meter. The operating rangewas 1ml/min to 200 ml/min with 1% uncentainity.

4.3.3 Pressure

The TMP was measured withthe IFM PG2454 electronic manometer. The pressure gauge operating was -1 bar to 10 bars with 1% uncertanity.

4.3.4 Ancillary equipment

The bench-scale UF membrane unit operation was controlled using the DeltaDOP 4.3-inch HMI. The polymeric coagulant / raw water stirring duration, peristaltic pump speed,filtration run time, airscouring frequency, air scouring mode (continuous/periodic) and membrane backwashing were all controlled using the HMI. The air scouring rate was manually adjustedusing the needle valve.

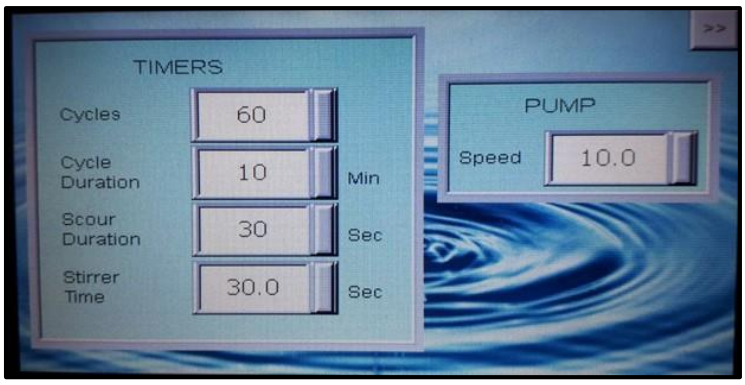

Figure 4-4: Filtration run time operation input screen

Figure 4-4 shows the filtration run-time,the filtration duration in 60 cycles representing 60 min filtration run time.The cycle duration and scour duration were synchronised. The cycle duration was the blocking of the air scouring frequency, and the scour duration was the air scouring duration within a specified block.In Figure 4-4 air scouring was blocked into 10 min and within the 10 min block air scouring was active in the last 30 s of the block, i.e. the air scouring initiated from 9 min 30 s until 10 min. At 19 min 30 s air scouring initiated again and stopped at 20 min, etc. for the duration of filtration run time.

The stirrer time referred to the duration the stirrer ran to mix the polymeric coagulant added with raw water. The stirrer ran for the set mixing duration. Upon the lapsing of the mixing duration, the stirrer stopped, the actuated ball valve opened, and the coagulated water gravitated into the membrane tank. The conductivity sensor was installed and synchronised with the actuated valve to prevent water from overflowing in the membrane tank.

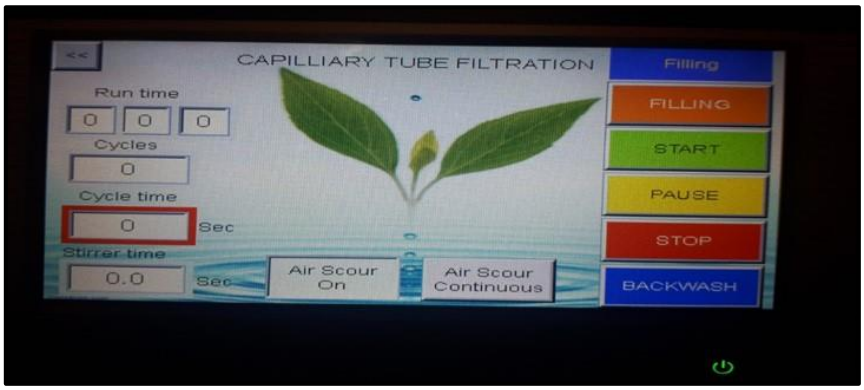

Figure 4-5: HMI process initiation and monitoring screen

Figure 4-5 shows the main screen of the HMI, the arrow on the left corner of the main screen was used to move fromone page to another. The filtration, air scouring, and backwashing were initiated and terminated from the main screen.

4.4 Bench scale UF membrane operating methodology

The methodology describes step-by-step instructions of the operation of the bench-scale submerged ultrafiltration system.

I. CYCLES was set to 60 to give a filtration of 60 min (Figure 4-4)
II. For the periodic air scouring, the CYCLE DURATION was set to 20 min, AIR SCOUR DURATION was set to 60 (Figure 4-4).
III. The STIRRER TIME was set to mix for 90 s (Figure 4-4).
IV. The PUMP speed was set at 12 to achieve an initial flux of 120 LMH (Figure 4-4).
V. The deionized water used to soak the membrane module tank was drained out (Figure 5-2).
VI. The raw water was filled into the raw water tank (Figure 4-2).
VII. The FILLING button (see Figure 4-5) was initiated and the stirrer started to rotate and mix raw water.
VIII. The coagulant was added after the first 30 s had elapsed. The coagulant and raw water mixed for 60 s.
IX. The powered actuated valve opened when the 90 s lapsed, the coagulated water gravitated into the empty membrane tank.
X. When the membrane tank was full, (see Figure 4-5) the filtration process was activated by pressing the START button.
XI. The needle next to the airflow meter was manually adjusted to the required airflow rate (see Table 4-5).
XII. The permeate flow rates, pressure readings (in bars), permeate turbidity and water temperature (in ^{o}C) were recorded every 5 min for the duration of the filtration cycle (60 min)
XIII. The remaining coagulated water in the membrane tank was drained out.
XIV. The membrane tank was filled with deionized water
XV. Membrane hydraulic backwash was initiated by pressing the BACKWASHING and START buttons (Figure 4-5). The backwashing was performed at the pressure of 1 bar for 1 min. The peristaltic pump served both purposes of filtration and backwashing.
XVI. The membrane module was then ready for the next experimental run.
XVII. The recorded permeate flow rates were converted into flux (in LMH) as follows: Flux = $\frac{\text{Permeate flow rate } (\frac{\text{mL}}{\text{min}})}{\text{membrane surface area}} \text{ x } \frac{1\text{l}}{1000\text{mL}} \text{ x } \frac{60 \text{ min}}{1\text{h}}$(membrane area = 0.051m^2)
XVIII. The membrane flux was normalised to 20 ^{o}C using equation (2-7).
XIX. The membrane resistance was calculated using equation 2-10. The pressure units were converted from bars to kg.m^{-1}. s^{-2} and the dynamic viscosity units were converted from centipoise (cP) to kg.m^{-1}. s^{-1} The flux units were converted from LMH to m^3.m^{-2}. s^{-1}

XX. The graph of time and the membrane resistance are drawn. The linear trend line was fitted. The results were accepted when the graph correlation coefficient (r^2) was greater than 0.95

XXI. The slope of the graph represented the rate of membrane resistance increase.

4.5 Membrane module characterisation

The membrane module was characterised using Scanning electron microscopy (SEM) fitted with Energy Dispersive X-Ray Spectroscopy (EDS) and Fourier Transform Infrared Spectrometer (FTIR) to determine the microtexture, structure and elemental analysis of the membrane material and deposits that had accumulated on the membrane material.

CHAPTER 5 RESULTS AND DISCUSSION

5.1 Overview

5.2 Characterisation of the UF membrane

Scanning Electron Microscopy (SEM),Energy Dispersive X-Ray Spectroscopy (EDS) and Fourier Transform Infrared Spectrometer (FTIR)techniques were used to characterise the UF membrane, both before and after fouling.

5.2.1 Characteristisation of the virgin membrane

Figure 5-1 below shows the microscopic view of the virgin hollow fibre membrane captured using Joel JSM-IT300 model SEM from Tokyo, Japan. To improved image resolution and avoid surface charging, Quorum Q150RES automatic sputter coater added a 5 nm gold layer to the sample of the membrane fibre surface.

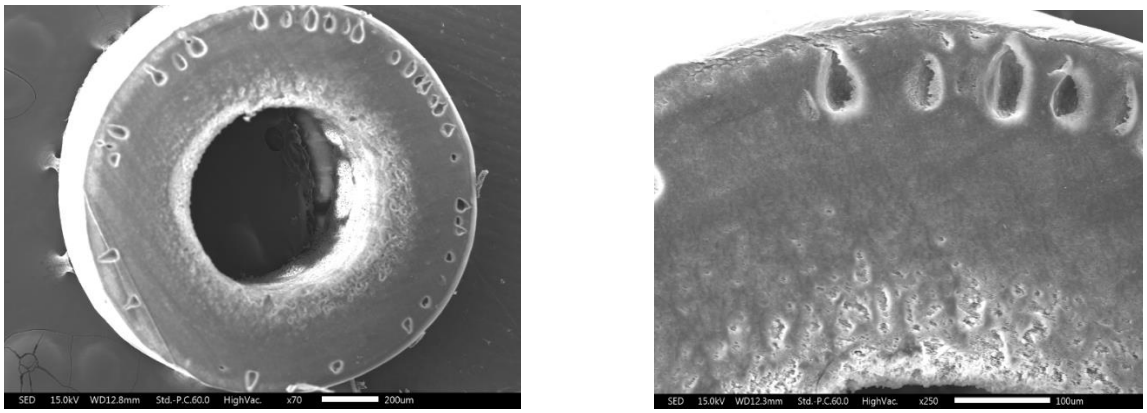

Figure 5-1: Cross-sectional view of the virgin UF membrane developed with SEM.

Figure 5-1 shows the virgin outside-in hollow fibre UF membrane. The membrane skin is the outer surface of the fibre with the supporting layer on the inner part of the fibre.

The EDS characterised the elemental composition of the membrane in terms of the structure and symmetry(Konno, 2016). Figure 5-2 is the EDS cross-section map of the UF membrane fibre.

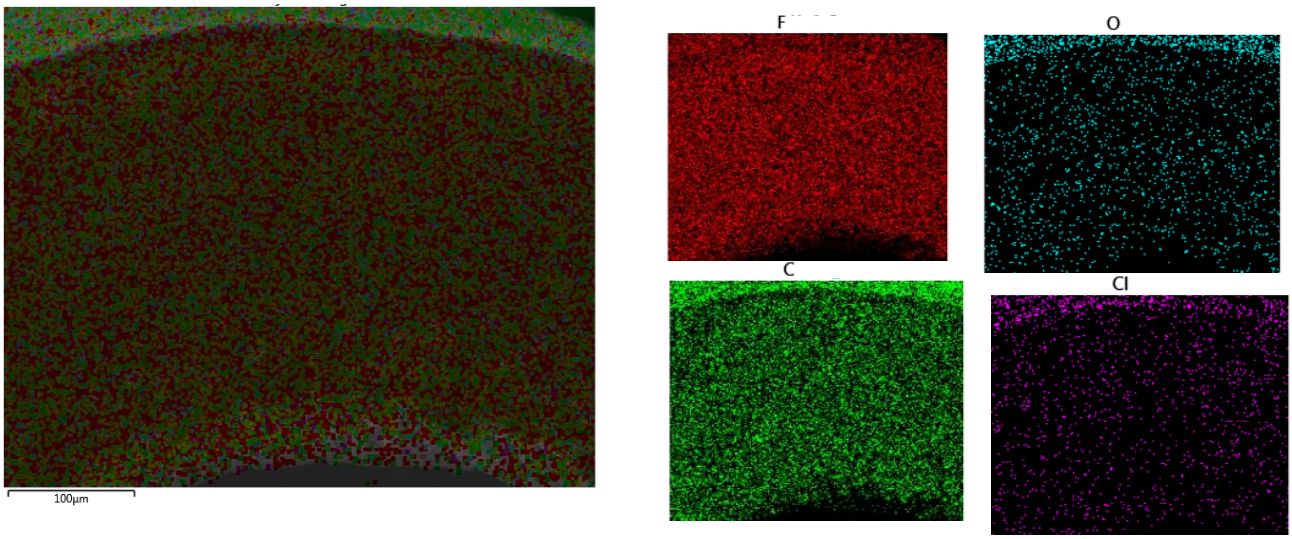

Figure 5-2: Characterisation of the virgin UF membrane using the EDS image.

The EDS characterised the UF membrane by bombarding the surface with an electron beam, the emitted energy characterisingthe elemental composition of the membrane. From Figure 5-2, the picture on the left with different colours indicates the distribution of elements across the membrane. The four pictures on the right with different colours show the distribution of individual elements, F, C, O and Cl. The picture on the far left showed an even spread of colours across the membrane cross-sectional area, indicating that the membrane was a homogeneous structure (symmetric) consisting of Fluoride (F) and Carbon (C) with a trace of Oxygen (O) and Chloride (Cl). Figure 5-3 shows the EDS spectrum for the UF membrane cross-sectional area.

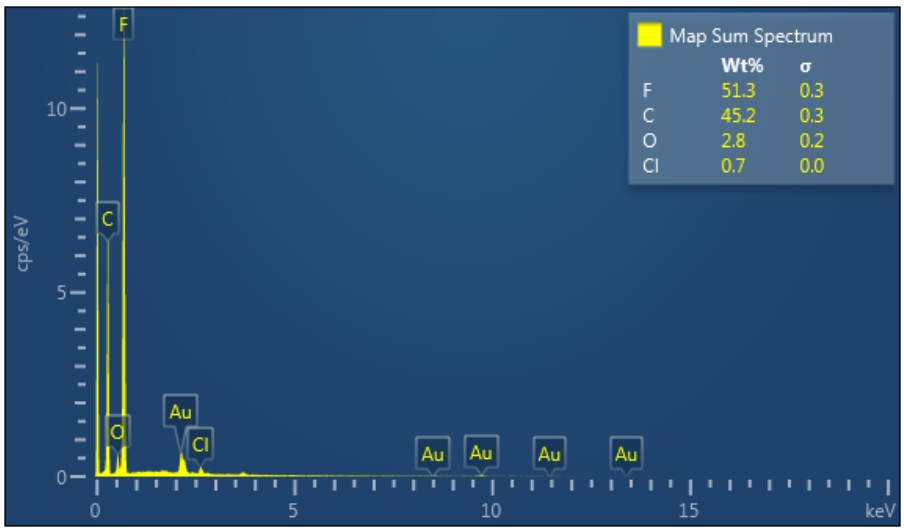

Figure 5-3: EDS spectrum for the virgin UF membrane.

From Figure 5-3, the map sum spectrum indicated that the predominant elements were C and F with O and Cl in trace quantities. The presence of O originates from the wet membrane, and the presence of Cl originates from the soaking solution used to prevent membrane pores from blockage.

A PerkinElmer FTIR fitted with the Attenuated Total Reflectance (ATR) sampling accessory at the spectrum region of between 600 – 4000 cm^{-1} characterised the primary functional groups of the membrane.The advantage of FTIR with spectrum region of between 600 – 4000 cm^{-1} is that it determines both organic and inorganic function group (Bradley, 2015). Figure 5-4 shows the virgin UF membrane IR spectrum.

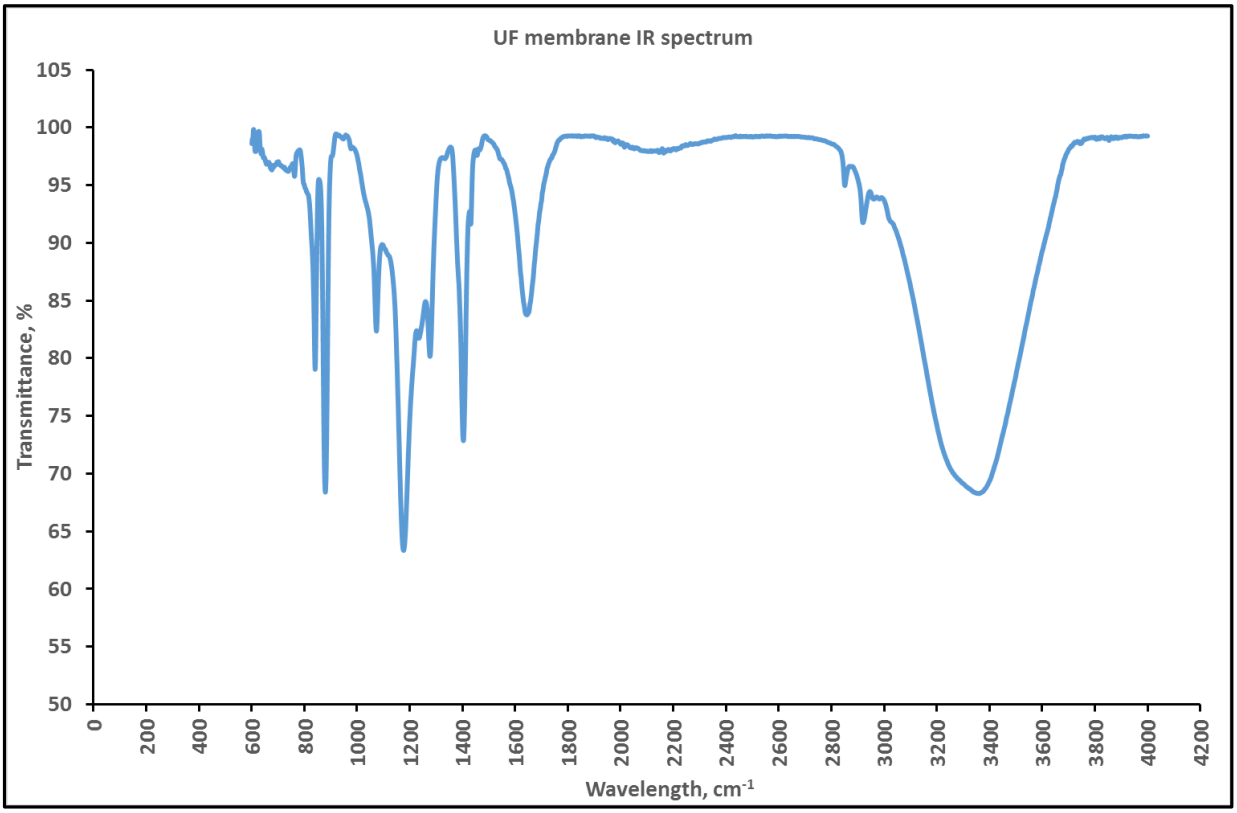

Figure 5-4: Virgin UF membrane IR spectrum

The IR spectra in Appendix 18 and 19 assisted in the interpretation of the functional groups represented in Figure 5-4. The transmittance peak at 3200 cm^{-1} indicated the O-H functional group from the water molecule. The results indicate analysis conducted on a wet virgin membrane fibre. The transmittance peaks between 1400 – 1600 cm^{-1} indicated the presence of C-F functional group. The transmittance peak at between 880 -1180 cm^{-1} indicated the presence of the vinyl/vinylidene functional group.

The information obtained from the EDS and FTIR confirmed the UF membrane was symmetric and fabricated with the PVDF material.

5.2.2 Characterisation of a fouled membrane

Membrane fouling was achieved by filtering untreated Vaal Dam raw water at 120 LMH for 60 min. SEM, EDS and FTIR analyses of a fouled membrane fibre were then conducted. Figure 5-5 shows the EDS of the used membrane.

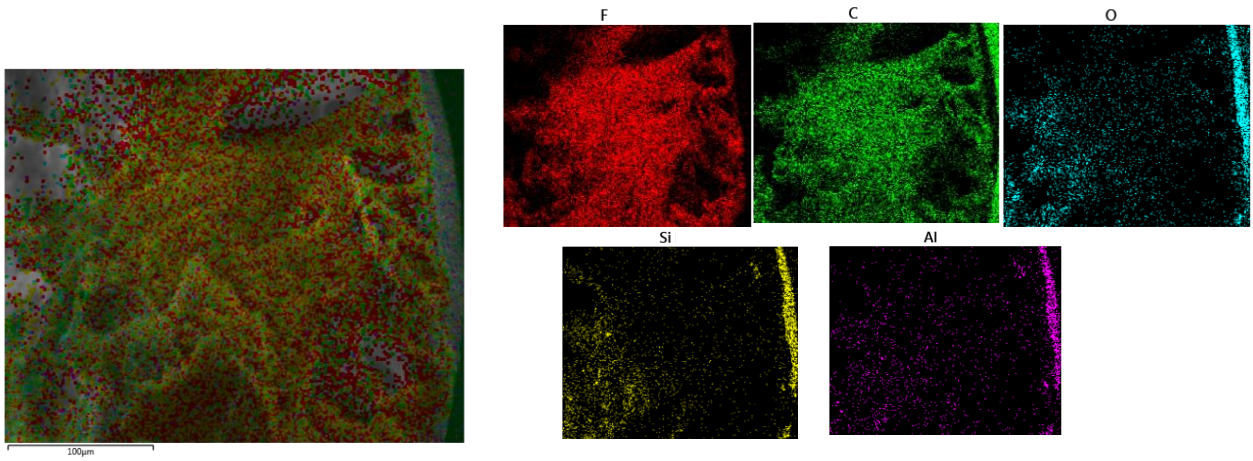

Figure 5-5: EDS image of the used UF membrane

From Figure 5-5, the fouled membrane shows the additional detection of Silica (Si) and Aluminium (Al). The accumulated Si and Al elements were on the membrane surface with some traces on the supporting layer.The presence of Si and Al indicated the foulant comprised of clay particles. Figure 5-6 shows the EDS spectrum for the cross-sectional area of the UF membrane fibre.

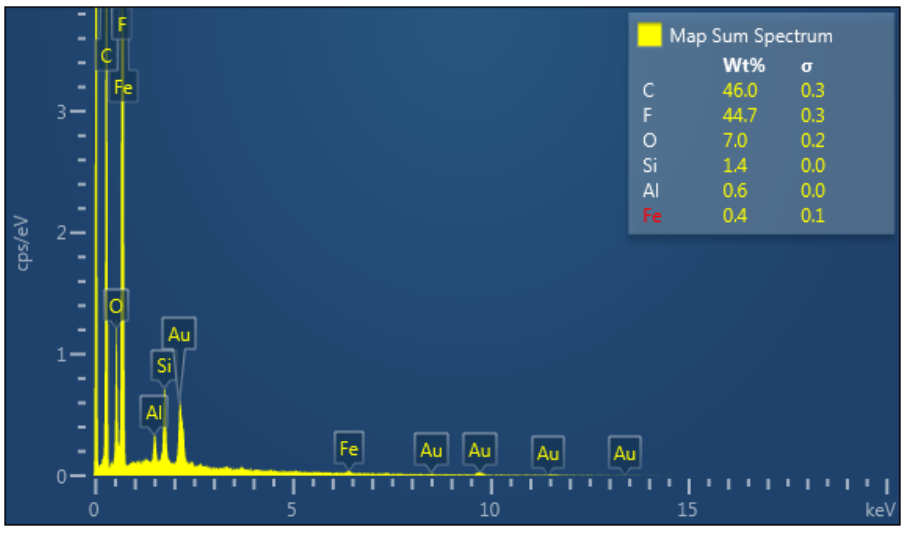

Figure 5-6: EDS spectrum for the cross-sectional area of the used UF membrane.

As expected C and F elements were the highest concentrations with moderate concentrations of Si, Al and traces of iron (Fe). The presence of Si, Al and traces of Fe originated from the foulant

accumulation on the membrane surface . Figure 5-7 compares the IR spectra of the virgin and used UF membrane.

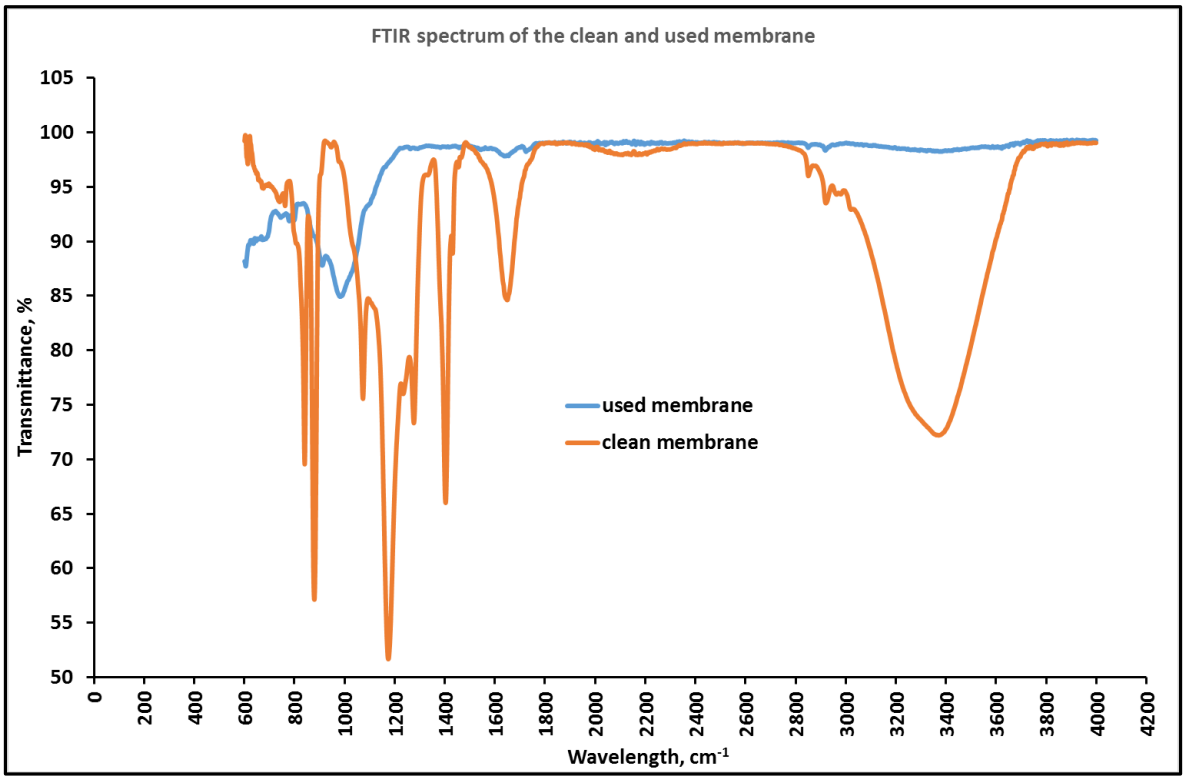

Figure 5-7: IR spectrum of the virgin and used UF membrane

From Figure 5-7, the used membrane had the transmittance peak at 980 cm^{-1} which corresponds to silicates (Povnnennykh, 1978). Figure 5-8 shows the SEM image of the used UF membrane.

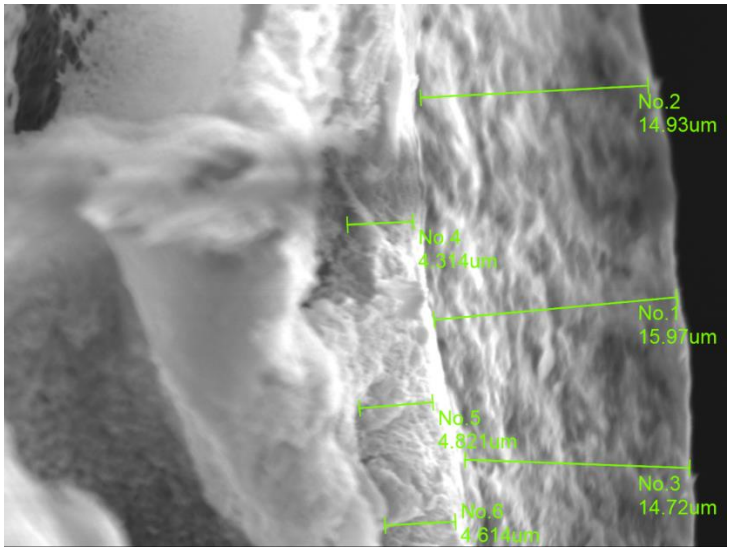

Figure 5-8: SEM Image of the fouled UF membrane

From Figure 5-8, the UF membrane skin had an average thickness of 4.583µm, and the cake thickness was 15.21µm. The cake formed on the membrane surface caused the membrane fouling resulting in a decline in flux and increase in TMP.

5.3 Selection and Validation of Operating Parameters and Air Sparger Geometry

5.3.1 Overview

Fouling of a membrane involves two competing mechanisms, viz. deposition of contaminants onto the membrane, and back transport of material away from the membrane by air scouring. The rate of deposition is directly related to the flux. The rate of back transport is a function of the size of the contaminants, and the size and frequency of the air bubbles. The latter in turn is determined by the air sparger design, the air scour flowrate and the air scour frequency.

The main objective of this study was to determine the combined effects of coagulant pretreatment, air scour rate and air scour frequency on the rate of fouling. It was firstly necessary to ensure that the values and ranges investigated for these parameters would have an impact on the rate of fouling.

Hence, this section focusses on how appropriate ranges and values for these parameters were selected.

5.3.2 Selection and validation of the membrane flux

The manufacturer of the pilot plant specified a maximum flux of 45 LMH. However, in laboratory scale investigations it is convenient to operate at a flux that accelerates the rate of fouling. This is both to emphasise the fouling effect and to enable more investigations to take place in a shorter time.

In preliminary scans in this investigation, it was found that the rate of fouling at 45 LMH was fairly slow. Various higher fluxes were scanned, and eventually a flux of 120 LMH was regarded as being adequate, i.e. it yielded a measurable rate of fouling.

The filtration flux and TMP profiles obtained at 45 LMH and 120 LMH are shown in Figures 5-9 and 5-10 respectively. For these runs there was no precoagulation or air scouring. The repeat runs data is shown in Apendix 7.

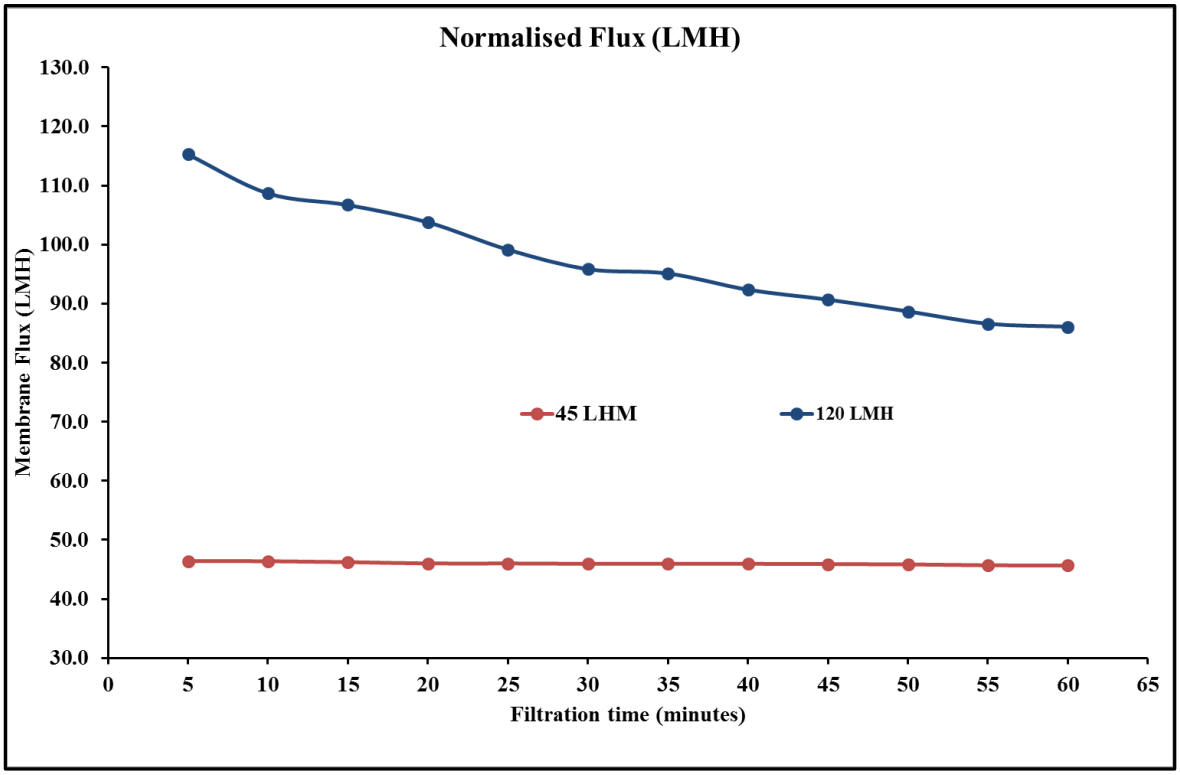

Figure 5-9: Filtration run time versus the initial fluxes of 45LMH and 120 LMH.

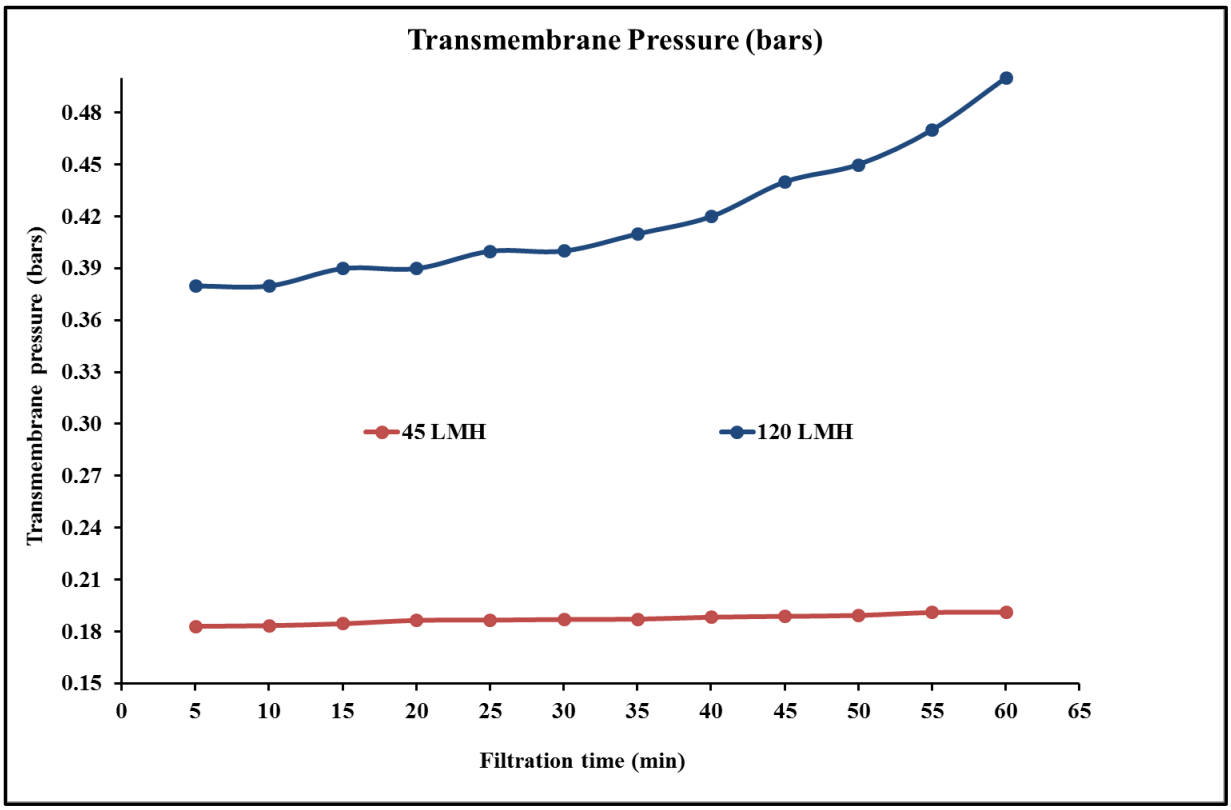

Figure 5-10: Filtration run time versus TMP for the 45LMH and 120 LMH fluxes.

In all investigations in this study, the flux decreased and the TMP increased with time. Hence the system wasn't operating in either a true constant flux or constant TMP modes.

From Figure 5-9, 45 LMH initial flux declined by 1.5%, from 46.6LMH to 45.7LMH, and 120LMH initial flux declined by 25%, from 115.3 LMH to 86.1 LMH. The 120LMH initial flux had a higher rate of membrane flux decline within 60 min of filtration run time relative to 45LMH.

From Figure 5-10, at 45LMH the TMP increased from 0.18 bars to 0.19 bars (6% TMP increase) in 60 minutes' filtration run time. At the 120 LMH operating flux, the transmembrane pressure increased from 0.38 bars to 0.50 bars (32% transmembrane pressure increase) in 60 minutes' filtration run time.The 120 LMH had a higher rate of TMP increase relative to 45LMH.

As discussed in earlier sections, when both the flux and the TMP change with time, the rate of fouling is best obtained from total resistance plots. Figure 5-11 shows the filtration run time versus the calculated membrane resistance using equation 2-13.

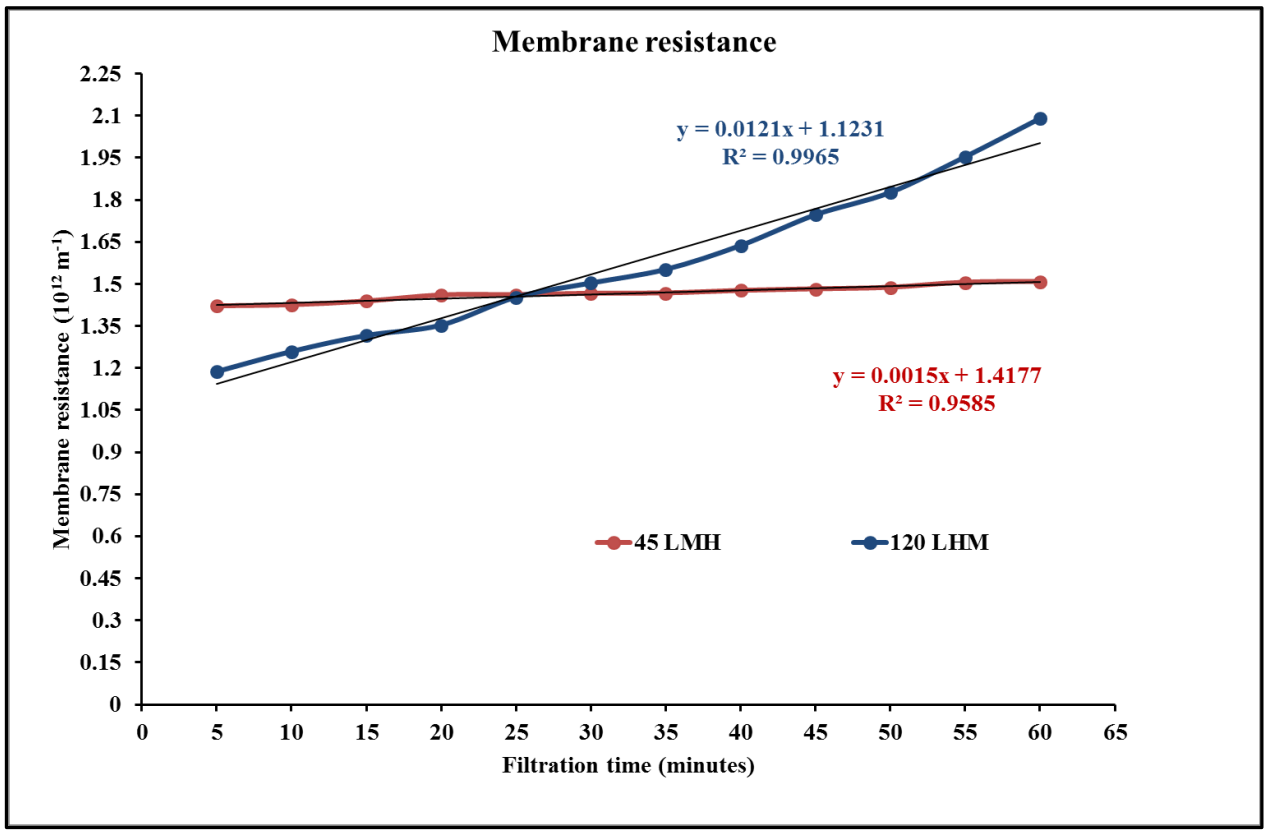

Figure 5-11: Total resistance increase comparison for 45LMH and 120 LMH membrane operating fluxes, filtration time 60 minutes.

From Figure 5-11,at the 45 LMH, the membrane resistance increased from 1.42 x 10^{12} $m^{-1}$to 1.51x 10^{12} m^{-1}(6% increase) in 60 minfiltration run time withtherate of membrane resistance increase(slope)of 0.0015 x $10^{12}m^{-1}$ min^{-1}. At the 120 LMH operating flux, the membrane resistance increased from 1.19 x 10^{12} m^{-1} to 2.1 x 10^{12} m^{-1} (76% membrane resistance increase) in 60 min

filtration run time with the rate of membrane resistance increase of 0.0121 x $10^{12}m^{-1}$ min^{-1}. The rate of membrane resistance increase of 120 LMH was 88% higher than the 45 LMH flux. These results indicated that at 120 LMH, the membrane was fouling 88% faster than the 45 LMH flux. The replicates of these experiments are shown in the appendix 4. For the rest of the investigation a flux of 120 LMH was used.

5.3.3 Selection and Validation of polymeric coagulant dosage

The range of coagulant doses to be investigated on the bench-scale UF unit was obtained fromjar test investigations,following jar test procedure in Appendix 1. The polymeric coagulant dosage investigated in the jar tests ranged from 0 to 50 mg/l. Figure 5.12showsthe effect of dosage on residual turbidity.

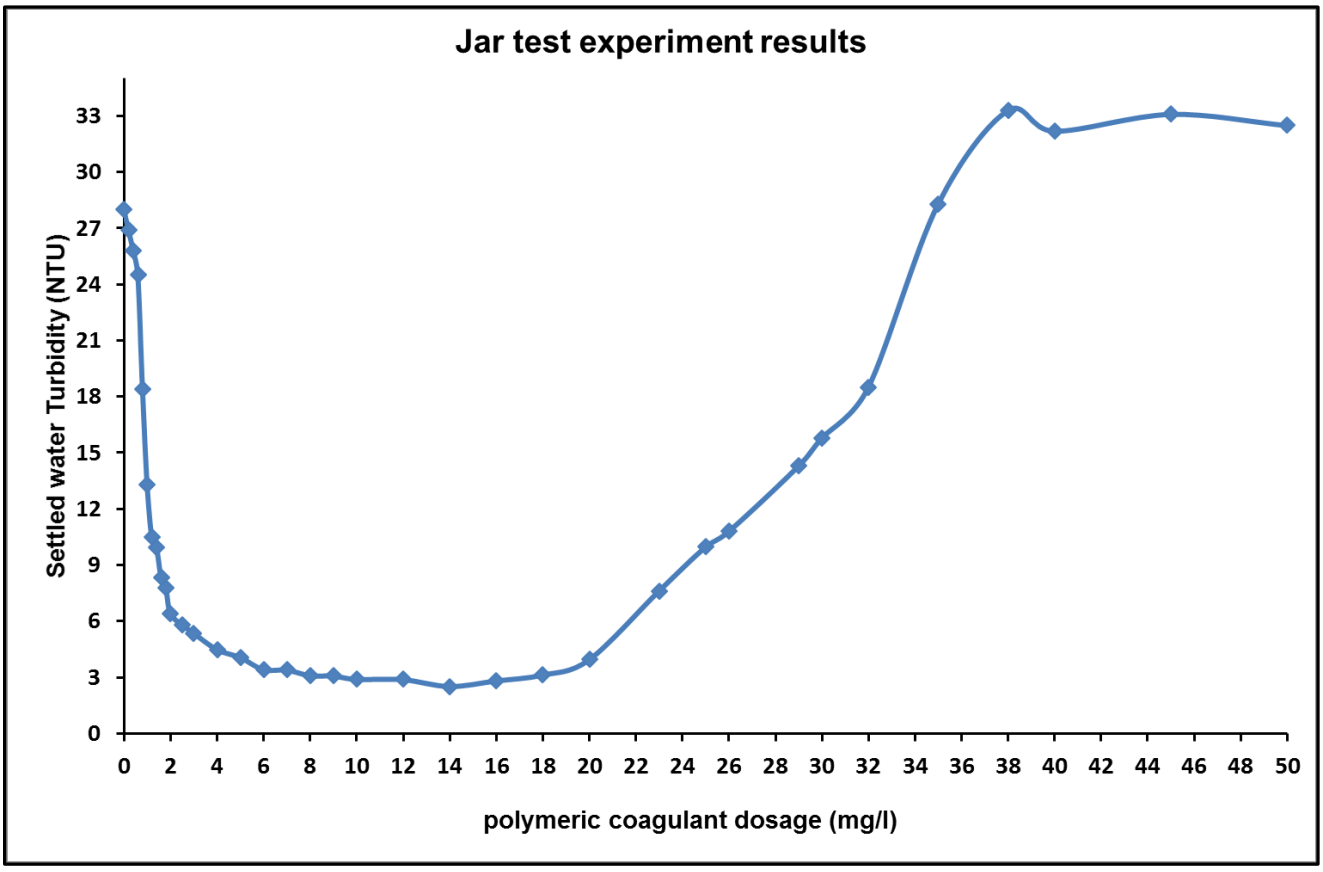

Figure 5-12: Jar test experiment results obtained using Vaal dam raw water.

The jar test investigations were replicated three times, shown in AppendixA.4. The settled water turbidity decreased from 28 NTU to 4 NTU as the polymeric coagulant dosage increased from 0 mg/l to 8 mg/l. The settled was turbidity remained relatively constant at 4 NTU as the polymeric coagulant dosage further increased from 8 mg/l to 18 mg/l polymeric coagulant dosage. The settled water turbidity steadily increased from 4 NTU to 32 NTU as the polymeric coagulant dosage was increased

from 20 mg/l to 32 mg/l. This follows the expected profile in standard jar tests, i.e. a decrease in residual turbidity with increasing dose followed by a subsequent increase at higher dosages.

For the validation on the bench-scale UF unit, three coagulant doses were selected in the region where polymeric coagulant addition resulted in a decrease in settled water turbidity (1 – 8 mg/l) and a further three doses were selected in the region where polymeric coagulant addition increased settled water turbidity (18 – 36 mg/l). The selected coagulant dosages were 0,1,3,8,20,26 and 32 mg/l respectively.

The effects of the coagulant doseson membrane fouling wereinvestigated on the bench-scale UF membrane unit.Runs were conducted at 120 LMH and no air scouring was used. The flux profiles and TMP profiles are shown in Appendix 6. The resistance profiles obtained at the different doses are shown in Figure5-13, and the average rate of resistance increase is shown in Figure 5-14.The error bars were calculated using standard deviation.

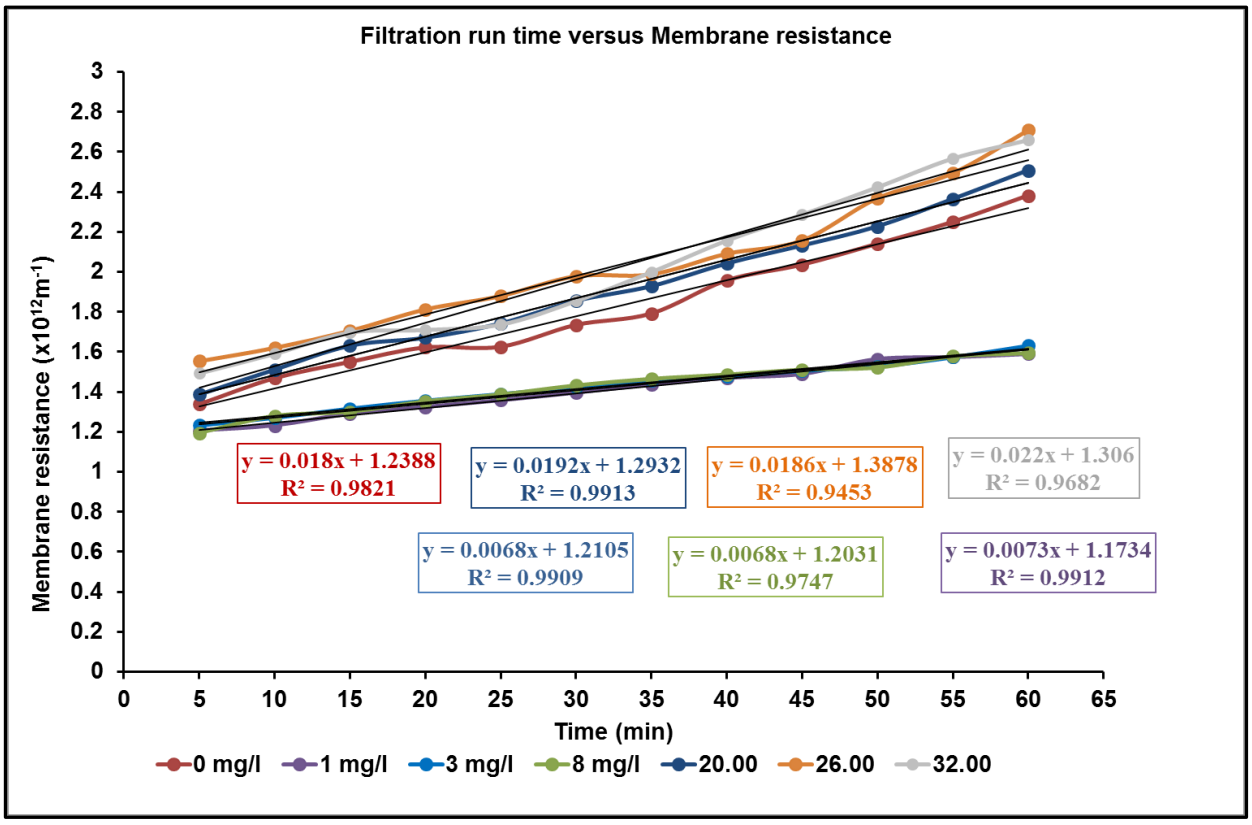

Figure 5-13: Membrane resistance increase at different coagulant dosage

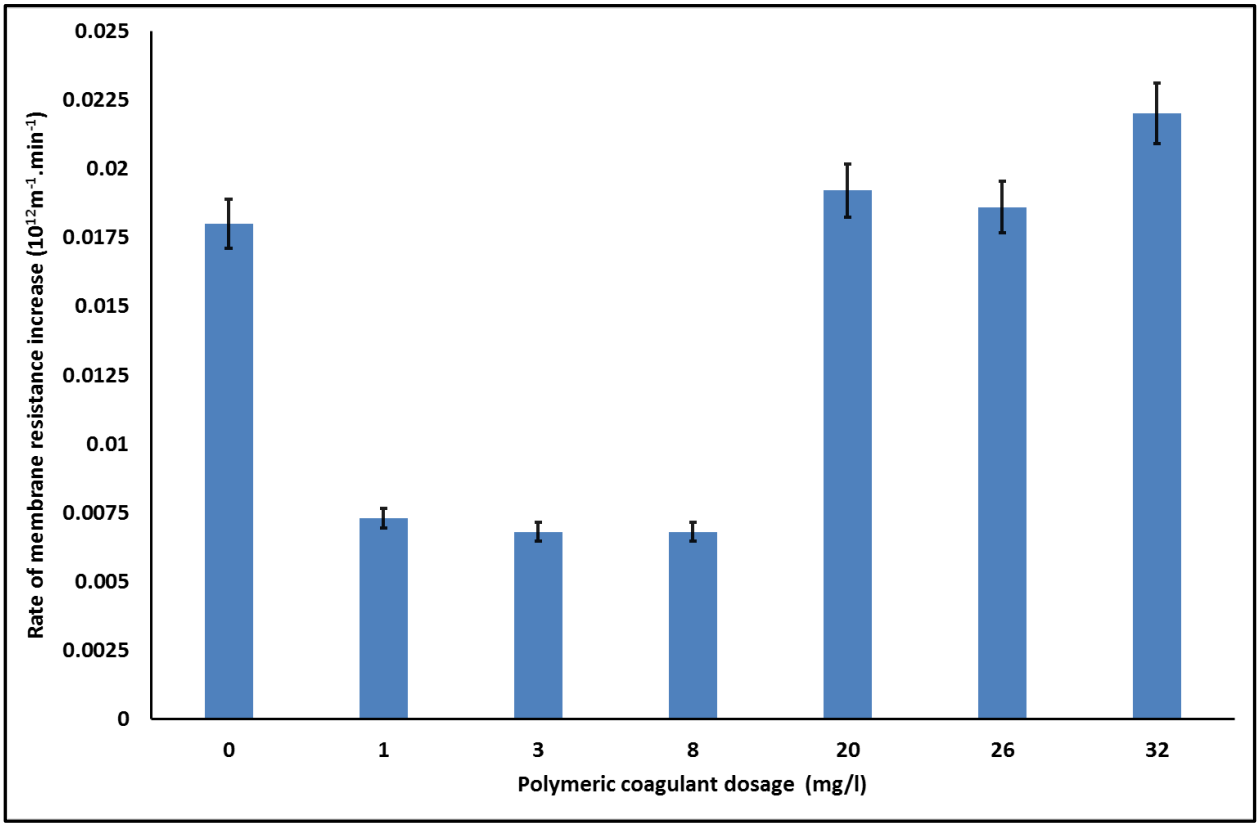

Figure 5-14: Averages of the rate of membrane resistance increase for the selected polymeric coagulant dosages

Figure 5-14the rate of membrane resistance increase reduced by 60% for the 1,3 and 8 mg/l when compared with 0mg/l polymeric coagulant dosage. The difference in the rate of membrane resistance increase between 1,3 and 8 mg/l polymeric coagulant dosages was approximately 7%. The rate of membrane resistance increased by 7%, 3% and 22% for the polymeric coagulant dosages of 20,26 and 32mg/l respectively. The polymeric dosage range of 1 – 8mg/l reduced the rate of membrane fouling, while polymeric dosages of 20, 26 and 32 mg/l increased the rate of membrane fouling. The difference between the rate of membrane resistance increase for polymeric coagulant dosages 1,3 and 8mg/l was insignificant.

Polymeric coagulant dosages of 0 and 1 mg/l weresubsequently selected for the DoE experiments.

5.3.4 Validation and selection of the air scouringrate

In the Experimental Design the range selected for air scouring rates was 0.4 to 12m^3/m^2.h based on the manufacturer recommendations and literature values. However the minimum air scour rate had to be changed to the rate at which air bubblesbegan rising on both gaps of the membrane module (see Figure 5-15). At air scour ratesbelow 1 m^3/m^2.h, air bubbles rose in either of the gaps but not both gaps. The minimum air scour rate was selected to be 1 m^3/m^2.h. The maximum air scouring rate of 12 m^3/m^2.h for the validation was adopted from the literature(Tian, et al., 2010).

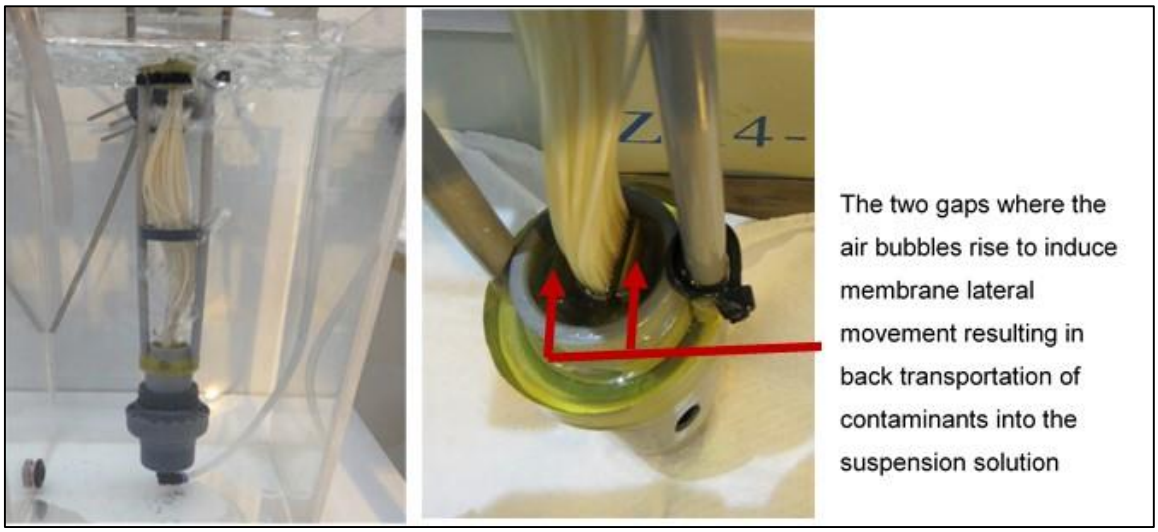

Figure 5-15: Membrane module, the gap width was 4mm and length 15mm

Based on the above, air scouring rates of 1,3,5,7,10 and 12 $m^3/m^2.h$ were selected for validation. The investigation and validationof the air scouring rate wereconducted with 1mg/l polymeric coagulant dosage,120LMH membrane flux, continuous air scouring and a 60 min filtration run time. Figure 5-16 shows themembrane resistancesfor the selected air scouring rates. Figure 5-17shows the averages of therate of membrane resistance increasesfor the selected air scouring rate. The error bars were the stanadard deviations of the three replicates. The replicated experiments are shown in Appendix 8.The error bars were calculated using standard deviation.

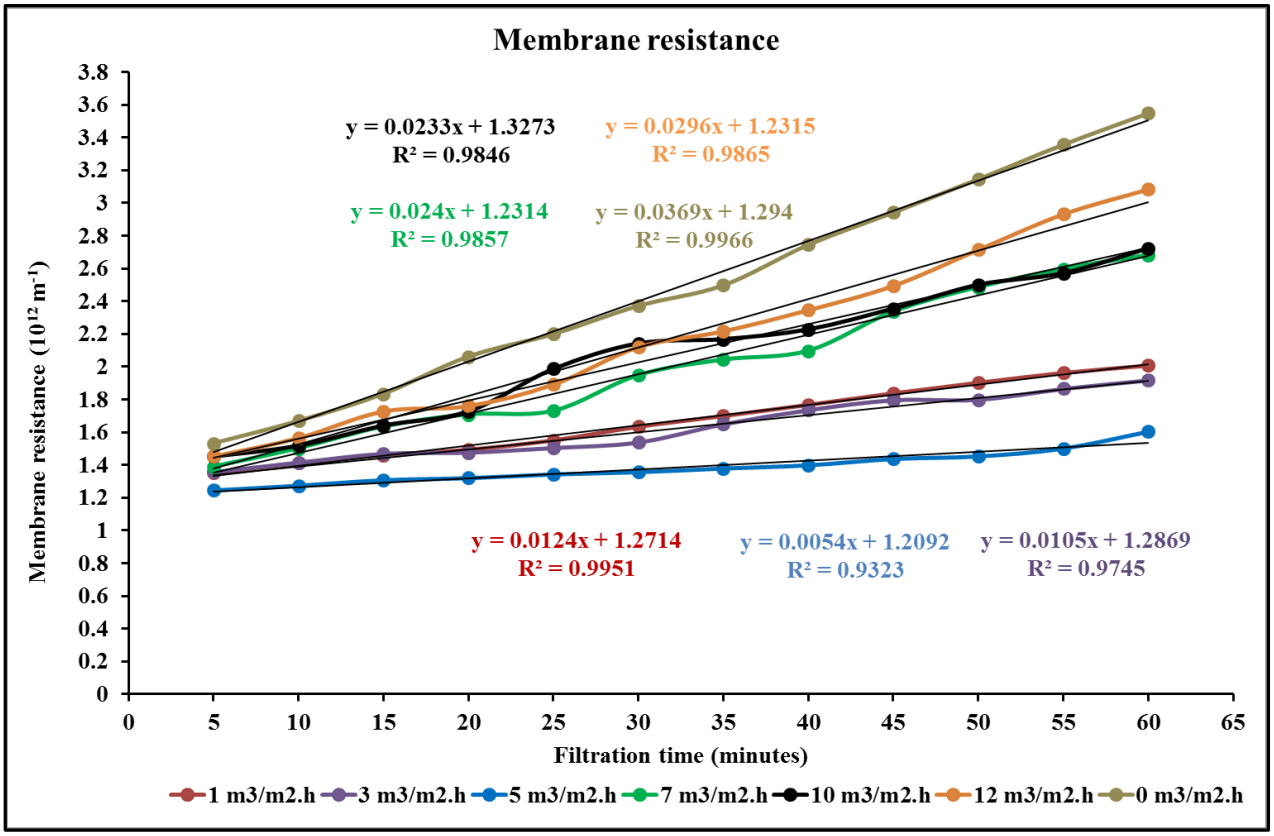

Figure 5-16: Membrane resistance at different air scour rates

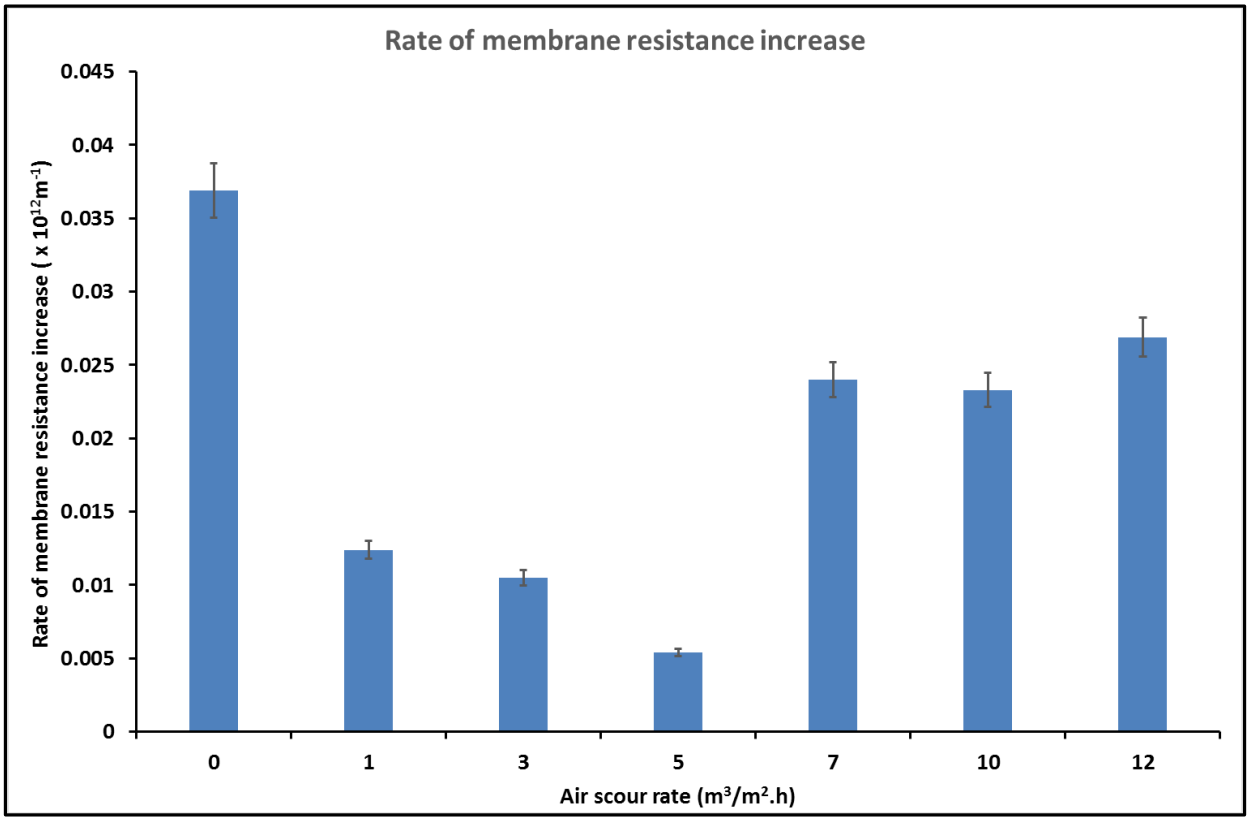

Figure 5-17: Average rate of membrane resistance increase at different air scour rates.

From Figure 5-17, as the air scouring rate increased from 1,3 5, 7, 10 and 12 m^3/m^2.h, the rate of membrane resistance increase decreased by 66%, 72%, 85%, 35%, 37% and 27% respectively, relative to the 0 m^3/m^2.h air scouring rate. The minimum rate of membrane resistance increase was at 5 m^3/m^2. h air scouring rate. Air scouring rates higher than 5 m^3/m^2.h increased the rate of membrane resistance increase relative to the 5 m^3/m^2.h air scouring rate. According to Liu et al., 2014, excessive air scouring rates resulted in the floc breakage into small colloids which leads to accelerated membrane fouling. The air scouring rates greater than 5m^3/m^2.h demonstrated this phenomenon.

For the DoE experiments, air scouring rates of 1 and 5 m^3/m^2.h were selected.

5.3.5 Selection and Validation of Sparger Pore Size

Figure 5-18 shows the sparger pore sizes investigated and Figure 5-19 shows the installation of each sparger into the UF membrane module

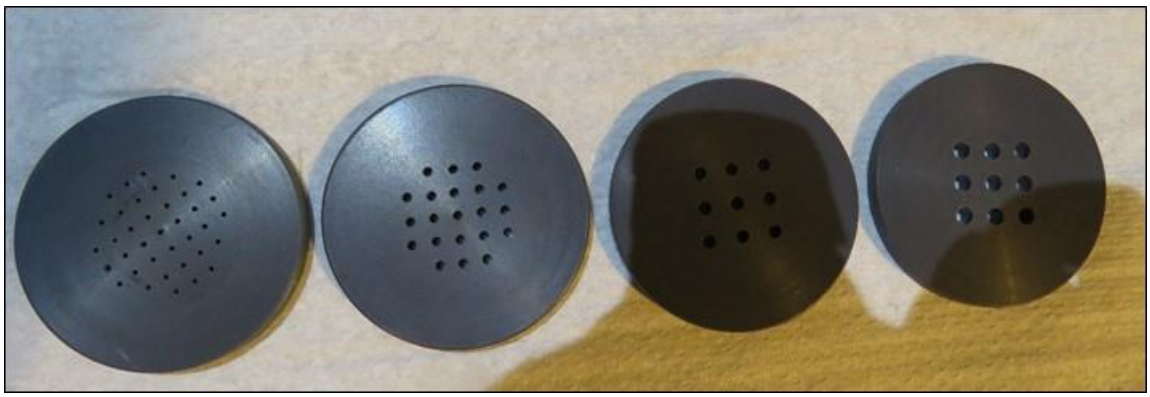

Figure 5-18: Sparger pore sizes validated, from left to right, 1mm, 2mm, 3mm,and 4mm sparger pore size.

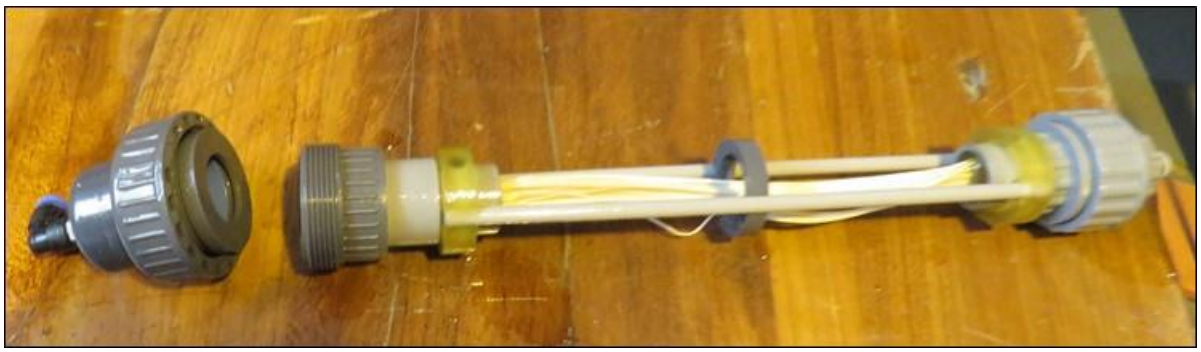

Figure 5-19: Membrane module with the union where spargers were inserted.

The operating conditions for the sparger pore size validation investigations were 1 mg/l polymeric coagulant dosage, a flux of 120 LMH, 60 minutes of filtration time, and continuous air scouring at rates of 1, 3 and 5 $m^3/m^2.h$.

The rate of membrane resistance increase was first grouped per air scouring rate using different sparger pore sizes, and is shown in Figure 5-20. The replicates data is shown in Appendix 5. The error bars were calculated using standard deviation.

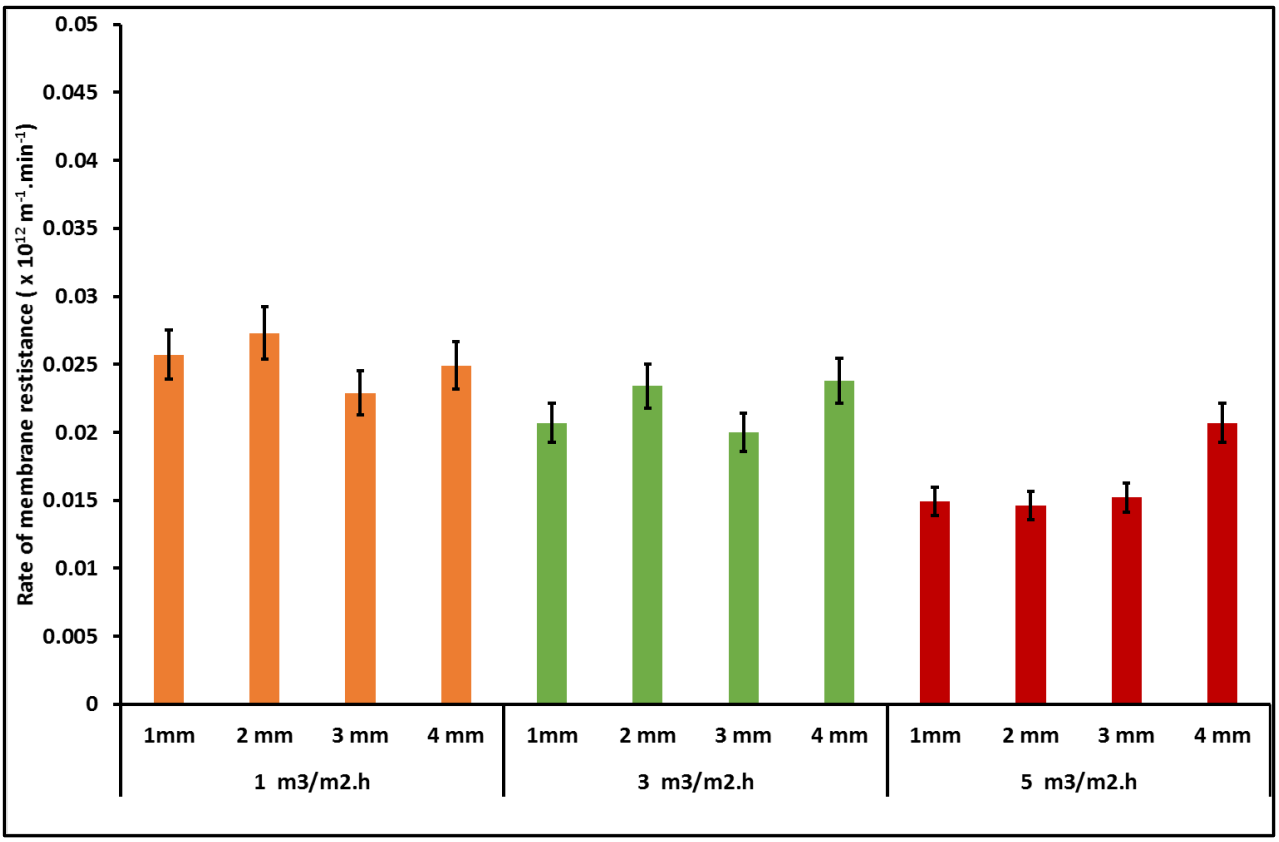

Figure 5-20: Averages of the rate of membrane resistance increase for different sparger pore sizes grouped by air scour rates.

From Figure 5-20, there was no observable trend correlating sparger pore size to the rate of membrane resistance increase. The rate of membrane resistance increase was then grouped by the sparger pore size with different air scouring rate, as shown in Figure 5-21 below.

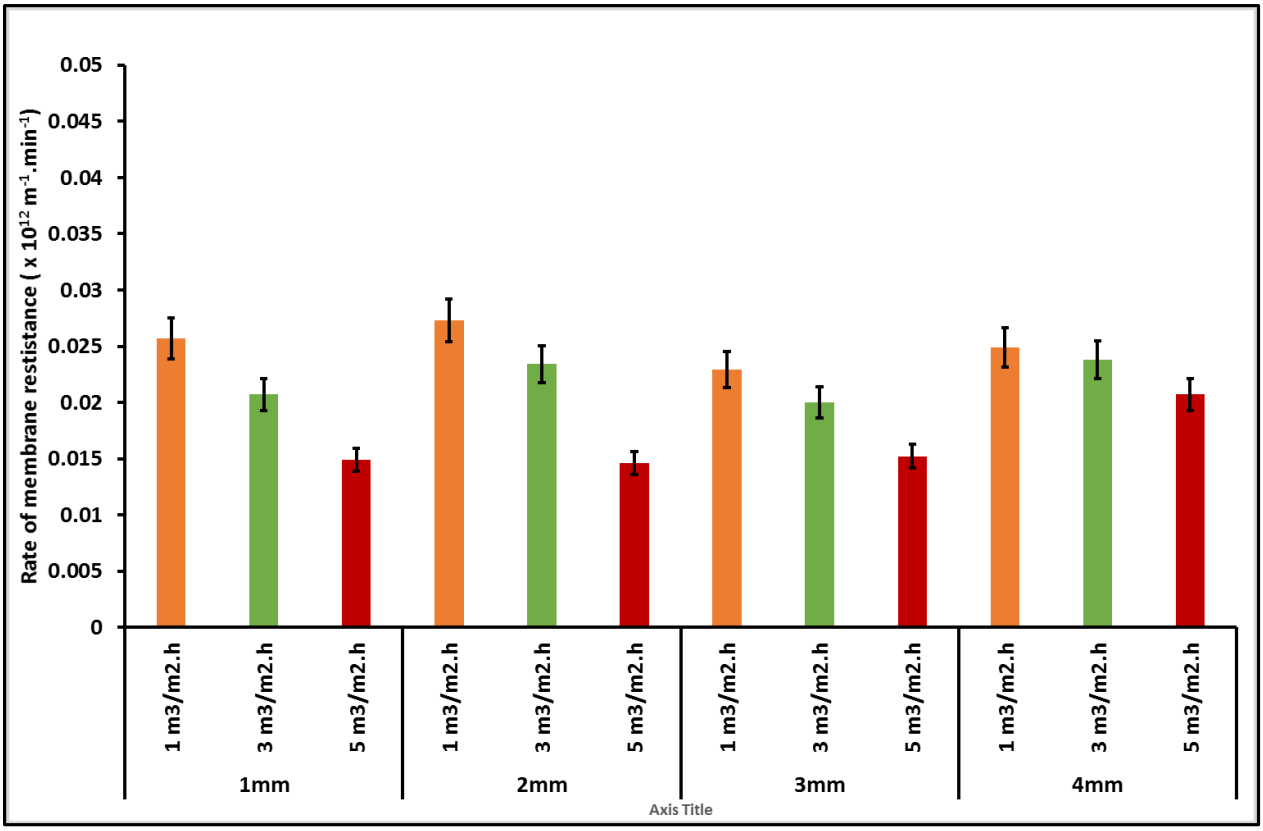

Figure 5-21: Averages of the rate of membrane resistance increase for different air scouring rates grouped by sparger pore sizes

From Figure 5-21, in all sparger pore sizes, the rate of membrane resistance increase decreased with increasing air scouring rate. The analysis of variance (ANOVA) was then used to analysethe effect of the sparger pore sizes in combination with the air scour rates on the rate of membrane resistance increase. The probability value (p-value) at a 95% confidence interval (CI) validated the effect of the combination of the sparger pore sizes and air scouring rate on the rate of membrane resistance increase. Table 5-1 below shows the schematic analysis of how the ANOVA was applied.

Table 5-1: Application of the ANOVA to determine the combined effect of sparger pore sizes and air scouring rates on membrane fouling

Between the groups, sparger pores sizes

Within the groups

Air scouring rate, $m^3/m^2.h$	Sparger pore sizes, mm			
	1	2	3	4
1				
3				
5				

The null hypothesis forthe validation of the effect of the sparger pore sizes effect on membrane fouling was “no differencein the rate of membrane resistance increase amongst the different sparger pore sizes”. Table 5-2 below shows the ANOVA results.

Table 5-2: ANOVA for the validation of the different sparger pore sizeson the rate of membrane resistance increase i.e. between the groups.

Source	DF	Sum of Squares	Mean square	F-value	p-value
Pore Size	3	3.57×10^{-09}	1.19×10^{-09}	3.96	0.0229
Error	20	6.01×10^{-09}	3.01×10^{-10}		

The true null hypothesis at 95% CI required a p-value to be higher than 0.05. From Table 5-2, the p-value of the validation of different spargers on the rate of membrane resistance increase was 0.0229; hence the null hypothesis rejected. However, the results did not explicitly indicate which sparger pore size had the least or the most effect on the rate of membrane resistance increase.

The limitation of the in-between groups ANOVA was that it did not provide further information as to which groups significantly contributed to the difference in the rate of membrane resistance increase. Table 5-3 shows the ANOVA validating the effect of air scouring of different sparger pore sizes on the rate of membrane resistance increase. The null hypothesis of this validation was the change in the rate of membrane resistance increase within the sparger pore sizes was not significant.

Table 5-3: ANOVA for the validation of the effect of the air scouring rates on the rate of membrane resistance increase.

Source	DF	Sum of Squares	Mean square	F-value	p-value
Air Rate	2	3.62×10^{-11}	1.81×10^{-11}	0.32	0.7322
Error	21	1.20×10^{-09}	5.72×10^{-11}		

The p-value of the effect of the air scouring rates within the sparger pores on the rate of membrane resistance increase was 0.7322. The calculated p-value was higher than 0.05, hence the null hypothesis was not rejected. The air scouring within the sparger pore sizes had an insignificant effect on the rate of membrane resistance increase.

The effect of sparger pore size on the rate of membrane resistance increase was selected by plotting air scouring rate versus the rate of membrane resistance increase, for the different sparger pore sizes.It was decided that the sparger pore size selected would have the lowest slope and an r^2, close to 1, indicating the least interaction between sparger pore size and air scour rate.

Figure 5-22 shows the graph of air scouring rate versus the rate of membrane resistance increase using different sparger pore sizes.

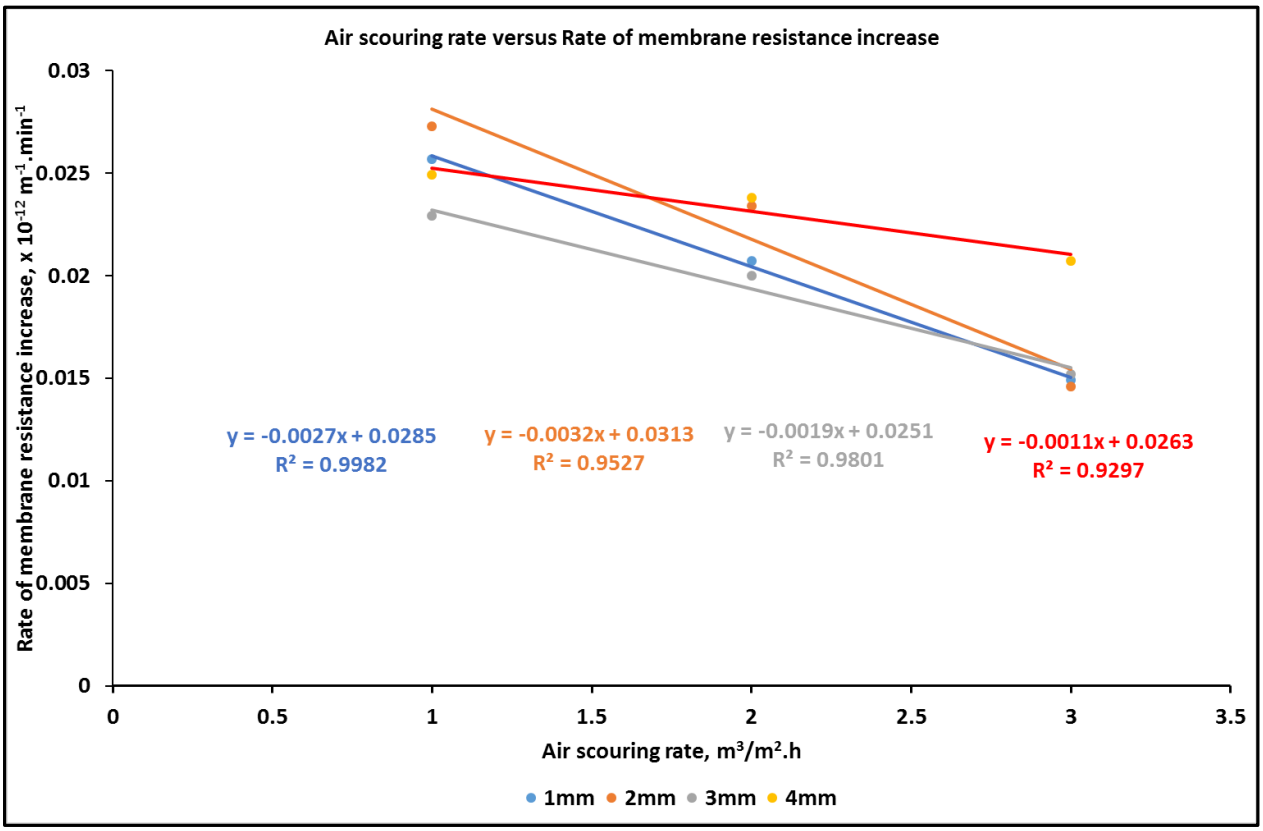

Figure 5-22: Air scouring rate versus the rate of membrane resistance increase using different sparger pore sizes.

From Figure 5-22, the 4 mm pore size had a poor r^2 of 0.9297. The slope for the 1mm and 2mm pores were -0.027 and -0.0032 respectively, with r^2values of 0.9982 and 0.9527 respectively. The difference in slope of the 1mm and 2mm pores was 16% with 2mm having the lowest slope. However, the r^2 for the 1mm pores was higher than that of the 2mm pores.On the above basis, a 1mm sparger pore size was selected for the DoE experiments.

5.3.6 Validation and selection of Frequency of Air Scouring

The periodic air scouring was blocked into 20 min slots, indicating three blocks in 60 min filtration run time. The frequencies of air scouring investigated were: no air scouring (0%);five minutes (25%); 10 min (50%); and 15 min (75%) of air scouring in every 20 minblockfor the duration of the filtration runtime.Theoperating conditions for this were 120 LMH membrane flux, 1 m^3/m^2.h air scouring rate, 1 mg/l polymeric coagulant dosage, 1 mm sparger pore size and 60 min filtration run time.

Figure 5-23 shows the membrane resistance profiles for the frequencies investigated. The replicate experiments are shown in Appendix9. Table 5-4 shows the averages of the rate of membrane resistance increase for the selected periodic air scouring frequencies.

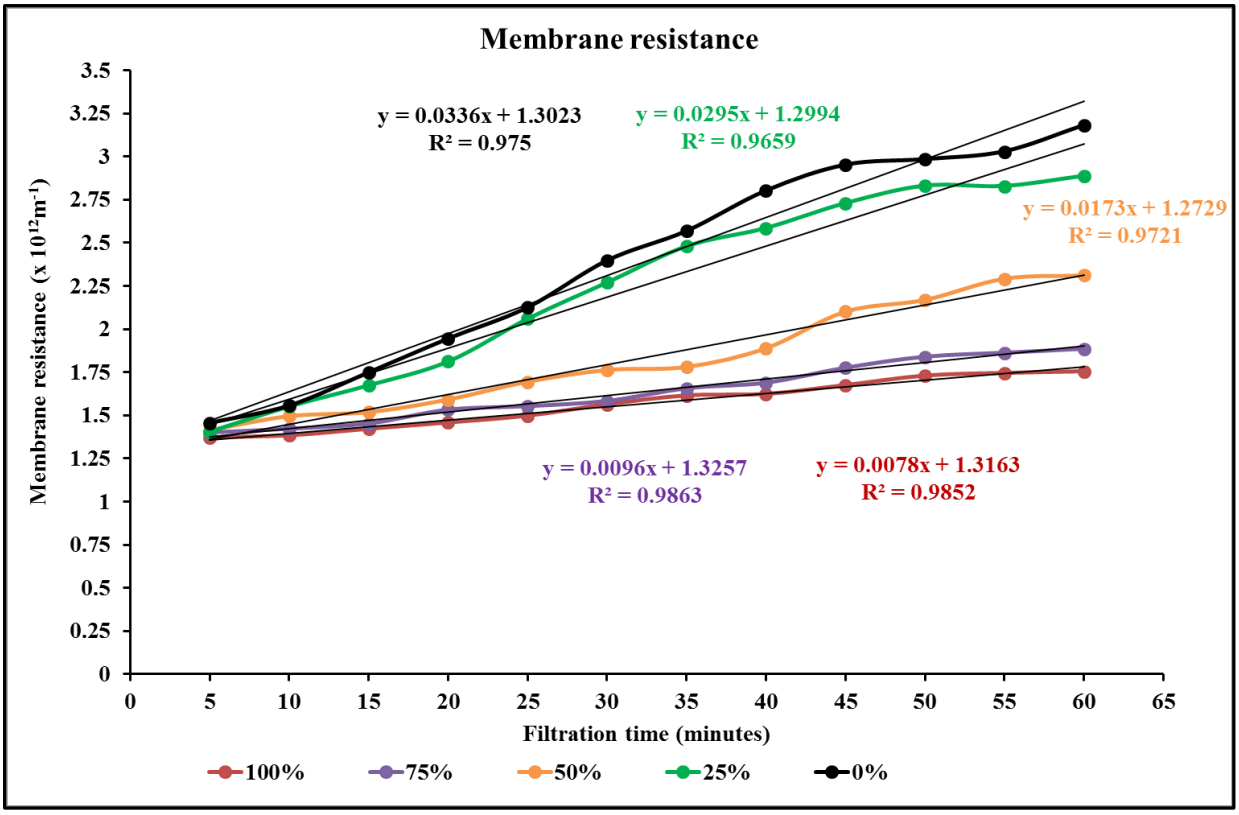

Figure 5-23: Effect of the frequency of air scouring on the rate of membrane resistance.

Table 5-4: The average values of the rate of membrane resistance increase for the selected air scouring frequency

The frequency of air scouring (in 20 minutes block)	**The rate of membrane resistanceincrease ($x10^{12}m^{-1}.min^{-1}$)**	**% reduction relative to no air scouring (0%)**
No air scouring (0%)	0.0360	-
25% (five minutes of air scouring)	0.0295	19%
50% (10 minutes of air scouring)	0.0173	52%
75% (15 minutes of air scouring)	0.0096	73%
100% (continuous air scouring)	0.0078	78%

From Table 5-4,the calculated percentage differences in the rate of membrane resistance increase were relative to no air scouring (0%). The difference in the rate of membrane resistance increase between 75% and 100% air scouring frequency (0.0336 $x10^{12}m^{-1}.min^{-1}$ and $0.0295x10^{12}\,m^{-1}.min^{-1}$) was moderate. Similarly with 0% and 25% air scouring frequency ($0.0096x10^{12}\,m^{-1}.min^{-1}$and $0.0078x10^{12}\,m^{-1}.min^{-1}$). The significant change in the rate of membrane resistance increase was

between 0%, 50% and 100% air scouring frequency, 0.0336 x10^{12} $m^{-1}.min^{-1}$, 0.0173 x10^{12} $m^{-1}.min^{-1}$ and 0.0078 x10^{12} $m^{-1}.min^{-1}$ respectively.

The 50% and 100% air scouring frequencieswereselected for the DoE experiments.

5.3.7 Summary for the validation of polymeric coagulant, air scouring rate and frequency of air scouring on the rate of membrane fouling

Table 5-5 below is the summary of the selected ranges from the validation experiments.

Table 5-5: Factor ranges showed a positive effect in minising the rate of membrane fouling

Factor	Range	
	Lower	Upper
Polymeric coagulant, mg/l	0	1
Air scouring rate, $m^3/m^2.h$	1	5
Air scouring frequency, 20 min block	50%	100%

5.4 The Combined Effects of Coagulant Dose, Air Scouring Rate and Air Scouring Frequency on Membrane Fouling

5.4.1 Treatment combinations

Table 5-6 shows the experiments' treatment combinations and labels as per the three factors, two levels DoE. The legends represented in labels on the graphs show the operating conditions.

Table 5-6: Experiment treatment combinations for the three factors two-level DoE

Design Run	Factors			Labels
	Air scour frequency (A)	Air scour rate (B)	Coagulant dose (C)	
1	Low	Low	Low	1
2	High	Low	Low	a
3	Low	High	Low	b
4	High	High	Low	ab
5	Low	Low	High	c
6	High	Low	High	ac
7	Low	High	High	bc
8	High	High	High	abc

5.4.2 Water quality

5.4.2.1 Turbidity removal

Figures 5-24 and 5-25 below show the turbidity log removal and final water quality measured as turbidity for the different treatment combinations indicated in Table 5-6. The replicate turbidity data are shown in Appendix 11 and 12

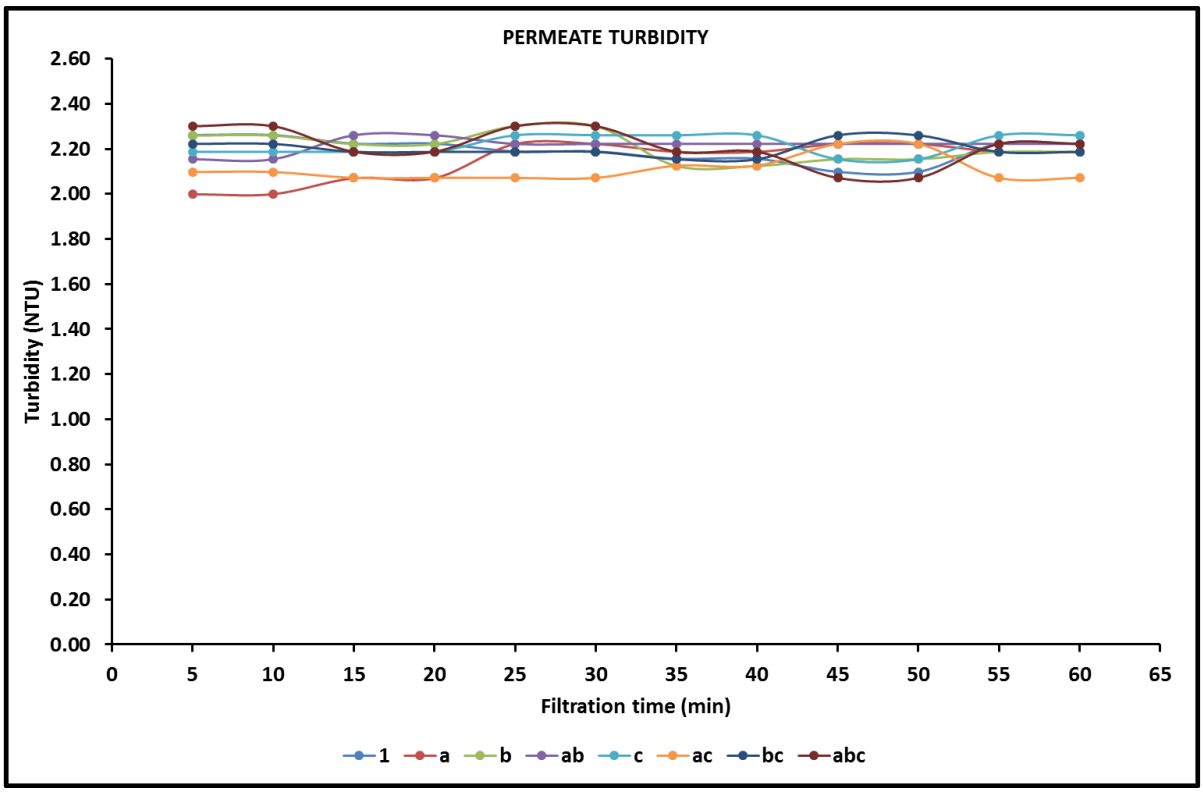

Figure 5-24: Turbidity log removal graph for the different treatment combinations

(1 log removal = 90% turbidity removal, 2 log removal = 99% turbidity removal, 3log removal = 99.9% turbidity removal)

From Figure 5-24, an average 2.2 turbidity log removal achieved irrespective of the treatment combinations. The turbidity log removal results showed that turbidity removal was independent of the treatment combination, but was mainly determined by the membrane pore size.

Figure 5-25 shows the final turbiditiesfor the treatment combinations.

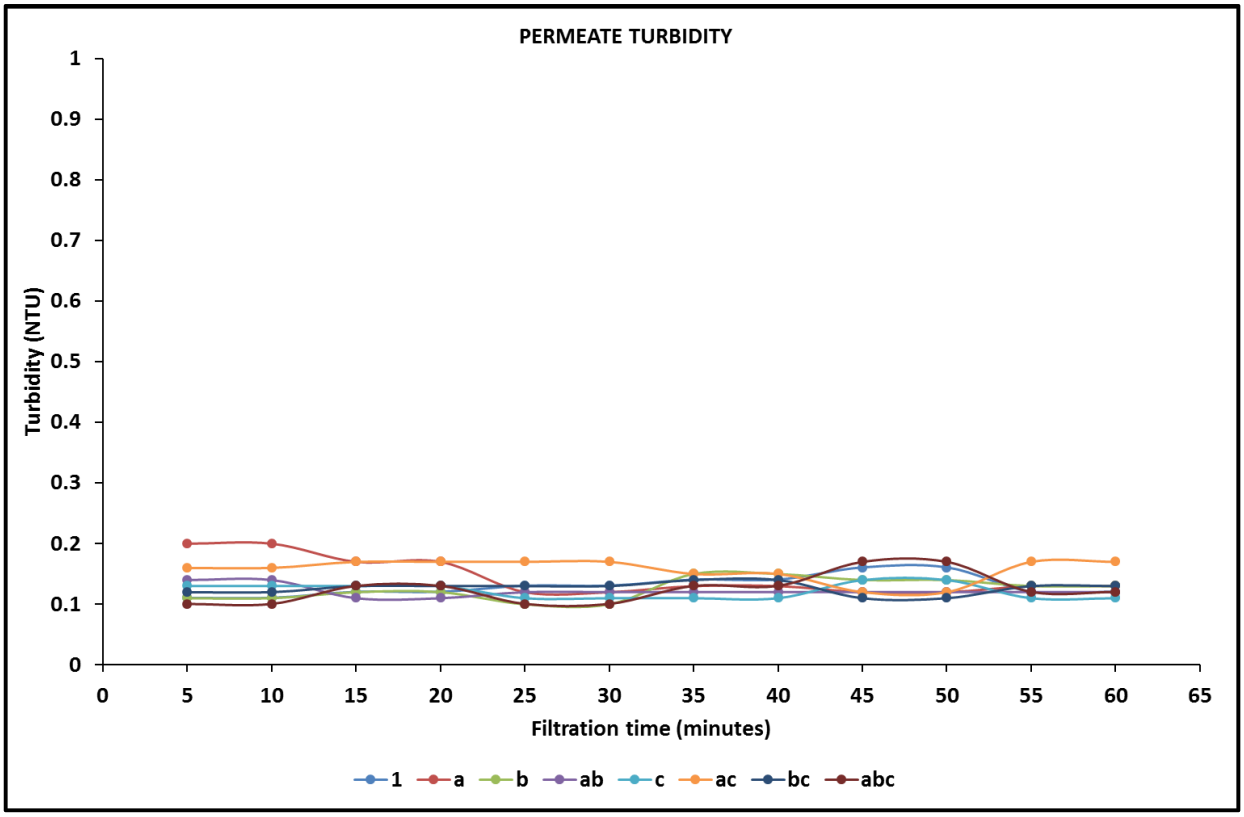

Figure 5-25: Permeate turbidity at different treatment combinations (operating conditions) denoted by a legend (see Tables 5-5 and 5-6 for operating conditions)

The SANS 241: 2015 drinking water quality standard regulatesthe final water turbidity of less than 1 NTU be acceptable for human consumption. In all treatment combinations, the average permeate turbidity was 0.15NTU, and less than SANS 241 standard of 1NTU. In the study conducted by Walsh, et al., 2009 on the effect of UF membrane pre-treatment with coagulation and flocculation on the permeate water quality concluded that coagulant addition does not improve the permeate quality but the rate of the membrane fouling.The conclusions from the Walsh, et al., 2009 study correspond with the results obtained in this studyon the permeate water quality measured as turbidity.

5.4.2.2 Total Dissolved Solids (TDS) removal

Figure 5-26 below indicates the effects of the UF membrane on TDS removal.

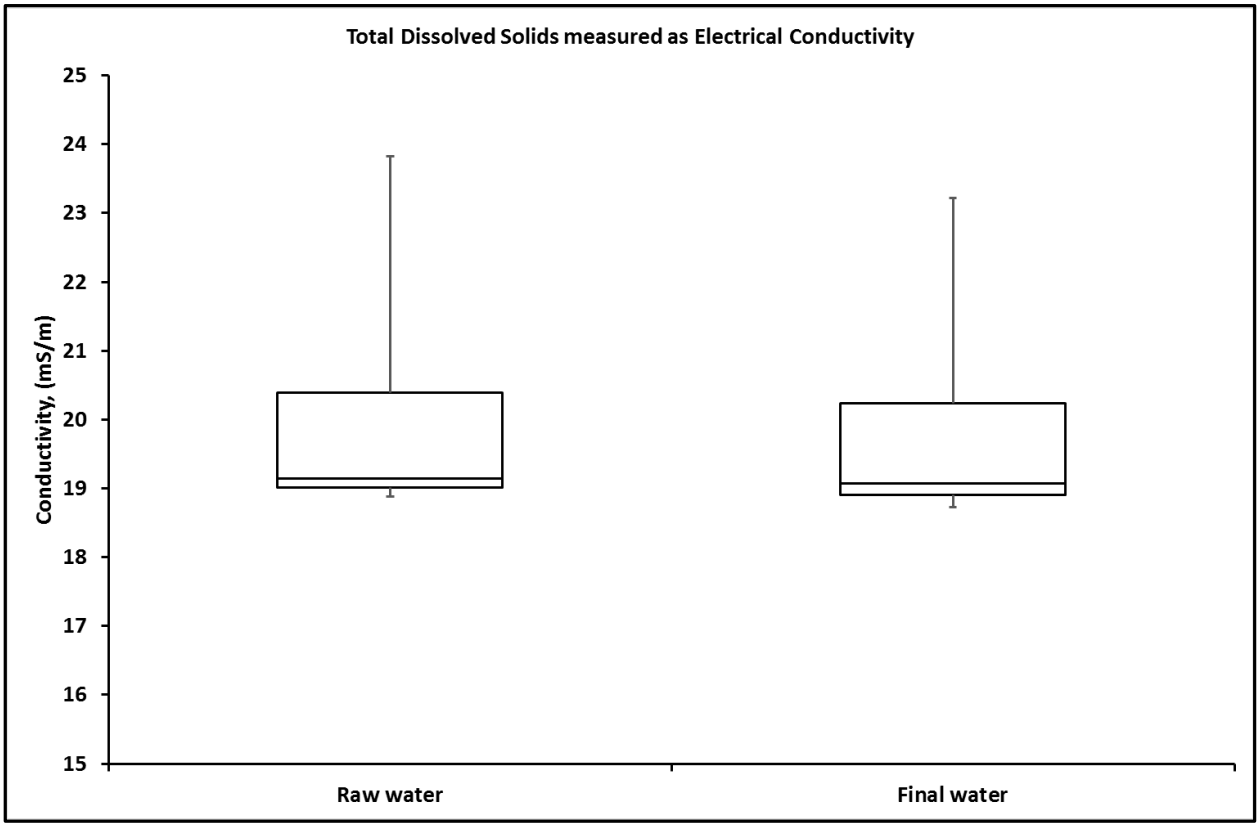

Figure 5-26: The box and whisker plot indicating the effectiveness of the UF membrane on TDS removal.

There was an insignificant difference in the conductivities of the raw and final water. The minimum and maximum final water conductivity was 18.8 and 23.5 mS/m respectively for both raw water and final water. The box and whisker plot was left-skewed with 19 mS/m median. The particle sizes of the TDS are <1nm (Schutte, 2006) and the UF membrane nominal pores were 0.1µm, hence explaining the negligible removed by the UF membrane.

5.4.2.3 Natural Organic Matter (NOM) removal

Figure 5-27 below shows the effect of UF treatment on NOM removal.

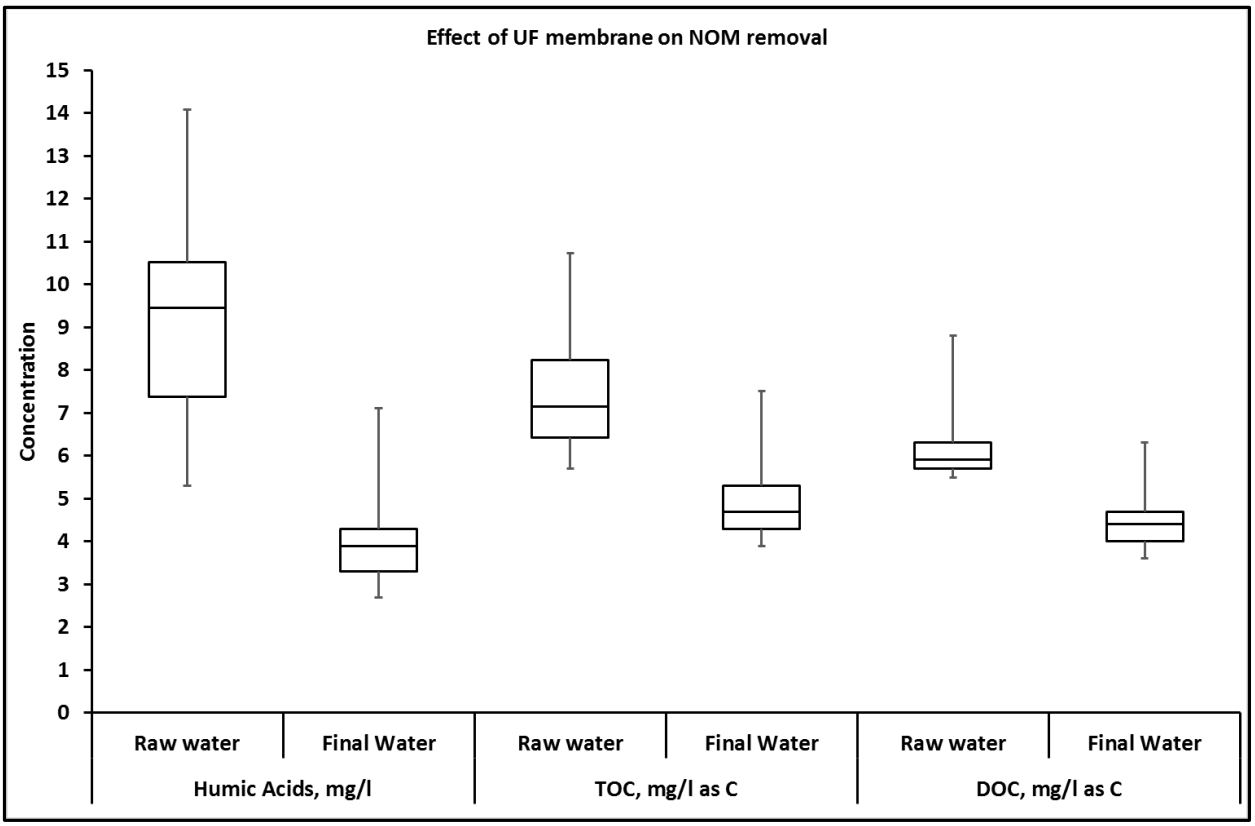

Figure 5-27: The box and whisker plot indicating the effect of UF membrane on NOM removal.

The raw water had minimum and maximum concentrations of 5mg/l and 14 mg/l with the inter-quartile range of between 7.5 mg/l and 10 mg/l. The median value was 7.5 mg/l. The humic acid concentrations distribution were right-skewed, i.e. 75% of the humic acid concentrations had a minimum concentration higher than 7.5mg/l with the maximum of 14mg/l.The final water had humic acids minimum and maximum concentrations of 2.5mg/l and 7 mg/l with the inter-quartile range of between 3.2 mg/l and 4.3 mg/l.The average removal of the humic acids by the UF membrane was 55%.

The humic acids with particle size greater than UF membrane nominal pore size of 0.1µm were strained out by the UF membrane. The attachment of humic acids onto the membrane surface resultedinorganic membrane fouling.

Similar trends were observed for TOC and DOC concentrations. The average DOC and TOC removal by the UF membrane was 30% and 35% respectively. The attachment of TOC and DOC particles onto the membrane surface resulted in organic membrane fouling. Figure 5-30 shows the SUVA for raw water and final water.

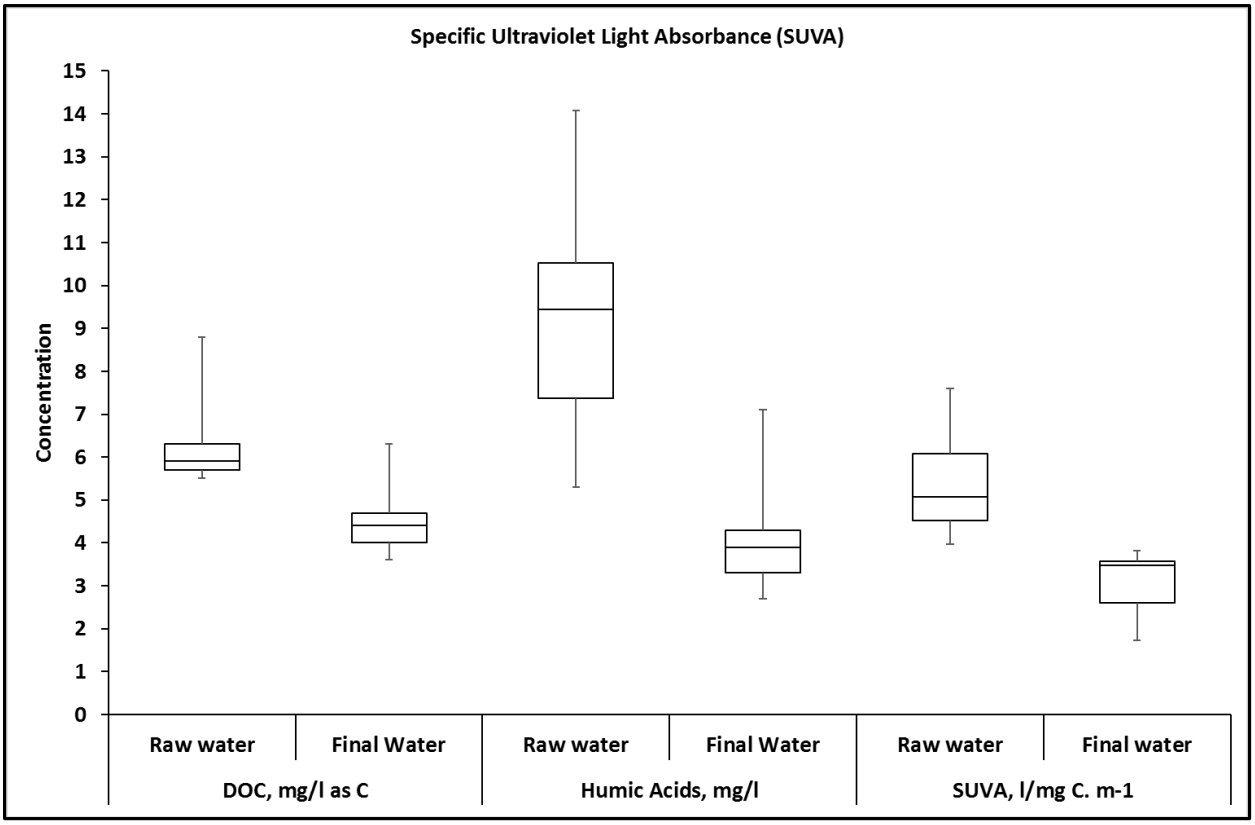

Figure 5-28: The box and whisker plot indicating the effect of UF membrane on SUVA removal.

The SUVA is the indicator of the distribution of the different NOM fraction in water. Table 2-5 shows the NOM fraction measured as SUVA values. From Figure 5-28, the raw water minimum and maximum SUVA values were 3l/mg $C.m^{-1}$and 7 l/mg $C.m^{-1}$ respectively with an inter-quartile range of 4 and 6 l/mg $C.m^{-1}$and median of 4.5 l/mg $C.m^{-1}$. The SUVA range values in the raw water indicated a predominance of hydrophobic NOM fraction. The SUVA value of the final water had minimum and maximum concentrations of 2 and 3.5 l/mg $C.m^{-1}$ with inter-quartile ranged between 2.4 and 3.3 l/mg $C.m^{-1}$and3 l/mg $C.m^{-1}$ median.

The SUVA value range in the final water indicated the prevalence of transphilic and hydrophilic of NOM fraction. The UF membrane removed a significant portion of the hydrophobic NOM fraction from the raw water. The presence of the NOM on the membrane surface caused organic membrane fouling.

5.4.2.4 Microbial removal

Figure 5-29 shows the Total Coliform (TC), Heterotrophic Plate Count (HPC) and pathogenic Escherichia coli (E. Coli)microbiological water quality parameters of the raw water.

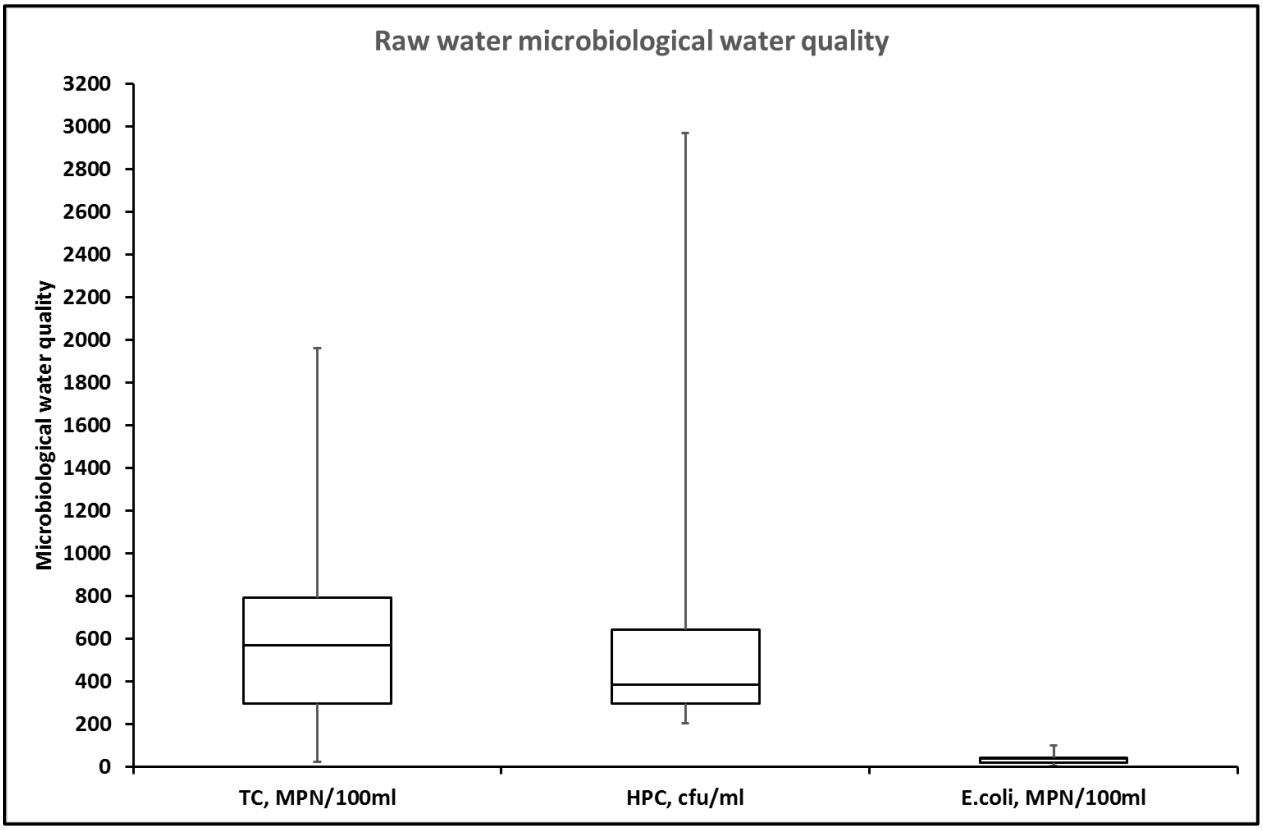

Figure 5-29: The box and whisker plot of the raw water microbiological water quality fed into the UF membrane system

The HPC does not directly indicate the presence of pathogenic bacteria. (Khan, 2004; Cabral, 2010).Instead, the HPC reduction demonstrates the efficacy of treatment processes (SANS 241:2015 and WHO,2011). The raw water had a minimum and maximum concentration of HPC of 200cfu/ml and 2900cfu/ml with inter-quartile ranges of 250cfu/ml and 650cfu/ml and median of 300cfu/ml. No HPCwas detected on the final water quality for all treatment combinations applied.

The TC valuesin water treatment is an operation indicator of the process efficiency (SANS 241:2015 and WHO, 2011).The minimum and maximum raw waterTC concentrations were 20MPN/100ml and 2000MPN/100ml,respectively, with the inter-quartile range of between 300 MPN/100ml and 820MPN/100ml and median of 620 MPN/100ml. There were no TC detected on the final water for all treatment combinations applied.

The E. coli are indicators of recent faecal pollution and infer that pathogens (diseases causing microorganisms) may be present(Khan, 2004; Cabral, 2010). The minimum and maximum concentrations of E. coli in raw water were 0 MPN/100ml, and 100 MPN/100ml with inter-quartile

range of 50MPN/100ml and 70MPN/100ml and median of 60 MPN/100ml. There were no E. coli detected on the final water irrespective of the treatment combinations.

The detection of no microorganisms in the final water indicated microorganisms accumulated or remained on the raw water side of the membrane surface.

The presence of algae in the raw and final water was determined using the chlorophyll a method. In both raw and final water, the chlorophyll a (used a measure of algal content) was below the method detection limit. The water quality data of the raw water and final water is shown in Appendix 13 and 14 respectively.

5.4.3 Effect of the treatment combinations on the rate of membrane fouling

Figure 5-30 below shows the membrane resistance profiles for the different treatment combinations.The replicate data is shown in Appendix 10.

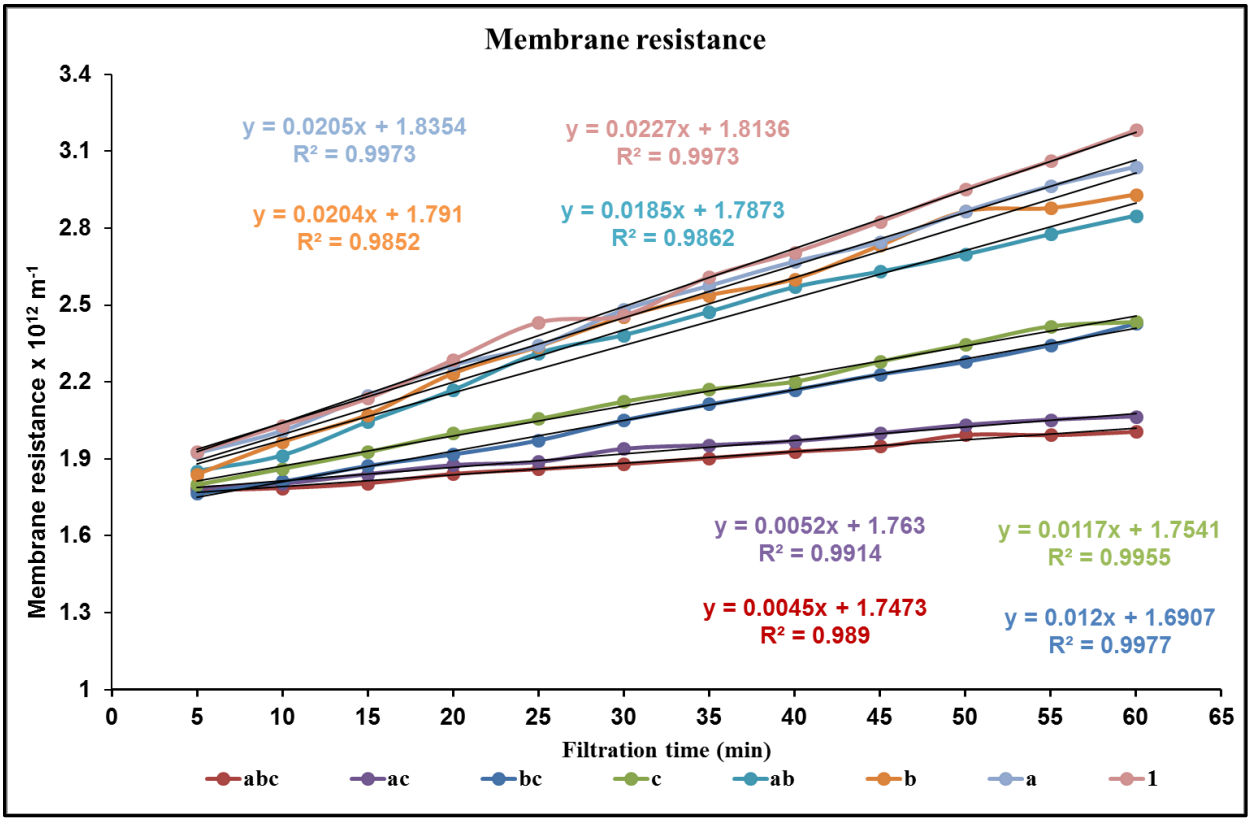

Figure 5-30: The graph of the membrane resistance for the different treatment combinations (operating conditions).

The slope of each line indicates the rate of membrane resistance increase,i.e. the rate of membrane fouling.Figure 5-31 shows the average rates of membrane resistance increase for different treatment combinations. The errors were the standard deviations of the three replicates of each treatment combination.

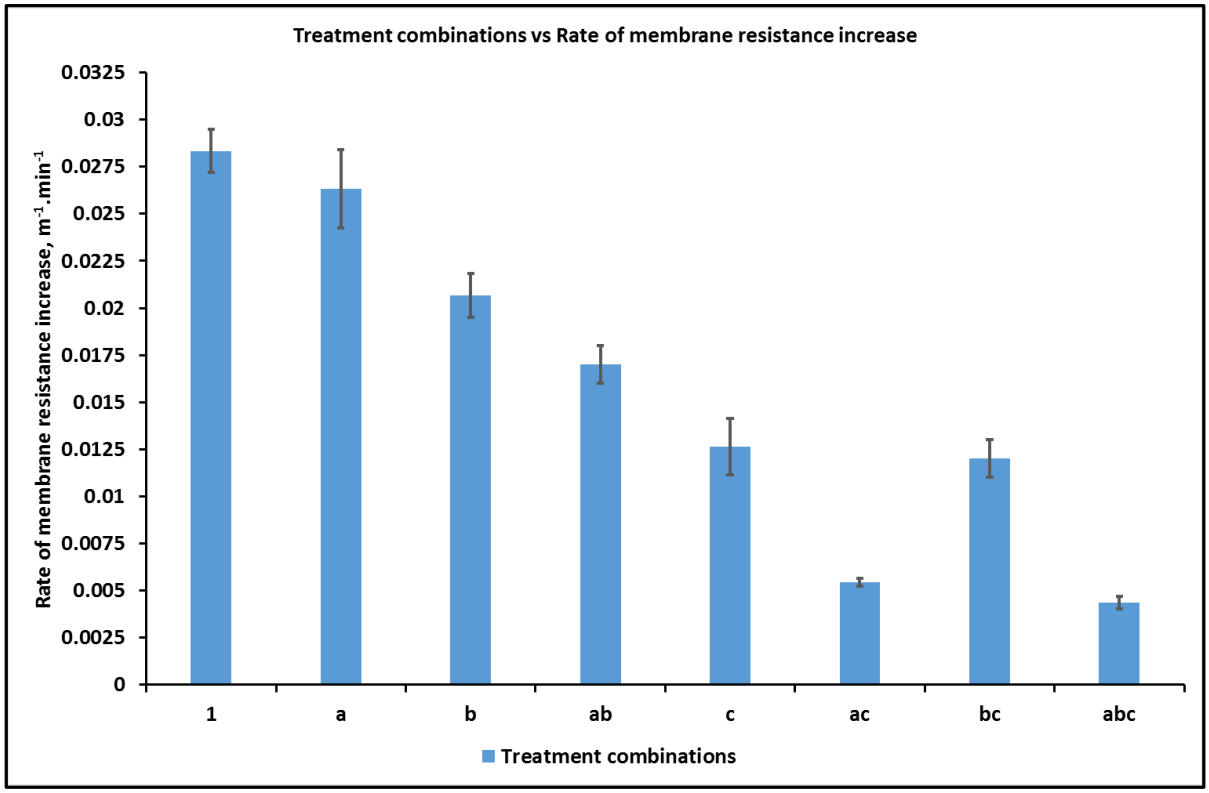

Figure 5-31: Average rate of membrane resistance increase for different treatment combinations arranged in the design run format.

From Figure 5-31, the treatment combinations without coagulant addition (i.e. **1, a, b,** and **ab**) had higher rates of membrane resistance increase compared to the treatment combinations with coagulant addition (i.e. **c, ac, bc,** and **abc**).

In the treatment combinations without coagulant dosage (0 mg/l polymeric coagulant dosage), the difference in the rate of membrane resistance increase between the treatment combinations **1** and **a** was 7%, 0.028 x 10^{12} $m^{-1}.min^{-1}$ and 0.026 x 10^{12} $m^{-1}.min^{-1}$ respectively. The error bars of the two treatment combinations suggested that the difference was insignificant. These results indicated that irrespective of the 1 $m^3/m^2.h$ or 5$m^3/m^2.h$ air scouring rate, periodic air scouring without coagulant addition caused the membrane to foul quicker. For the treatment combinations **b** and **ab**, the rate of membrane resistance increase was 0.021 x 10^{12} $m^{-1}.min^{-1}$ and 0.017 x 10^{12} $m^{-1}.min^{-1}$ respectively, i.e. 18% difference. The error bars suggest that the difference in the rate of membrane resistance increase was significant. The results indicate that application of 5 $m^3/m^2.h$ air scouring rate continuously reduced the rate of membrane fouling compared to 1$m^3/m^2.h$ air scouring rate.

In the treatment combinations with 1mg/l coagulant dosage, the rate of membrane resistance increase between treatment combinations **c** and **ac** was0.013 x 10^{12} $m^{-1}.min^{-1}$ and 0.0054 x 10^{12} $m^{-1}.min^{-1}$respectively i.e.57% difference. The error bars indicates that the difference was significant. The results indicates that for the periodic air scouring, the 5 $m^3/m^2.h$ air scouring rate reduced the

rate of membrane fouling relative to the 1m^3/m^2.h air scouring rate. A similar trend was observed for the treatment combinations **bc** and **abc**.The percentage difference was 63% and significant. The 5 m^3/m^2.h air scouring rate at continuous air scouring resulted in a substantially reduced rate of membrane fouling compared to 1m^3/m^2.h air scouring rate.

The difference in the rate of membrane resistance increase between treatment combinations **c** and **bc** was 5%. The error bars indicate that the difference in the rate of membrane resistance was insignificant. The rate of membrane resistance increases for 1 mg/l polymeric dosage with 50% periodic air scouring, 5 m^3/m^2.h air scouring rate (0.013 x 10^{12} $m^{-1}.min^{-1}$) was similar to 50% air scouring,1m^3/m^2.h air scouring rate (0.012 x 10^{12} $m^{-1}.min^{-1}$).

The difference in the rate of membrane resistance increase between **ac**(0.0054 x 10^{12} $m^{-1}.min^{-1}$) and **abc (**0.0043 x 10^{12} $m^{-1}.min^{-1}$) was 18%. The error bars indicate a significant difference in the rate of membrane resistance increase. The result indicates that at the continuous air scouring, the 5 m^3/m^2.h air scouring rate reduced the rate of membrane fouling compared to 1m^3/m^2.h air scouring rate. Figure 5-32 shows decreasing order arrangement of the membrane resistance increase (average values).

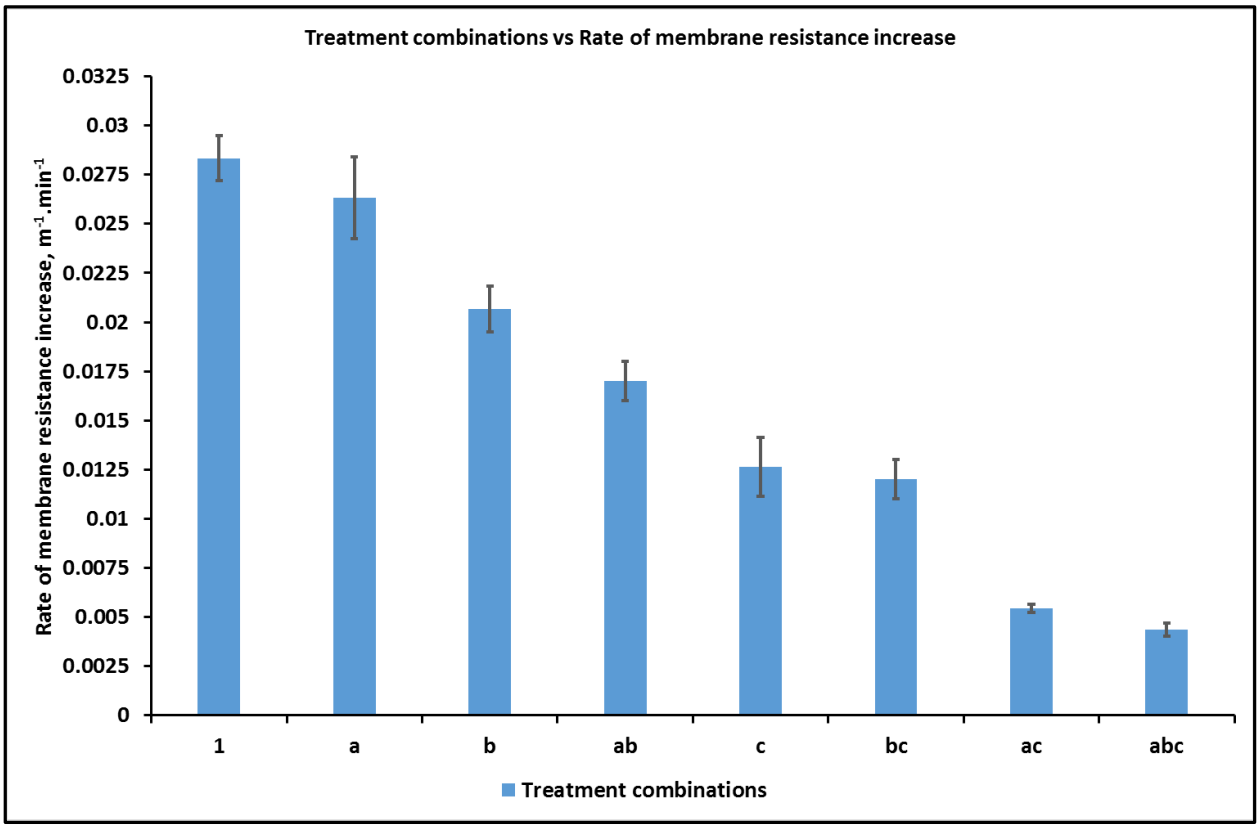

Figure 5-32: Rate of membrane resistance increase arranged in decreasing order

From Figure 5-32, treatment combinations **1** and **a** had the highest rate of membrane resistance increase with the lowest obtained at **abc** treatment combination. The major difference in the three

treatment combinations was the polymeric coagulant addition. There was no polymeric coagulant addition on the combinations that resulted in the highest rate of membrane resistance while the lowest rate of membrane resistance increase was obtained with 1mg/l polymeric coagulant addition.

5.4.4 Statistical analyses

A statistical analysis of the individual and combined effects of polymeric coagulant addition, air scouring rate, and air scour frequency onmembrane resistance increase was conducted (Appendix 3, Table 6-1). The data normality was tested. Figure 5-33 shows the results.

According to Montgomery, 2007, for the data to conform to normality:

i. A frequency data distribution plot must be bell-shaped,
ii. A cumulative probability plot of the empirical data compared with predicted values should fall along a straight line
iii. The box plot should be symmetrically distributed from the median (middle value), i.e. a data points on one side of the median should be the mirror image of the other side in both length and size.

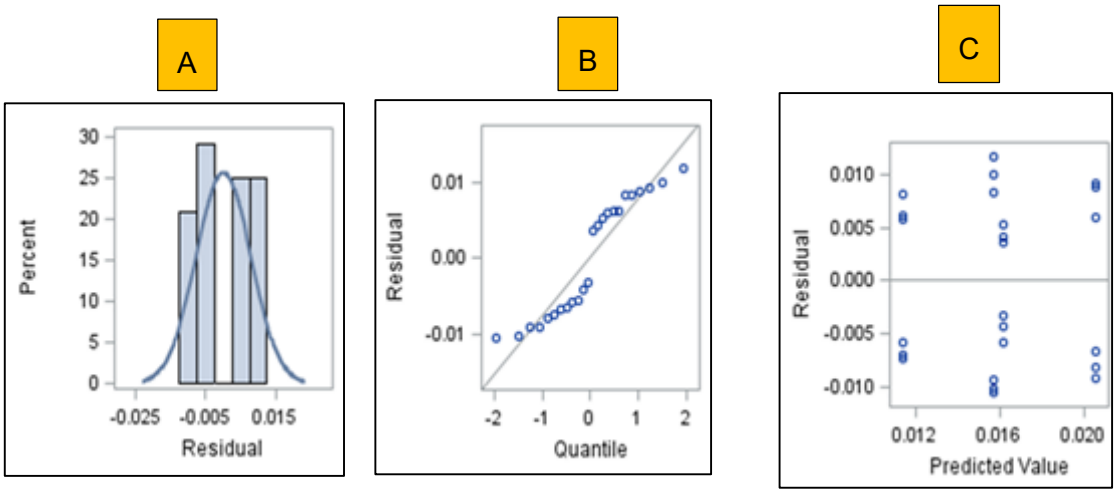

Figure 5-33: Test for data normality.

In Figure 5-33, symbols A, B and C represent the frequency distribution, cumulative probability plot, and box plot respectively. All conformed to data normality.

A Pareto plot was used to illustrate the relative effects of polymeric coagulant dosage, air scouring rate, air scouring frequency, and their interactions, using calculated main effects on the rate of membrane resistance increase. The main effects of each input factor and the interacting factors were calculated using equations (6-1) up to (6-6) in Appendix 16. Table 5-7 shows the calculated effects of the treatment combinations.

Table 5-7: Main effects of each factor and interactions

Factor	Contrasts	Effect
A	-0.0580	-0.0048
B	-0.1065	-0.0089
C	-0.1742	-0.0145
AB	0.0004	3.3333E-05
AC	-0.0260	-0.0022
BC	0.0414	0.0035
ABC	-0.0020	-0.0002

The contrasts were used to calculate the sum of squares (SS) as shown in equation (6-8) under Appendix 16. The Pareto plot, Figure 5-34,was developed using the SS and the percentage of the cumulative SS. The x-axis indicates the factors and interactions, and the primary and secondary (y-axis) indicates SS and % cumulative percentage, respectively.

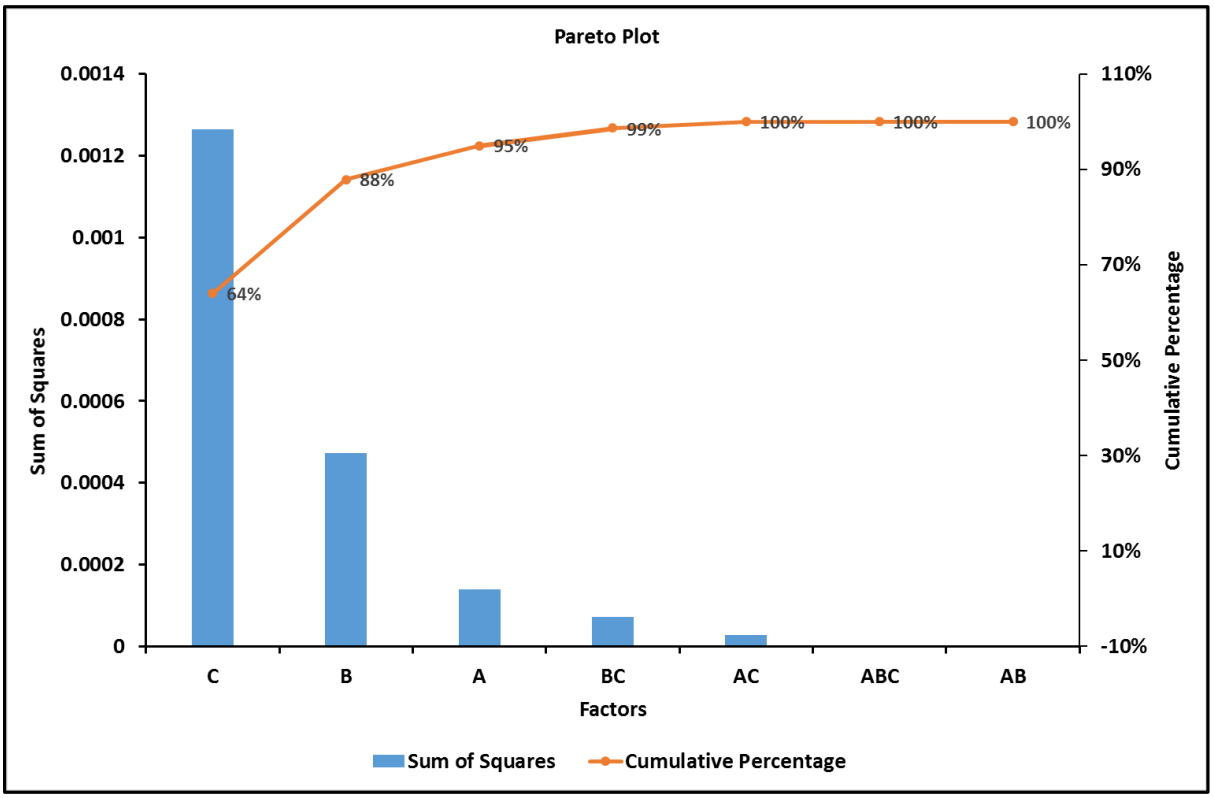

Figure 5-34: Pareto Plot of the factors and factor interactions versus SS and % cumulative SS

From Figure 5-34, 99% cumulative percentage was contributed by the polymeric coagulant dosage, air scouring rate, frequency of air scouring and the interaction between air scouring and the frequency of air scouring. The major contributingfactor was the polymeric coagulant dosage**(C)**at 64% followed by the air scouring rate**(B)** at 24%, the air scouring frequency (A) at 7%. The interaction of the air scouring rate and the air scouring frequency**(BC)**was 4%. The remaining interacting factors (**AB, AC, and ABC**) contributed less than 1% to the rate of membrane resistance increase. Therefore, the effect of these interacting input factors on the rate of membrane resistance increase was negligible and not considered in the development of the regression model.

5.4.5 Regression model and surface plot

A regression model was used to determine the treatment combination that will result in the lowest rate of membrane resistance increase. The calculated effects of the identified factors developed the regression model. The effect of each contributing factor was halved and used in developing the regression model (Montgomery (2013)).

$$\gamma = \beta_0 + A(\frac{\text{Main effect}}{2}) + B(\frac{\text{Main effect}}{2}) + C(\frac{\text{Main effect}}{2}) + BC(\frac{\text{Main effect}}{2})$$

$$\gamma = \beta_0 + A(\frac{-0.0048}{2}) + B(\frac{-0.0089}{2}) + C(\frac{-0.0145}{2}) + \frac{0.0035}{2}(BC) \qquad \text{Equation (5-1)}$$

β_0= is the average of all rate of change in membrane resistance = 0.0160

$$\gamma = 0.0160 - 0024*A - 0.0045*B - 0073*C + 0.0017*BC \qquad \text{Equation (5-2)}$$

Negative main effects indicated the following:

i. The rate of membrane resistance increase reduced with increasing air scouring frequency from 50% to 100%.
ii. The rate of membrane resistance increase reduced with increasing air scouring rate from 1 $m^3/m^2.h$ to 5 $m^3/m^2.h$.
iii. The rate of membrane resistance increase reduced with increased polymeric coagulant dosage from 0 mg/l (no addition) to 1 mg/l.

The effect of the air scouring rate and the air scouring frequency interaction was positive. The positive effect indicated that the combination of air scouring rate and air scouring frequency increased the rate of membrane resistance increase.

5.4.5.1 : Response surface plot blocked by coagulant dosage

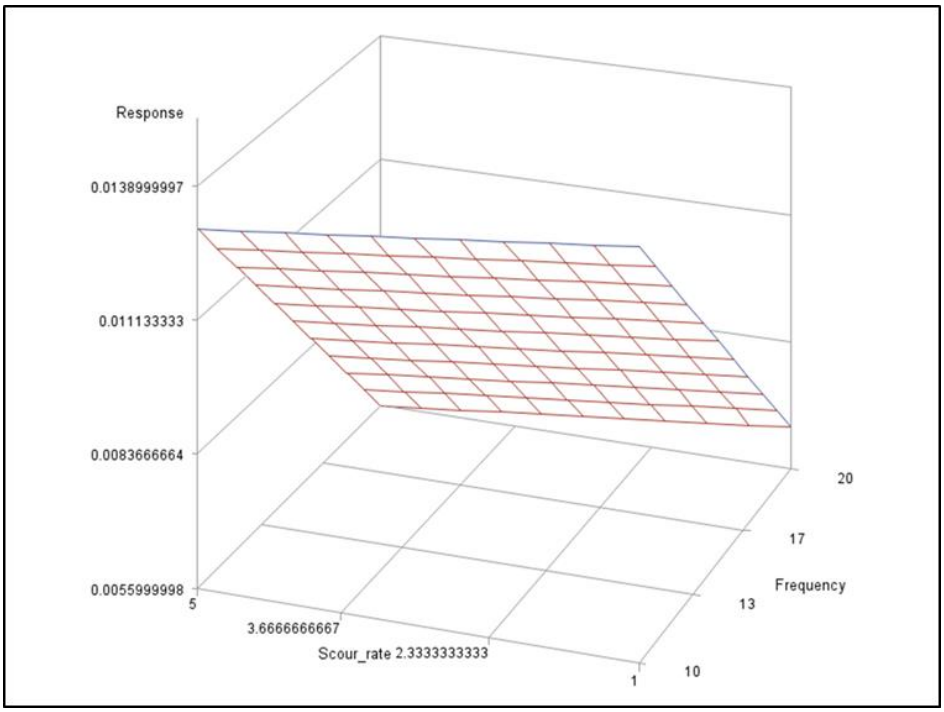

Figure 5-35: Response surface plot for 1 mg/l coagulant dosage treatment combination.

From Figure 5-35, the response surface plot graph, the lowest rate of membrane resistance increase was obtained at a higher air scour rate and continuous air scouring frequency. The surface plot indicated that the air scouring frequency was a critical input factor as compared to the air scouring rate.

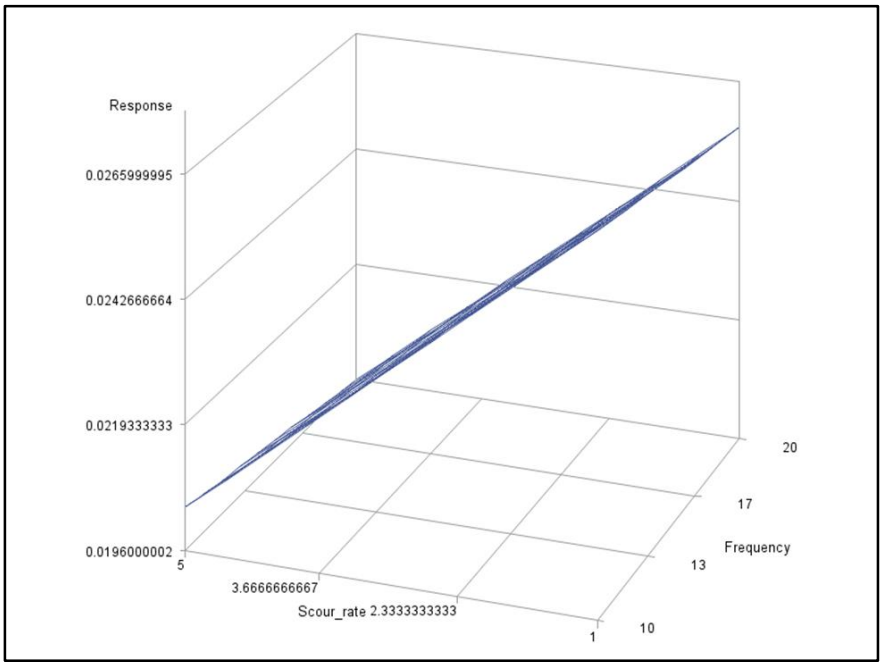

Figure 5-36: Response surface plot without coagulant dosage treatment combination

Figure 5-36 indicates that both the air scour rate and the frequency of air scouring were the critical input factors in lowering the rate of membrane resistance increase.

5.4.6 Validation of the regression model

Two treatment combinations were used on the validation of the regression model. The two treatment combinations, together with the predicted rate of membrane resistance increase, are shown in Table 5-8 below. Figure 5-37and Figure 5-38 show the experimental data validated against the regression model.

Table 5-8: Treatment combinations and the predicted rate of membrane resistance increase using the regression model (Equation 5-2).

Air scour frequency	Air scour rate	Coagulant dose	The predicted rate of resistance increase (x 10^{12} $m^{-1}.min^{-1}$)
- (periodic)	+(5)	+ (1 mg/l)	0.0083
+ (continuous)	+ (5)	+ (1 mg/l)	0.0035

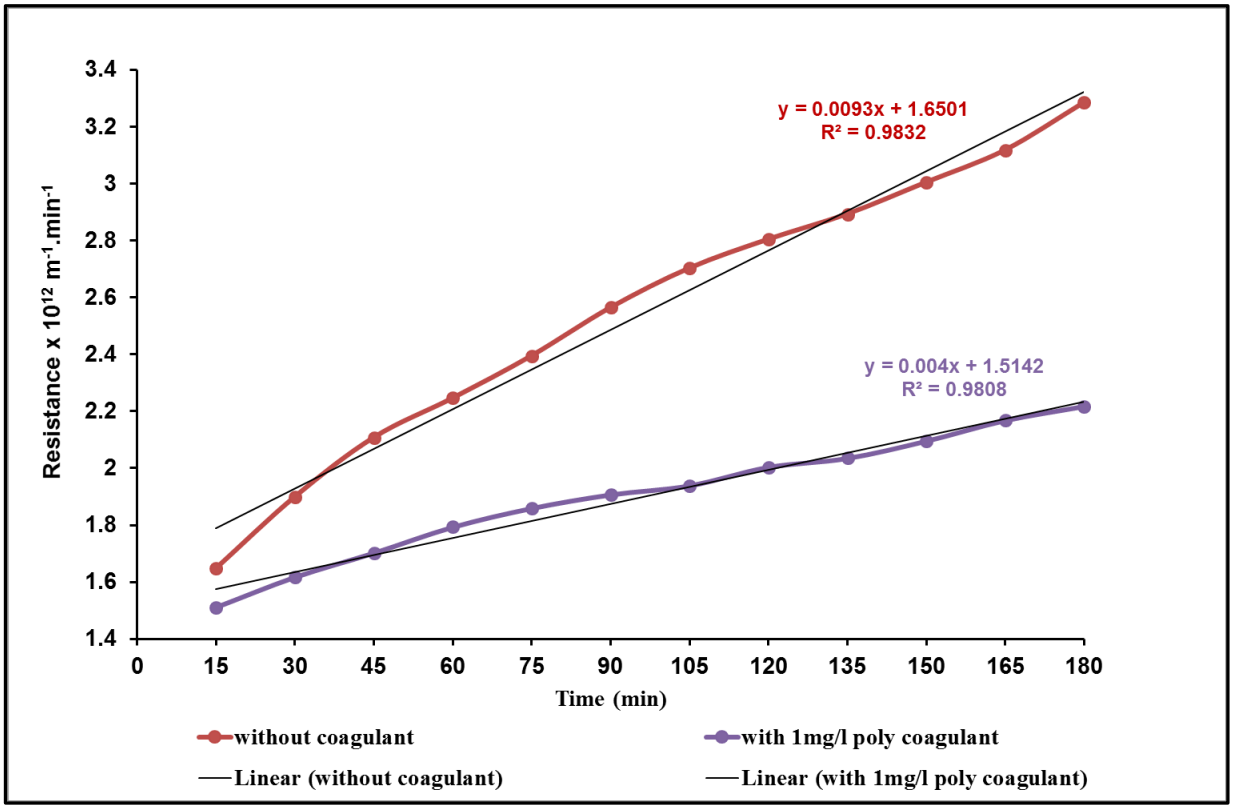

Figure 5-37: Rate of membrane resistance increase at 3 hours filtration run time

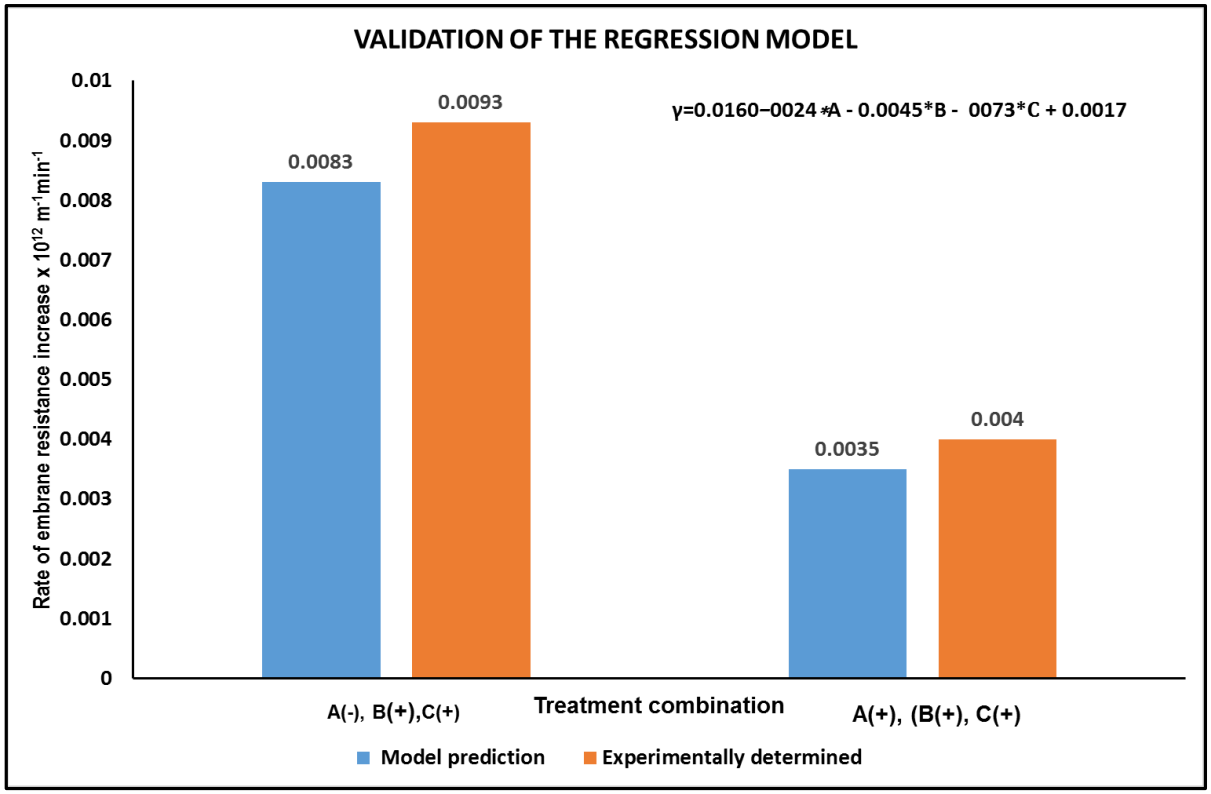

Figure 5-38: Comparison of the predicted value of the rate of membrane resistance increase and the experimentally determined value

The percentage difference between the predicted value and the experimentally determined rate of membrane resistance increase for the A(-)B(+)C(-) treatment combination was 11%. The difference was higher than 10%, and therefore the model required further optimization. Similarly, with the A(+)B(+)C(-) treatment combination, the percentage difference between the predicted value and experimental value was 13%. The predicted values of the rate of membrane resistance increase and the experimentally determined values were moderately similar. The developed regression model was reasonably accurate but required further optimization to improve accuracy.

5.5 Impact of the findings

Polymeric coagulant addition contributed significantly tominimisingthe rate of membrane resistance increase. The results showed that 1mg/l polymeric coagulant dosage was sufficient to effect a significant reduction on rate of membrane resistance increase. Excessive polymeric coagulant additionhad a detrimental effect on the rate of membrane resistance increase.

The use of air scouring during permeation reduced the rate of membrane resistance increase. However, higher air scouring rates seeminglybroke flocs into tiny particles plugging the membrane pores, hence causing an increase in the rate of membrane resistance increase.

Bubbles produced by the spargers with smaller pore sizes reduced the rate of membrane resistance increase. The rate of membrane resistance increase reduced with increasing air scouring frequency.The effect of the interaction of the air scouring rate and the frequency of air scouringon the rate of the membrane resistance increase is dependent on individual factors.

CHAPTER 6 CONCLUSIONS AND RECOMMENDATIONS

6.1 Conclusions

This study investigated the effects of polymeric coagulant dosage, air scouring rate and the frequency of air scouring on the rate of membrane fouling and final water quality in a submerged UF membrane systemfiltering Vaal Dam raw water. The rate of membrane resistance increase was used as a measure of therate of membrane fouling.

Firstly the individual effects of polymeric coagulant dosage, air scouring rate and the frequency of air scouring was investigated using an OFAT approach. The findings were as follows:

i. The rate of membrane fouling was highwith no coagulant (0 mg/l polymeric coagulant dosage). The rate of membrane fouling reduced significantly for polymeric coagulant dosage in the range 1 – 8 mg/l (particle destabilisation region). There was an insignificant difference in the rate of membrane fouling when polymeric coagulant dosages of 1, 3,5 and 8 mg/l were applied. The excessive polymeric dosages of 20, 26 and 32 mg/l (restabilization region) increased the rate of membrane fouling. The residual polymeric coagulant accumulation on the membrane surface caused membrane blinding, and hence an increase in the rate of membrane fouling.The rate of membrane fouling was similar at 0, 20, 26 and 32 mg/l polymeric coagulant dosages.

ii. Air spargers with smaller pore sizes (1mm and 2mm) resulted in a reduction in the rate of membrane fouling. The spargers with bigger pore sizes had an insignificant effect on the rate of membrane fouling.

iii. The air scouring rate in the range of 1 m^3/m^2.hto 5 m^3/m^2.h reduced the rate of membrane fouling. Air scouring rates higher than 5 m^3/m^2.h increased the rate of membrane fouling.The higher air scouring rate broke the formed microflocs into smaller particles blocking the membrane pores, hence the higher rate of membrane fouling.

iv. The continuous (100%) and 75% periodic air scouring frequency resulted in a significantly reduced rate of membrane fouling.The 0% and 25% periodic air scouring frequency adversely affect the rate of membrane fouling.

Based on the above scanning and validation investigations, polymeric coagulant dosages of 0 mg/l and 1 mg/l, air scouring rates of 1 m^3/m^2.h and 5 m^3/m^2.h and the 50% and 100% air scouring frequencies were selected for a three-factors two-levels DoE. The DoE had eight (8) treatment combinations (experiments). The outcomes of the DoE were as follows:

i. All eight treatment combinations achieved a 2.2 log turbidity removal. The average permeate turbidity was 0.15NTU in all treatment combinations.

   a. There were no HPC, TC and E. coli detected on the permeate.
   b. The UF membrane did not remove any TDS.
   c. The UF membrane removed approximately 43% of the NOM fraction, mostly hydrophobic.
   d. The SUVA value was reduced from 4.5 l/mg C.m^{-1}on the raw water to 2.7 l/mg C.m^{-1} on the permeate.

ii. The treatment combinations of (1 mg/l polymeric coagulant dosage; 5 m^3/m^2.h air scouring rate; 100% air scouring frequency) and (1 mg/l polymeric coagulant dosage; 1 m^3/m^2.h air scouring rate; 100% frequency) resulted in the lowest rate of membrane fouling.

iii. The treatment combinations of (0 mg/l polymeric coagulant dosage; 5 m^3/m^2.h air scouring rate; 50% air scouring frequency) and (0 mg/l polymeric coagulant dosage; 1 m^3/m^2.h air scouring rate; 50% frequency) resulted in the highest rate of membrane fouling.

iv. The treatment combinations of (1 mg/l polymeric coagulant dosage; 5 m^3/m^2.h air scouring rate; 50% air scouring frequency) and (1 mg/l polymeric coagulant dosage; 1 m^3/m^2.h air scouring rate; 50% frequency) resulted in a moderate rate of membrane fouling.

v. The Pareto plot showed that the polymeric coagulant is the most critical factor in minimising the rate of membrane fouling followed by the air scouring rate and lastly the air scouring frequency.

vi. The interaction of the air scouring rate and frequency of air scouring had a marginal effect on the rate of membrane fouling.

vii. The other interactions such as polymeric coagulant and air scouring rate, polymeric coagulant and air scouring frequency and polymeric coagulant, air scouring rate, air scouring frequency had minimal effect on the rate of membrane fouling.

In summary, the UF membrane system operated at 1mg/l polymeric coagulant, air scouring rate of either 1 m^3/m^2.h or 5 m^3/m^2.h and 100% air scouring frequency had a similar rate of membrane fouling when the UF membrane system was operated at 1mg/l polymeric coagulant, air scouring rate of either 1 m^3/m^2.h or 5 m^3/m^2.h and 50% air scouring frequency.

The results indicates contionous air scouring with polymeric coagulant dosage significantly minimise the rate of membrane fouling, periodic air scouring maybe the cost effective method of membrane operation as it will reduce the air blower energy consumption by 50%. Futhermore, the rate of

membrane fouling between periodic and continuous air scouring when polymeric coagulant was applied were reasonably similar.

6.2 Recommendations

Future studies should include the following:

i. Application of the inorganic coagulants as pre-treatment to low-pressure membrane filtration system for raw water with high turbidity.

ii. The effects of filtration run time longer than 60 min on the membrane restoration (irreversible fouling).

iii. The effect of mechanical backwashing on the irreversible fouling.

iv. The effects of other membrane materials.

v. The effect of coagulant dosage on pressurised UF/MF fouling rate.

vi. The rate of membrane fouling on a membrane module with slacked membrane fibres when air scouring is applied.

REFERENCES

Akhondi, E., Wicaksana, F., & Fane, A. G. (2014). Evaluation of fouling deposition, fouling reversibility and energy consumption of submerged hollow fibre membrane system with periodic backwash. *Journal of membrane science, 452*, 319 - 331.

Ang, W. L., & Mohamma, A. (2015). Mathematical modeling of membrane operations for water treatment. In B. Angelo, C. Alfredo, & R. K. Navin (Eds.), *Advances in Membrane Technologies for Water Treatment - Materials, Processes and Applications* (pp. 379 -407). Cambridge: Woodhead Publishing is an imprint of Elsevier.

Ao, L., Liu, W., Zhao, L., & Wang, X. (2016). Membrane fouling in ultrafiltration of natural water after pretreatment to different extents. *Journal of environmental sciences, 43*(Elsevier B.V.), 234 – 243.

Arnal, J., Garcia-Fayos, Verdu, B., & Lora, G. J. (2009). Ultrafiltration as an alternative membrane technology to obtain safe drinking water from surface water: 10 years of experience on the scope of the AQUAPOT project. *Desalination, 248*(Elsevier B.V.), 34 -41.

Atasi, K., Crawford, G., Hudkins, J. M., Livingston, D., Reardon, R., & Schmidt, H. (2006). Chapter 4: Low-pressure membranes for effluent filtration. In L. Hager, *Membrane systems for wastewater treatment* (pp. 1 (4.1) - 23 (4.7)). USA: McGraw Hill.

Atkinson, J. W., Palin, A., & Schull, K. E. (2010). *Chemical oxidation methods in water treatment.* Retrieved August 17, 2019, from https://doi.org/10.1080/10643387309381600

AWWA. (2005). *Microfiltration and Ultrafiltration Membranes for Drinking Water - manual of water supply practice -M53, First Edition.* United States of America: Glacier Publishing Services, Inc.

AWWA. (2010). *Algae - Source to Treatment - manual of water supply practices, M57 First Edition.* United States of America: Glacier Publishing Services, Inc.

AWWA. (2011). *Operational Control of Coagulation and Filtration Processes - Manual of Water Supply Practices - M37, Third Edition.* United States of America: American Water Works Association.

AWWA. (2016). *Microfiltration and Ultrafiltration Membranes for Drinking Water - manual of water supply practices - M53, Second Edition.* United States of America: Glacier Publishing Services, Inc.

AWWA, 2. (2016). *Microfiltration and Ultrafiltration Membranes for Drinking Water - Manual of Water Supply Practices—M53, Second Edition.* United States of America: American Water Works Association.

Botes, J., Jacobs, E., & Bradshaw, S. (1998). Long-term evaluation of a UF pilot plant for potable water production. *Desalination 115, 115*(Elsevier Science B.V.), 229 - 238.

Bradley, M. (2015). *ThermoFisher Scientific*. Retrieved March 14, 2020, from https://www.thermofisher.com/blog/materials/a-gift-for-you-an-ftir-basic-organic-functional-group-reference-chart/

Bratby, J. (2006). Chapter 3: Coagulants. In *Coagulation and Flocculation in Water and Wastewater Treatment* (pp. 31-69). London: IWA Publishing, London, UK.

Cabral, J. P. (2010). Water Microbiology. Bacterial Pathogens and Water. *Environmental Research and Public Health, 7*(doi:10.3390/ijerph7103657), 3657-3703;.

Carollo, E. (1997). *Carollo Engineering*. Retrieved November 6, 2018, from https://www.carollo.com/sites/default/files/docs/low-pressure-membranes.pdf

Chang, H., Liang, H., Qu, F., Liu, B., Yu, H., Du, X., . . . Snyder, S. A. (2017). Hydraulic backwashing for low-pressure membranes in drinking water treatment: A review. *Journal of Membrane Science 540 (2017) 362–380, 540*(Elsevier B.V), 362 - 380.

Chang, H., Liang, H., Qub, F., Liu, B., Yub, H., Dub, X., . . . Snyderc, S. A. (2017). Hydraulic backwashing for low-pressure membranes in drinking water treatment: A review. *Journal of Membrane Science, 540*(Elsevier B.V), 362 - 380.

Cohn, P. D., & Cox, M. (1999). Health and aesthetic aspects of water quality . In R. D. Letterman (Ed.), *Water quality and treatment - A Handbook of Community Water Supplies* (pp. 50 - 121). United States of America: McGraw-Hill.

Crittenden, J. C., Trussell, R. R., Hand, D. W., Howe, K. J., & Tchobanoglous, G. (2012). Coagulation and Flocculation. In J. H. Borchardt (Ed.), *MWH's Water Treatment* (pp. 541 - 637). Canada: John Wiley & Sons, Inc.

Crittenden, J. C., Trussell, R. R., Hand, D. W., Howe, K. J., & Tchobanoglous, G. (2012). Membrane filtration. In J. H. Borchardt (Ed.), *MWH's Water Treatment - Principles and Design* (pp. 819 - 901). Canada: John Wiley & Sons, Inc.

Crittenden, J. C., Trussell, R. R., Hand, D. W., Howe, K. J., & Tchobanoglous, G. (2012). Physical and Chemical Quality of Water. In J. H. Borchardt (Ed.), *MWH's Water Treatment* (pp. 17 - 71). Canada: John Wiley & Sons, Inc.

Cui, Z., Chang, S., & Fane, A. (2003). The use of gas bubbling to enhance membrane processes. *Journal of membrane science, 221*(Elsevier B.V.), 1-35.

Dar Lin, S. (2014). *Water and Wastewater Calculations Manual* (3 ed.). New York: McGraw Hill.

Davis, C. C., & Marc, E. (2014). Coagulation With Hydrolyzing Metal Salts:Mechanisms and Water Quality Impacts. *Critical Reviews in Environmental Science and Technology, 44:4*(DOI: 10.1080/10643389.2012.718947), 303-347.

DWS. (2019, June 3). *Department of Water and Sanitation*. Retrieved from The Reservoir: https://www.reservoir.co.za/

Fan, X., Tao, Y., Wang, L., Zhang, X. L., Wang, Z., & Noguchi, H. (2014). Performance of an integrated process combining ozonation with ceramic membrane ultra-filtration for advanced treatment of drinking water. *Desalination, 335*(Elsevier B.V.), 47 - 54.

Galvañ, C., Casas, S., Llombart, M., Mesa, J., Ferrer, O., Gibert, O., & Bernat, X. (2014). Direct pre-treatment of surface water through submerged hollow fibre ultrafiltration membranes. *Water Science & Technology: Water Supply, 14.3*(IWA Publishing), 461 - 469.

Gao, W., Liang, H., Ma, J., Han, M., Chen, Z.-l., Han, Z.-s., & Li, G.-b. (2011). Membrane fouling control in ultrafiltration technology for drinking water production: A review. *Desalination, 272*(Elsevier B.V.), 1-8.

Gora, S., Chaulk, M., & Sheppard, G. (2011). *Study on Characteristics and Removal of Natural Organic Matter in Drinking Water Systems in Newfoundland and Labrador.* Newfoundland: CBCL limited, consulting engineers.

Guigui, C., Bonnelye, V., Bourlier, D. L., Rouch, J. C., & Aptel, P. (2001). Combination of coagulation and ultrafiltration for drinking water production: impact of process configuration and module design. *Water Science and Technology: Water Supply , 1*(IWA Publishing), 107 - 118.

Guigui, C., Mougenot, M., & Cabassud, C. (2003). Air sparging backwash in ultrafiltration hollow fibres for drinking water production. *Water Science and Technology: Water Supply , 3*(IWA Publishing), 415 - 422.

Guigui, C., Roucha, J., Durand-Bourlier, B. L., & Aptel, V. P. (2002). Impact of coagulation conditions on the in-line coagulation/UF process for drinking water production. *Desalination, 147*(Elsevier Science B.V), 95 - 100.

Guo, C., Liu, B., Chen, C., Chang, H., Wang, S., He, M., & Crittenden, J. (2018). Development of an efficient approach for separating bubbles and flocs in a submerged membrane ultrafiltration process. *Water Science and Technology, 18:3*(IWA Publishing), 808 - 818.

Guo, W., Ngo, H.-H., & Vigneswaran, S. (2012). Fouling Control of Membranes with Pretreatment. In *membrane technology and environmental application* (pp. 533 - 578). Virginia: American Society of Civil Engineers.

Howe, K. J., Hand, D. W., Crittenden, J. C., Trussell, R. R., & Tchobanoglous, G. (2012). Chapter 8: Membrane filtration. In *Principles of water treatment* (pp. 281 - 326). Canada: John Wiley & Sons, Inc.

Howe, K. J., Hand, D. W., Crittenden, J., Trussell, R. R., & Tchobanoglous, G. (2012). Chapter 5: Coagulation and floccultion. In *Principles of water treatment* (pp. 139 - 188). Canada: John Wiley & Sons, Inc.

Howe, K. J., Hand, D. W., Crittenden, J., Trussell, R., & Tchobanoglous, G. (2012). Chapter 2: Water quality and public health. In *Principles of water treatment* (pp. 5-24). Canada: John Wiley & Sons, Inc.

Huang, H., Chwab, K., & Jacangelo, J. G. (2009). Pretreatment for Low Pressure Membranes in Water Treatment: A Review. *Environmental Science and Technology, 43 No.9*(American Chemical Society), 3011 - 3018.

John, W., & Trollip, D. (2009). *National Standards for drinking treatment chemicals.* South Africa: Water research commission.

Kao, C. M., Yang, B. M., Surampalli, R. Y., & Zhang, T. C. (2012). Limitation of Membrane Technology and Prevention of Membrane Fouling. In T. C. Zhang, R. Y. Surampalli, S. Vigneswaran, R. D. Tyagi, S. L. Ong, & C. M. Kao (Eds.), *Membrane technology and environmental applications* (pp. 504 - 525). Virginia: American Society of Civil Engineers.

Kawamura, S. (2000). Chapter 3: Design of basic treatment process units. In *Intergrated design and operation of water treatment facilities* (pp. 74 - 138). Canada: John Wiley & Sons.

Kawamura, S. (2000). Chapter 7: Specific water treatment processes. In *Intergrated design and operation of water treatment facilities* (pp. 579 - 594). Canada: John Wiley & Sons.

Khan, W. (2004). *Microbial interaction in drinking water systems.* Stellenbosch, South Africa: Stellenbosch University .

Kolarik, L., & Booker, N. (1995). Physcio-chemical process in water and wastewater treatment. In L. Kolarik, & A. Priestley (Eds.), *Morden techniques in water and wastewater treatment* (pp. 7 - 14). Australia: CSIRO Cataloguing.

Konieczny, K., Bodzek, M., & Rajca, M. (2006). A coagulation–MF system for water treatment using ceramic membranes. *Desalination, 198*(Elsevier B.V), 92 -101.

Konieczny, K., Sąkol, D., & Bodzek, M. a. (2006). Efficiency of the hybrid coagulation–ultrafiltration water treatment process with the use of immersed hollow-fiber membranes. *Desalination , 198*(Elsevier B.V.), 102 - 110.

Konno, H. (2016). X-ray Photoelectron Spectroscopy. In *Materials Science and Engineering of Carbon: Characterization* (pp. 153-171). Japan: Elsevier Inc.

Koyuncu, I., Sengur, R., Turken, T., Guclu, S., & Pasaoglu, M. (2015). Advances in water treatment by microfiltration, ultrafiltration and nanofiltration. In A. Basile, A. Cassano, & N. K. Rastogi (Eds.), *Advances in membrane technologies for water treatment - Materials, Processes and Applications* (pp. 84 - 127). United Kingdom: Elsevier Science & Technology.

Laîné, J., Campos, C., Baudin, I., & Janex, M. (2003). Understanding membrane fouling: a review of over a decade of research. *Water Science and Technology: Water Supply, 3*(IWA publishing), 155 - 164.

Lazarova, V., Gallego, S., Molina, V. G., & Rougé, P. (2007). *Problems of operation and main reasons for failure of membranes in tertiary treatment systems.* Retrieved July 20, 2019, from https://www.genesysro.com/uploads/docs/Problems_of_operation_and_main_reasons_for_failure_of_membrane_in_tertiary_treatment_systems.pdf

Lebeau, T., Lelievre, C., Buisson, H., Cleret, Van de Venter, D., W, L., & Cote, P. (1998). Immersed membrane filtration for the production of drinking water: combination with PAC for NOM and SOC removal . *Desalination, 117*(Elsevier Science B.V.), 219 - 231.

Lee, M., & Kim, J. (2012). Analysis of local fouling in a pilot-scale submerged hollow-fiber membrane system for drinking water treatment by membrane autopsy. *Separation and Purification Technology , 95*(Elsevier B.V.), 27 - 234.

Leopold, P., & Freese, S. D. (2009). *A simple guide to the chemistry, selection and use of vhemicals for water and wastewater treatment.* South Africa: Water Reaserch Commission - TT 405/09.

Letterman, R. D., Amirtharajah, A., & O'Melia, C. R. (1999). Chapter 6: Coagulation and Flocculation. In R. D. Letterman (Ed.), *Water quality and treatment - A Handbook of Community Water Supplies* (pp. 226 - 286). United States of America: McGraw-Hill, Inc.

Li, K., Liang, H., Qu, F., Shao, S., Yu, H., Han, Z. S., . . . Li, G. (2014). Control of natural organic matter fouling of ultrafiltration membrane by adsorption pretreatment: Comparison of mesoporous adsorbent resin and powdered activated carbon. *Journal of Membrane Science, 471*(ElsevierB.V.), 94 - 102.

Li, L., Wray, H. E., Andrews, R. C., & Bérubé, P. R. (2014). Ultrafiltration Fouling: Impact of Backwash Frequency and Air Sparging. *Separation Science and Technology, 49*(DOI: 10.1080/01496395.2014.948964), 2814 - 2823.

Li, M., Wu, G., Guan, Y., & Zhang, X. (2011). Treatment of river water by a hybrid coagulation and ceramic membrane process. *Desalination , 280*(Elsevier B.V.), 114 - 119.

Liang, S., Zhang, H., Zhao, Y., & Song, L. (2016). Performance Modeling and Analysis of a Hollow Fiber Membrane System. *Membrane Science & Technology, 6:1*(DOI: 10.4172/2155-9589.1000144), 3-8.

Liu, J., Liu, B., Liua, T., Bai, Y., & Yu, S. (2014). Coagulation–bubbling–ultrafiltration: Effect of floc properties on the performance of the hybrid process. *Desalination, 333*(Elsevier B.V.), 126-133.

Lok, A., Wray, H., Bérubé, P., & Andrews, R. C. (2017). Optimization of air sparging and in-line coagulation for ultrafiltration fouling control. *Separation and Purification Technology , 188*(Elsevier B.V.), 60 - 66.

Lu, Y., Ding, Z., Liu, L., Wang, Z., & Ma, R. (2008). The influence of bubble characteristics on the performance of submerged hollow fiber membrane module used in microfiltration. *Separation and Purification Technology , 61*(Elsevier B.V.), 89 - 95.

MacCormick, A. (1995). The application of microfiltration in water and wastewater treatment . In L. KOLARIK, & P. A.J (Eds.), *Modern techniques in water and wastewater treatment* (pp. 45 - 51). Australia: CSIRO Cataloguing.

Meier-Haacka, J., Bookerb, N., & Carrollc, T. (2003). A permeability-controlled microfiltration membrane for reduced fouling in drinking water treatment. *Water Research, 37*(Elsevier Science Ltd), 585 - 588.

Montgomery, D. C. (2013). Chapter 6: The 2k factorial design . In *Design and analysis of experiments* (pp. 233 - 292). United States: John Wiley & Sons, Inc.

Morrison, I. (2006). Treatment processes - Caogulation and Flocculation. In F. Schutte (Ed.), *Handbook for the operation of water treatment works* (pp. 76 - 92). South Africa: Water Research Commision - TT 265/06.

Mosqueda-Jimenez, D. B., Huck, P. M., & Basu, O. D. (2008). Fouling characteristics of an ultrafiltration membrane used in drinking water treatment. *Desalination 230 (2008) 79–91, 230*(Elsevier B.V.), 79 - 91.

Nakatsuka, S., Ase, T., & Miyano, T. (2010). High flux ultrafiltration membrane for drinking water production. *Water Science and Technology: Water Supply, 1 No. 5/6*(IWA Publishing), 177 - 184.

Nakatsuka, S., Nakate, I., & Miyano, T. (1996). Drinking water treatment by using ultrafiltration hollow. *Desalination 106 (1996) 55-61, 106*(Elsevier Science B.V.), 55 - 61.

Nguyen, S. T. (2012). *Mitigation of membrane fouling in microfiltration and ultrafiltration of activated sludge effluent for water reuse.* Melbourne, Australia: RMIT University, School of Civil, Environmental & Chemical Engineering, Department of Chemical Engineering.

Nkambule, T. I., Krause, R. W., Haarhoff, J., & Mamba, B. B. (2012). Natural organic matter (NOM) in South African waters: NOM characterisation using combined assessment techniques. *Water SA, 38 No5*(Water South Africa), 697 - 706.

Park, Y. J., & Kim, Y. C. (2014). Effect of Coagulation on Submerged Ultrafiltration Membrane. *APCBEE Procedia, 10*(B.V. Sele), 214 - 218.

Pearce, G., Stephenson, Daigger, T., Glen, Verrecht, B., Germain, E., . . . Le-Clech, P. (2011). Chapter 2: Fundamentals. In S. Judd, & J. Claire (Eds.), *Principles and Applications of Membrane Bioreactors for Water and Wastewater Treatment* (pp. 54 - 197). Oxford: Butterworth-Heinemann Elsevier.

Peiris, R. H., Budman, H., Moresoli, C., & Legge, R. L. (2013). Fouling control and optimization of a drinking water membrane filtration process with real-time model parameter adaptation using fluorescene and permeate flux measurement. *Journal of process control, 23*(Elsevier Ltd.), 70-77.

Porcelli, N., & Judd, S. (2010). Chemical cleaning of potable water membranes: A review. *Separation and Purification Technology, 71*(Elsevier B.V.), 137 - 143.

Povnnennykh, A. S. (1978). The use of infrareds pectra for the determination of minerals. *American Mineralogist, 63*, 956 - 959.

Proctor, C. R., & Hammes, F. (2015). Drinking water microbiology — from measurement to management. *Environmental biotechnology, 33*(Elsevier Ltd.), 87–94.

Ratnayaka, D., Lee, M. F., Tiew, K., . Chua, H., Sanmuganathan, D., Lim, D. H., . . . Currie, J. (2009). *Application of membrane technology to retrofit large-scale conventional water treatment plant in Singapore.* Singapore: Singapore public utility board.

Robinson, S., & Berube, P. R. (2020). Membrane ageing in full-scale water treatment plants. *Water Research, 169*(Elsevier Ltd), 1-11.

Rojas-Serrano, F., Perez, J. I., & Gomez, M. A. (2015). Integrated in-line coagulation-aerated ultrafiltration for drinking-water production: A case study from laboratory to pilot plant. *Environmental Science and Health, Part A 50:13, 50*(DOI: 10.1080/10934529.2015.1064284), 1376 -1385.

SANS-241_1. (2015). *SANS 241-1: 2015 Microbiological, physical, aesthetic and chemical determinands.* South Africa: SABS standards division.

SANS-241_2. (2015). *SANS 241 Application of SANS 241-1.* South Africa: SABS standards division.

Schutte, F. (2006). Part A: Introduction to water quality and treatment. In F. Schutte (Ed.), *Handbook for the operation of water treatment works* (pp. 3-58). South Africa: Water Research commission TT 265/06.

Shon, H., Phuntsho, S., Vigneswaran, S., Kandasamy, J., R, A., & Jegatheesan, V. (2012). Physical, Chemical, and Biological Characterization of Membrane Fouling. In T. C. Zhang, R. Y. Surampalli, S. Vigneswaran, R. D. Tyagi, S. L. Ong, & C. M. Kao (Eds.), *Membrane technology and environmental applications* (pp. 457 - 499). Virginia: American Society of Civil Engineers.

Singh, R. (2015). Chapter 1: Introduction to membrane technology. In *Membrane technology and engineering for water purification* (pp. 1-79). Colorado Springs: Butterworth-Heinemann.

Singh, R. (2015). Chapter 1: Introduction to Membrane Technology. In R. Singh (Ed.), *Membrane technology and engineering for water purification - Application, Systems Design and Operation* (pp. 1 - 78). Oxford: Butterworth-Heinemann Elsevier.

Smith, R. (1995). Membrane processes: An overview. In L. Kolarik, & A. Priestley (Eds.), *Morden techniques in water and wastewater treatment* (pp. 41 - 43). Australia: CSIRO Cataloguing.

Szymanska, K., Zouboulis, A., & Zamboulis, D. (2014). Hybrid ozonation–microfiltration system for the treatment of surface water using ceramic membrane. *Journal of Membrane Science 468(2014)163–171, 468*(ElsevierB.V.), 163 - 171.

Taylor, J. S., & Wiesner, M. (1999). Chapter 11: Membranes. In R. D. Letterman (Ed.), *Water quality and treatment - A Handbook of Community Water Supplies* (pp. 629 - 695). United States of America: McGraw-Hill, Inc.

Tian, J.-y., Xu, Y.-p., Chen, Z.-l., & Nan Jun, L. G.-b. (2010). Air bubbling for alleviating membrane fouling of immersed hollow-fiber membrane for ultrafiltration of river water. *Desalination 260 (2010) 225–230, 260*(Elsevier), 225 - 230.

Tng, K., Antony, A., Wang, Y., & Leslie, G. (2015). Membrane ageing during water treatment: mechanisms, monitoring, and control. In A. Basile, A. Cassano, & N. K. Rastogi (Eds.), *Advances in Membrane Technologies for Water Treatment - Materials, Processes and Applications* (pp. 349 - 378). USA: Woodhead Publishing.

Tuan, L. A. (2008). *Treatment of surface water and municipal wastewater by hybrid ceramic microfiltration systems.* Thailand: Asian Institute of Technology, School of Environment, Resources and Development.

Twain, M. (2015). Water and Membrane Treatment. In R. SINGH (Ed.), *Membrane technology and engineering for water purification* (pp. 81 - 175). Oxford,: Butterworth-Heinemann Elsevier.

Van Doesburg, J., Pease, S., & Sherman, M. (2009). Immersed ultrafiltration membranes for treatment of organically laden surface water. Hurghada, Egypt: International Water Technology Conference, IWTC 13.

van Duuren, F. A. (1997). *Water Purification Works Design.* South Africa: Water Reaserch Commission.

Vigneswaran, S., Nguyen, T. V., Kandasamy, J., Aimc, B. R., & Visvanathan, C. (2012). Membrane Processes for Drinking Water Treatment. In T. C. Zhang, S. R. Y, S. Vigneswaran, R. D. Tyagi, L. Ong See, & C. M. Kao (Eds.), *Membrane technology and environmental applications* (pp. 140 -167). Virginia: American Society of Civil Engineers.

Vincent, D. N., Cabassud, C., & Cabassud, M. (2000). Neural networks for long term prediction of fouling and backwash efficiency in ultrafiltration for drinking water production. *Desalination, 131*(ELSEVIER), 353-362.

Walsh, M., Zhao, N., Gora, S., & Gagnon, G. (2009). Effect of coagulation and flocculation conditions on water quality in an immersed ultrafiltration process. *Environmental Technology, Vol. 30, No. 9,*(Taylor & Francis), 927-938.

Wang, D. (2016). Raw water quality assessment for the treatment of drinking water. *Environmental Earth Science, 75:1327*(pringer-Verlag), 1- 9.

Wang, Z., Nan, J., Yao, M. ,., & Yang, Z. X. (2017). Insight into the combined coagulation-ultrafiltration process: The role of Al species of polyaluminum chlorides. *Journal of Membrane Science 529 (2017) 80–86, 529*(Elsevier B.V.), 80 - 86.

Watanabe, Y., Kimura, K., H, Y., Yonekawa, H., & T, S. (2009). Mechanism and Control of Membrane Fouling in Water Purification. Kobe: 8th International Symposium on Water Supply Technology.

WHO. (2011). *Guidelines for Drinking-water Quality - Fourth Edition .* Switzerland: World Health Organization.

Xia, S., Li, X., Liu, R., & Li, G. (2004). Study of reservoir water treatment by ultrafiltration for drinking water production. *Desalination , 167*(Elsevier B.V.), 23 - 26.

Xia, S., Li, X., Liu, R., & Li, G. (2005). Pilot study of drinking water production with ultrafiltration of water from the Songhuajiang River (China). *Desalination, 179*(ELSEVIER), 369 - 374.

Xing, J., Liang, H., Cheng, X., Yang, H., Xu, D., Gan, Z., & Luo, X. (2018). Combined effects of coagulation and adsorption on ultrafiltration membrane fouling control and subsequent

disinfection in drinking water treatment. *Environmental Science and Pollution Research, 16-1*(Springer-Verlag), 18 - 24.

Yao, M., Nan, J., Chen, T., Zhan, D., Li, Q., Wang, Z., & Li, H. (2015). Influence of flocs breakage processon membrane fouling in coagulation/ultrafiltrationprocess—Effect of additional coagulant of poly-aluminumchloride and polyacrylamide. *Journal of MembraneScience 491(2015), 491*(ElsevierB.V.), 63–72.

Yu, W. Z., Liu, H. J., Xu, L., Qu, J. H., & Graham, N. (2013). The pre-treatment of submerged ultrafiltration membrane by coagulation—Effect of polyacrylamide as acoagulant aid. *Journal of Membrane Science, 446*(Elsevier B.V.), 50-58.

Yu, W., & Graham, N. J. (2015). Performance of an integrated granular media – Ultrafiltration membrane process for drinking water treatment. *Journal of Membrane Science, 492*(Elsevier B.V.), 164 - 172.

Yu, W., Yang, Y., & Graham, N. (2016). Evaluation of ferrate as a coagulant aid/oxidant pretreatment for mitigating submerged ultrafiltration membrane fouling in drinking water treatment. *Chemical Engineering Journal, 298*(Elsevier B.V.), 234 - 242.

Yu, W., Zhang, D., & Graham, N. J. (2017). Membrane fouling by extracellular polymeric substances after ozone pre-treatment: Variation of nano-particles size. *Water Research, 120*(Elsevier Ltd.), 146 - 155.

Zhang, Y., Zhao, X., Zhang, X., & Peng, S. (2015). A review of different drinking water treatments for natural organic matter removal. *Water Science & Technology: Water Supply, 15.3*(IWA Publishing), 442 - 455.

Zirehpour, A., & Rahimpour, A. (2016). *Membranes for wastewater treatment: Application.* Iran: Scrivener Publishing LLC.

Zsirai, T., Buzatu, P., Aerts, P., & Judd, S. (2012). Efficacy of relaxation, backflushing, chemical cleaning and clogging removal for an immersed hollow fibre membrane bioreactor. *Water research, 46*(Elsevier Ltd.), 4499 - 4507.

Zupančič, M., Novak, D., Diaci, J., & Golobič, I. (2014). An evaluation of industrial ultrafiltration systems for surface water using. *Desalination 344 (2014) 321–328, 344*(Elsevier B.V.), 321 - 328.

APPENDICES

Appendix 1. Jar test procedure

MATERIALS

i. PHIPPS and BIRD 6 paddle programmable jar stirrer
ii. Concentrated polymeric coagulant
iii. 1 x HACH 2100Q Turbidimeter
iv. 10 x 10mL plastic syringes
v. 50 L of Vaal Dam raw water sample
vi. 1 x 1000mL volumetric flask
vii. 1 x 1000mL measuring cylinder
viii. 6 x 1000mL tall form beakers
ix. 6 x 60mL plastic syringe

PROCEDURE

i. Prepare 1000 mg/L polymeric coagulant solution by weighing 1g of the concentrated polymeric coagulant into 1000 mL of distilled or deionized water in a volumetric flask.
ii. Shake the solution properly to form a homogeneous solution.
iii. Allow the solution to stand for 1 h.
iv. Determine the turbidity of the raw water sample using the turbidimeter, as per the instrument instruction manual.
v. Measure 1000mL of raw water using a measuring cylinder and transfer it into each of the six 1000 tall form beakers.
vi. Place the beaker into the jar stirrer and immerse the blades into the beaker containing raw water samples
vii. Centre the beakers on the 6 paddle jar stirrer.
viii. Calculate the volumes of stock solution needed to achieve the target dosages (C_{beaker}).

$$C_{stock}V_{stock} = C_{beaker}V_{beaker}V_{stock} = (C_{beaker}V_{beaker})/C_{stock}$$

ix. Measure out the correct volumes of polymeric coagulant stock solution into 10 mL small syringes and for six beakers containing 1000 mL of raw water samples.

x. Start the mixers at 300 RPM speed. When you are ready to start timing, add the pre-measured polymeric coagulant stock to all the beakers simultaneously. After 30 s, reduce the mixer's speed to 60 rpm and allow it to stir for 10 minutes.

xi. After stirring for 10 minutes at 60 rpm, turn off the mixer and allow the formed agglomerates to settle for 15 minutes.

xii. Use the 60 ml plastic syringe and draw 50 mL of supernatant from each beaker and measure the turbidities of these samples.

xiii. Plot turbidity as a function of polymeric coagulant dosed.

Appendix 2. Process and instrumentation diagram

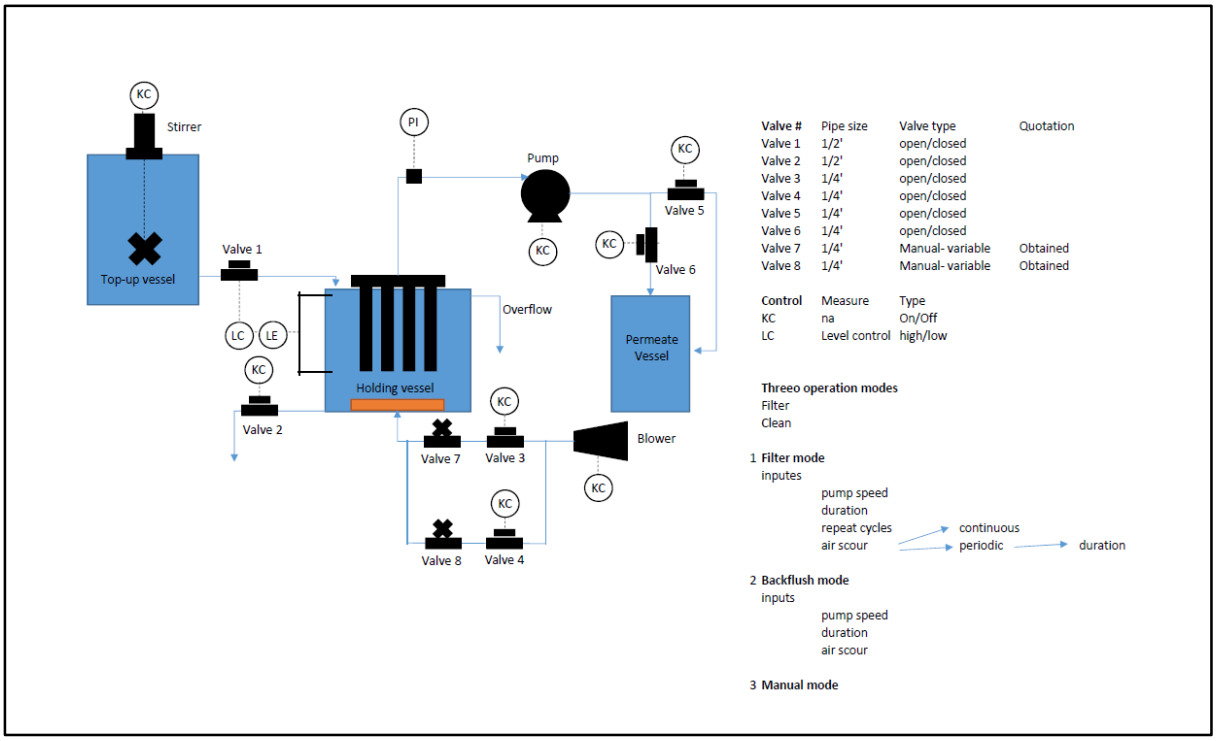

Valve #	Pipe size	Valve type	Quotation
Valve 1	1/2'	open/closed	
Valve 2	1/2'	open/closed	
Valve 3	1/4'	open/closed	
Valve 4	1/4'	open/closed	
Valve 5	1/4'	open/closed	
Valve 6	1/4'	open/closed	
Valve 7	1/4'	Manual- variable	Obtained
Valve 8	1/4'	Manual- variable	Obtained

Control	Measure	Type
KC	na	On/Off
LC	Level control	high/low

Threeo operation modes
Filter
Clean

1 **Filter mode**
inputes
pump speed
duration
repeat cycles → continuous
air scour → periodic → duration

2 **Backflush mode**
inputs
pump speed
duration
air scour

3 **Manual mode**

Appendix 3. Table of the rate of membrane resistance increase

Air scour frequency)	Air scour rate $m^3/m^2.h$	Coagulant dosage, mg/L	The rate of membrane resistance increase, (x 10^{12} $m^{-1}.min^{-1}$)
Periodic	1	0	0.0266
Periodic	1	0	0.0297
Periodic	1	0	0.0294
Continuous	1	0	0.0257
Continuous	1	0	0.0274
Continuous	1	0	0.024
Periodic	5	0	0.0204
Periodic	5	0	0.0198
Periodic	5	0	0.0215
Continuous	5	0	0.0196
Continuous	5	0	0.0172
Continuous	5	0	0.0175
Periodic	1	1	0.0139
Periodic	1	1	0.0114
Periodic	1	1	0.0125
Continuous	1	1	0.0056
Continuous	1	1	0.0055
Continuous	1	1	0.0052
Periodic	5	1	0.013
Periodic	5	1	0.0105
Periodic	5	1	0.012
Continuous	5	1	0.0046
Continuous	5	1	0.004
Continuous	5	1	0.0045

Appendix 4. Summary results of the rate of membrane resistance increase.

	Factors			Rate of membrane resistance increase (x 10^{12} $m^{-1}.min^{-1}$)			
Design Run	**Air scour frequency (A)**	**Air scour rate (B)**	**Coagulant dose (C)**	**Labels**	**1**	**2**	**3**
1	Low	Low	Low	1	0.027	0.029	0.029
2	High	Low	Low	a	0.028	0.024	0.027
3	Low	High	Low	b	0.02	0.022	0.02
4	High	High	Low	ab	0.016	0.018	0.017
5	Low	Low	High	c	0.013	0.011	0.0139
6	High	low	High	ac	0.0052	0.0055	0.0056
7	Low	High	High	bc	0.012	0.011	0.013
8	High	High	High	abc	0.0045	0.004	0.0046

Appendix 5. Jar test experiments replicate results

Polymer dosage (mg/l)	Settled Turbidity (NTU)	Polymer dosage (mg/l)	Settled Turbidity (NTU)	
	run 1		run 2	run 3
0	28	0	16.7	25.6
0.2	26.9	0.2	16.6	25.5
0.4	25.8	0.4	16.6	25.6
0.6	24.5	0.6	16.3	25.3
0.8	18.4	0.8	16.4	24.8
1	13.3	1	15.9	23.6
1.2	10.5	1.2	15.8	21.6
1.4	9.96	1.4	12.7	20.1
1.6	8.35	1.6	12.8	17.8
1.8	7.78	1.8	12.6	16.9
2	6.42	2	11.7	14.8
2.5	5.82	3	9.5	9.4
3	5.37	4	6.89	8.11
4	4.49	5	5.81	7.62
5	4.07	6	3.69	5.88
6	3.42	7	3.42	4.64
7	3.4	8	2.11	3.35
8	3.1	9	1.47	2.69
9	3.08	10	1.4	2.39
10	2.9	12	1.81	1.99
12	2.89	14	1.69	2.32
14	2.52	16	4.88	2.8
16	2.82	18	7.6	4.41
18	3.13	20	7.48	6.76
20	3.95	22	11.7	9.36
23	7.62	25	13.3	15.7
25	9.97	30	20	23.3
26	10.8			
29	14.3			
30	15.8			

Appendix 6. Validadtion of rate of membrane resistance increase at different sparger pore sizes

run 1		
Sparger pore size (mm)	**Air scour rate $m^3/m^2.h$**	**Rate of membrane resistance increase (x 10^{12} m^{-1}. min^{-1})**
1mm	1 $m^3/m^2.h$	0.0257
	3 m3/m2.h	0.0207
	5 $m^3/m^2.h$	0.0149
2mm	1 $m^3/m^2.h$	0.0273
	3 m3/m2.h	0.0234
	5 $m^3/m^2.h$	0.0146
3mm	1 $m^3/m^2.h$	0.0229
	3 m3/m2.h	0.02
	5 $m^3/m^2.h$	0.0152
4mm	1 $m^3/m^2.h$	0.0249
	3 m3/m2.h	0.0238
	5 $m^3/m^2.h$	0.0207

run 2		
Sparger pore size (mm)	**Air scour rate $m^3/m^2.h$**	**Rate of membrane resistance increase (x 10^{12} m^{-1}. min^{-1})**
1	1	0.0229
	3	0.0194
	5	0.0154
2	1	0.0305
	3	0.0236
	5	0.0144
3	1	0.0305
	3	0.0181
	5	0.0146
4	1	0.0262
	3	0.0238
	5	0.0207

run 3		
Sparger pore size (mm)	**Air scour rate $m^3/m^2.h$**	**Rate of membrane resistance increase (x 10^{12} m^{-1}. min^{-1})**
1mm	1 $m^3/m^2.h$	0.0271
	3 m3/m2.h	0.0214
	5 $m^3/m^2.h$	0.0151
2mm	1 $m^3/m^2.h$	0.0267
	3 m3/m2.h	0.0228
	5 $m^3/m^2.h$	0.015
3mm	1 $m^3/m^2.h$	0.0221
	3 m3/m2.h	0.019
	5 $m^3/m^2.h$	0.0149
4mm	1 $m^3/m^2.h$	0.0247
	3 m3/m2.h	0.0241
	5 $m^3/m^2.h$	0.0197

Appendix 7. Validation of rate of membrane resistance increase at different polymeric coagulant dosages

Coagulant dosage, mg/l	Rate of membrane resistance increase, (x $10^{12} m^{-1}. min^{-1}$)		
	run 1	run 2	run 3
0	0.018	0.0195	0.0203
1	0.0073	0.0111	0.0121
3	0.0068	0.0113	0.0087
8	0.0068	0.0102	0.0095
20	0.0192	0.0189	0.0145
26	0.0186	0.0197	0.0157
32	0.022	0.0259	0.0173

MEMBRANE FLUX, (LMH)

RUN 1

	Polymeric coagulant dosage, mg/l						
Run time, min.	0	1	3	8	20	26	32
5	65.88	72.94	74.12	74.11	115.29	114.12	114.12
10	62.35	70.59	71.76	71.75	115.29	114.12	114.12
15	60.00	69.41	70.59	70.58	114.12	112.94	111.76
20	57.65	68.24	69.41	69.40	112.94	112.94	111.76
25	57.65	67.06	68.82	67.05	112.94	112.94	110.59
30	55.29	64.71	68.24	65.87	112.35	111.76	110.59
35	54.12	62.35	66.47	64.69	111.76	111.76	110.59
40	52.94	61.76	64.71	63.52	111.76	110.59	109.41
45	50.59	60.00	63.53	62.93	111.76	110.59	109.41
50	49.41	58.82	62.94	62.34	111.41	109.41	108.24
55	48.24	58.24	62.35	62.34	111.29	109.41	108.24
60	47.06	57.65	61.76	61.16	111.18	108.24	108.24

RUN 2

	Polymeric coagulant dosage, mg/l						
Run time, min.	**0**	**1**	**3**	**8**	**20**	**26**	**32**
5	106.74	115.30	112.85	116.86	107.34	98.36	103.97
10	100.51	113.79	110.80	111.07	101.14	95.00	100.00
15	95.45	110.79	108.48	109.41	96.14	92.00	97.00
20	93.21	108.10	105.96	108.19	94.00	90.00	97.00
25	93.00	105.53	104.15	106.00	93.00	89.00	95.00
30	91.30	103.69	102.73	103.96	90.00	88.00	93.00
35	88.40	102.39	101.98	102.28	88.00	87.00	90.00
40	84.60	101.12	100.83	101.52	85.00	85.00	88.00
45	83.10	99.05	99.59	100.06	83.00	83.00	85.00
50	82.40	97.63	98.64	99.34	83.00	80.00	83.00
55	81.60	96.02	97.67	98.14	81.00	78.00	80.00
60	80.10	95.07	97.09	97.11	78.00	74.00	78.00

RUN 3

	Polymeric coagulant dosage, mg/l						
Run time, min.	**0**	**1**	**3**	**8**	**20**	**26**	**32**
5	42.36	59.58	58.36	61.73	43.34	58.36	60.97
10	41.75	56.73	56.33	58.93	40.36	55.00	57.00
15	41.08	54.19	55.52	57.85	39.23	52.00	54.00
20	40.62	53.40	54.31	55.40	39.36	50.00	54.00
25	39.91	52.05	53.15	54.81	38.98	49.00	52.00
30	39.40	51.42	52.36	54.40	38.01	48.00	50.00
35	38.79	51.07	51.06	52.80	37.78	47.00	47.00
40	36.95	50.48	50.62	52.25	37.12	45.00	45.00
45	35.90	50.39	50.41	51.72	35.98	43.00	42.00
50	34.84	49.89	49.39	50.56	34.55	40.00	40.00
55	34.34	49.31	48.86	50.04	33.56	38.00	37.00
60	33.95	48.77	48.20	49.08	32.56	34.00	35.00

TRANSMEMBRANE PRESSURE, (TMP), (bars)

RUN 1

	Polymeric coagulant dosage, mg/l						
Run time, min	**0**	**1**	**3**	**8**	**20**	**26**	**32**
5	0.28	0.25	0.26	0.24	0.45	0.46	0.46
10	0.28	0.26	0.26	0.24	0.45	0.46	0.46
15	0.28	0.26	0.26	0.24	0.47	0.47	0.49
20	0.28	0.27	0.26	0.25	0.47	0.50	0.49
25	0.28	0.27	0.27	0.25	0.49	0.50	0.50
30	0.28	0.27	0.27	0.25	0.50	0.52	0.50
35	0.29	0.28	0.27	0.25	0.52	0.54	0.54
40	0.30	0.28	0.27	0.26	0.57	0.58	0.59
45	0.30	0.28	0.27	0.26	0.60	0.61	0.61
50	0.31	0.29	0.28	0.26	0.62	0.63	0.63
55	0.31	0.29	0.28	0.27	0.63	0.64	0.65
60	0.33	0.29	0.28	0.27	0.63	0.64	0.67

RUN 2

	Polymeric coagulant dosage, mg/l						
Run time, min	**0**	**1**	**3**	**8**	**20**	**26**	**32**
5	0.40	0.39	0.39	0.39	0.41	0.42	0.43
10	0.41	0.39	0.39	0.39	0.42	0.43	0.44
15	0.41	0.40	0.40	0.40	0.44	0.44	0.46
20	0.42	0.40	0.40	0.41	0.44	0.45	0.46
25	0.42	0.40	0.40	0.41	0.45	0.46	0.46
30	0.44	0.40	0.41	0.41	0.46	0.48	0.48
35	0.44	0.41	0.41	0.42	0.47	0.48	0.50
40	0.46	0.41	0.41	0.42	0.48	0.49	0.53
45	0.47	0.41	0.42	0.42	0.49	0.50	0.54
50	0.49	0.42	0.42	0.42	0.51	0.53	0.56
55	0.51	0.42	0.43	0.43	0.53	0.54	0.57
60	0.53	0.42	0.44	0.43	0.54	0.56	0.58

RUN 3

	Polymeric coagulant dosage, mg/l						
Run time, min	**0**	**1**	**3**	**8**	**20**	**26**	**32**
5	0.24	0.24	0.24	0.27	0.28	0.29	0.24
10	0.29	0.25	0.25	0.28	0.29	0.30	0.24
15	0.32	0.25	0.25	0.30	0.30	0.32	0.25
20	0.32	0.25	0.25	0.30	0.31	0.32	0.25
25	0.32	0.26	0.26	0.31	0.32	0.32	0.26
30	0.34	0.26	0.26	0.32	0.34	0.34	0.26
35	0.35	0.27	0.26	0.33	0.34	0.36	0.26
40	0.37	0.27	0.27	0.34	0.35	0.39	0.27
45	0.39	0.27	0.27	0.35	0.36	0.40	0.27
50	0.40	0.27	0.27	0.37	0.39	0.42	0.28
55	0.42	0.29	0.27	0.39	0.40	0.43	0.28
60	0.43	0.29	0.27	0.40	0.42	0.44	0.28

MEMBRANE RESISTANCE,(x $10^{12}m^{-1}$)

RUN 1

	Polymeric coagulant dosage, mg/l						
Run time, min	**0**	**1**	**3**	**8**	**20**	**26**	**32**
5	1.72	1.35	1.41	1.27	1.42	1.53	1.58
10	1.85	1.43	1.47	1.33	1.42	1.53	1.58
15	1.94	1.47	1.50	1.35	1.50	1.59	1.73
20	2.02	1.54	1.56	1.39	1.52	1.68	1.73
25	2.03	1.58	1.58	1.46	1.58	1.71	1.81
30	2.13	1.66	1.60	1.50	1.62	1.78	1.81
35	2.26	1.75	1.67	1.55	1.71	1.85	1.96
40	2.33	1.77	1.74	1.60	1.86	2.01	2.13
45	2.48	1.87	1.77	1.65	1.98	2.13	2.23
50	2.59	1.93	1.81	1.68	2.06	2.23	2.31
55	2.68	1.94	1.85	1.75	2.08	2.25	2.39
60	2.96	2.00	1.89	1.79	2.11	2.28	2.47

RUN 2

	Polymeric coagulant dosage, mg/l						
Run time, min	**0**	**1**	**3**	**8**	**20**	**26**	**32**
5	1.34	1.21	1.23	1.19	1.39	1.55	1.49
10	1.47	1.23	1.27	1.28	1.51	1.62	1.59
15	1.55	1.29	1.32	1.30	1.63	1.71	1.70
20	1.62	1.32	1.36	1.35	1.67	1.81	1.71
25	1.63	1.36	1.39	1.39	1.74	1.88	1.74
30	1.73	1.40	1.42	1.43	1.86	1.98	1.85
35	1.79	1.44	1.46	1.47	1.93	1.99	2.00
40	1.96	1.47	1.48	1.49	2.04	2.09	2.16
45	2.04	1.49	1.51	1.51	2.13	2.16	2.29
50	2.14	1.56	1.53	1.52	2.23	2.37	2.42
55	2.25	1.57	1.57	1.58	2.36	2.49	2.57
60	2.38	1.59	1.63	1.59	2.51	2.71	2.66

RUN 3

	Polymeric coagulant dosage, mg/l						
Run time, min	**0**	**1**	**3**	**8**	**20**	**26**	**32**
5	2.21	1.45	1.50	1.42	2.13	2.29	2.23
10	2.33	1.53	1.57	1.52	2.25	2.36	2.33
15	2.37	1.64	1.61	1.56	2.37	2.45	2.44
20	2.48	1.67	1.68	1.63	2.41	2.55	2.45
25	2.50	1.80	1.75	1.68	2.48	2.62	2.48
30	2.53	1.82	1.79	1.74	2.60	2.72	2.59
35	2.69	1.83	1.87	1.80	2.67	2.73	2.74
40	2.83	1.93	1.92	1.83	2.78	2.83	2.90
45	3.01	1.93	1.93	1.86	2.87	2.90	3.03
50	3.10	2.02	1.99	1.91	2.97	3.11	3.16
55	3.14	2.04	2.10	1.97	3.10	3.23	3.31
60	3.27	2.07	2.13	2.01	3.25	3.45	3.40

Appendix 8. Validation of rate of membrane resistance increase at 45 LMH and 120 LMH

Membrane Flux, LMH	Run No.	Rate of membrane resistance increase, x $10^{12} m^{-1}. min^{-1}$
45LMH	1	0.0026
	2	0.0028
	3	0.0015
120 LMH	1	0.0127
	2	0.0171
	3	0.0121

RUN 1

Run time, min	TMP		FLUX		MEMBRANE RESISTANCE	
	45 LMH	120 LMH	45 LMH	120 LMH	45 LMH	120 LMH
5.00	0.18	0.38	46.39	115.30	1.42	1.19
10.00	0.18	0.38	46.35	108.69	1.43	1.26
15.00	0.18	0.39	46.21	106.71	1.44	1.32
20.00	0.19	0.39	46.00	103.78	1.46	1.35
25.00	0.19	0.40	46.00	99.14	1.46	1.45
30.00	0.19	0.40	45.94	95.83	1.47	1.50
35.00	0.19	0.41	45.94	95.10	1.47	1.55
40.00	0.19	0.42	45.94	92.35	1.48	1.64
45.00	0.19	0.44	45.90	90.66	1.48	1.75
50.00	0.19	0.45	45.84	88.67	1.49	1.83
55.00	0.19	0.47	45.70	86.58	1.51	1.95
60.00	0.19	0.50	45.65	86.07	1.51	2.09

RUN 2

Run time, min	TMP		FLUX		MEMBRANE RESISTANCE	
	45 LMH	120 LMH	45 LMH	120 LMH	45 LMH	120 LMH
5.00	0.18	0.38	45.95	109.81	1.39	1.23
10.00	0.18	0.38	45.50	102.42	1.41	1.33
15.00	0.18	0.39	45.46	100.43	1.42	1.39
20.00	0.18	0.39	45.40	98.59	1.43	1.43
25.00	0.18	0.41	45.40	97.06	1.44	1.52
30.00	0.18	0.42	45.30	95.10	1.44	1.59
35.00	0.18	0.44	45.24	94.79	1.44	1.67
40.00	0.18	0.48	45.23	92.75	1.45	1.86
45.00	0.19	0.49	45.23	92.35	1.47	1.91
50.00	0.19	0.51	44.90	91.80	1.52	2.00
55.00	0.19	0.52	44.80	89.17	1.54	2.10
60.00	0.19	0.52	44.60	88.66	1.57	2.11

RUN 3

Run time, min	TMP		FLUX		MEMBRANE RESISTANCE	
	45 LMH	120 LMH	45 LMH	120 LMH	45 LMH	120 LMH
5.00	0.17	0.42	45.41	110.30	1.33	1.36
10.00	0.17	0.42	45.30	107.20	1.34	1.41
15.00	**0.17**	**0.44**	**45.20**	**103.00**	**1.34**	**1.54**
20.00	0.17	0.44	45.20	101.35	1.35	1.56
25.00	0.17	0.45	45.20	100.17	1.37	1.62
30.00	0.17	0.47	45.10	100.11	1.38	1.69
35.00	0.18	0.49	45.10	98.02	1.44	1.80
40.00	0.18	0.49	45.00	97.14	1.44	1.82
45.00	0.18	0.51	44.90	95.71	1.44	1.92
50.00	0.18	0.51	44.90	95.06	1.44	1.93
55.00	0.18	0.52	44.80	93.78	1.45	2.00
60.00	0.18	0.53	44.80	92.69	1.45	2.06

Appendix 9. Validation of the rate of membrane resistance increase at different air scouring rates

Air scouring rate, $m^3/m^2.h$	Run No.	Rate of membrane resistance increase, (x $10^{12} m^{-1}. min^{-1}$)
0	1	0.032
	2	0.034
	3	0.037
1	1	0.0088
	2	0.018
	3	0.012
3	1	0.0051
	2	0.0078
	3	0.011
5	1	0.0038
	2	0.0054
	3	0.0054
7	1	0.0135
	2	0.0151
	3	0.024
10	1	0.015
	2	0.014
	3	0.023
12	1	0.016
	2	0.019
	3	0.029

TRANSMEMBRANE PRESSURE (TMP), (bars)

RUN 1

Run time, min	Air scouring rates, $m^3/m^2.h$						
	1	3	5	7	10	12	0
5.00	0.37	0.37	0.35	0.38	0.40	0.38	0.40
10.00	0.37	0.38	0.35	0.41	0.40	0.41	0.43
15.00	0.38	0.38	0.36	0.41	0.41	0.42	0.45
20.00	0.38	0.39	0.36	0.43	0.42	0.43	0.45
25.00	0.39	0.39	0.37	0.44	0.42	0.43	0.47
30.00	0.41	0.39	0.37	0.45	0.44	0.45	0.49
35.00	0.42	0.40	0.37	0.45	0.45	0.47	0.53
40.00	0.43	0.40	0.37	0.47	0.47	0.50	0.55
45.00	0.43	0.41	0.38	0.49	0.47	0.52	0.57
50.00	0.44	0.41	0.38	0.50	0.49	0.53	0.60
55.00	0.46	0.42	0.38	0.53	0.52	0.55	0.61
60.00	0.47	0.43	0.40	0.54	0.53	0.56	0.61

RUN 2

Run time, min	Air scouring rates, $m^3/m^2.h$						
	1	3	5	7	10	12	0
5.00	0.38	0.37	0.37	0.41	0.39	0.40	0.42
10.00	0.38	0.38	0.37	0.41	0.40	0.42	0.43
15.00	0.39	0.38	0.38	0.43	0.42	0.43	0.44
20.00	0.39	0.38	0.38	0.43	0.42	0.43	0.45
25.00	0.39	0.38	0.38	0.44	0.43	0.45	0.48
30.00	0.41	0.38	0.38	0.45	0.44	0.46	0.51
35.00	0.41	0.39	0.39	0.45	0.46	0.49	0.53
40.00	0.42	0.39	0.39	0.46	0.48	0.51	0.54
45.00	0.42	0.40	0.39	0.47	0.48	0.51	0.56
50.00	0.43	0.40	0.39	0.47	0.49	0.53	0.59
55.00	0.43	0.40	0.40	0.49	0.51	0.54	0.64
60.00	0.43	0.41	0.40	0.49	0.52	0.54	0.65

RUN 3

Run time, min	Air scouring rates, $m^3/m^2.h$						
	1	3	5	7	10	12	0
5.00	0.37	0.37	0.35	0.38	0.40	0.38	0.40
10.00	0.37	0.38	0.35	0.41	0.40	0.41	0.43
15.00	0.38	0.38	0.36	0.41	0.41	0.42	0.45
20.00	0.38	0.39	0.36	0.43	0.42	0.43	0.45
25.00	0.39	0.39	0.37	0.44	0.42	0.43	0.47
30.00	0.41	0.39	0.37	0.45	0.44	0.45	0.49
35.00	0.42	0.40	0.37	0.45	0.45	0.47	0.53
40.00	0.43	0.40	0.37	0.47	0.47	0.50	0.55
45.00	0.43	0.41	0.38	0.49	0.47	0.52	0.57
50.00	0.44	0.41	0.38	0.50	0.49	0.53	0.60
55.00	0.46	0.42	0.38	0.53	0.52	0.55	0.61
60.00	0.47	0.43	0.40	0.54	0.53	0.56	0.61

Membrane Flux, (LMH)

RUN 1

Run time, min	Air scouring rates, $m^3/m^2.h$						
	1	3	5	7	10	12	0
5.00	108.00	108.40	108.90	96.60	96.70	96.80	97.80
10.00	106.00	105.87	108.40	94.54	95.10	95.29	95.30
15.00	104.00	103.12	106.01	92.99	94.10	94.25	90.20
20.00	103.00	102.66	105.13	91.78	93.40	94.15	87.30
25.00	102.00	100.91	103.81	90.74	92.40	93.00	85.60
30.00	100.80	97.93	102.87	89.89	91.60	92.80	83.40
35.00	99.45	95.04	99.66	87.25	90.30	91.15	79.60
40.00	96.30	94.15	99.04	86.35	89.70	88.30	75.40
45.00	93.00	96.30	101.84	88.60	88.20	86.40	73.70
50.00	92.50	94.00	98.28	85.50	87.50	85.10	71.80
55.00	89.89	92.95	97.08	85.36	86.60	83.50	69.80
60.00	87.78	91.36	95.88	84.83	85.30	82.10	67.50

RUN 2

Run time, min	Air scouring rates, $m^3/m^2.h$						
	1	3	5	7	10	12	0
5.00	98.55	98.49	98.81	99.12	97.50	98.78	98.30
10.00	96.90	97.28	97.06	97.30	95.20	94.97	97.39
15.00	96.66	96.50	97.41	95.60	94.20	92.94	95.48
20.00	96.14	95.82	96.76	93.97	93.10	88.80	93.01
25.00	94.68	94.96	96.58	90.90	90.10	87.30	88.91
30.00	93.33	94.12	96.44	89.80	88.40	86.40	84.20
35.00	92.62	94.05	95.97	86.70	85.80	83.80	82.29
40.00	91.85	93.49	95.83	84.30	81.40	81.50	80.00
45.00	91.31	93.03	95.27	80.90	79.50	78.40	78.25
50.00	90.85	92.20	94.52	78.40	75.30	74.70	75.47
55.00	0.46	0.42	0.38	0.53	0.52	0.55	0.61
60.00	0.47	0.43	0.40	0.54	0.53	0.56	0.61

RUN 3

Run time, min	Air scouring rates, $m^3/m^2.h$						
	1	3	5	7	10	12	0
5.00	95.23	98.69	99.65	98.81	101.40	98.54	99.59
10.00	93.76	95.37	99.51	98.75	99.35	97.83	95.86
15.00	93.47	94.99	98.52	96.37	97.30	95.08	90.67
20.00	92.19	94.80	98.06	96.05	96.61	93.42	88.54
25.00	91.65	94.51	97.50	93.84	95.25	92.40	86.48
30.00	91.65	94.26	97.39	93.31	94.00	92.34	82.87
35.00	91.44	93.71	96.27	92.52	91.89	91.85	80.75
40.00	91.16	93.01	96.24	91.69	91.07	91.70	78.80
45.00	91.09	92.78	96.14	91.25	88.84	90.63	76.90
50.00	90.67	92.74	95.72	90.65	87.80	90.36	75.30
55.00	90.61	92.67	95.44	90.38	87.40	89.46	75.00
60.00	90.58	92.03	95.21	90.19	85.92	87.96	74.70

MEMBRANE RESISTANCE, (x $10^{12}m^{-1}$)

RUN 1

Run time, min	Air scouring rates, $m^3/m^2.h$						
	1	3	5	7	10	12	0
5.00	1.23	1.23	1.16	1.42	1.49	1.41	1.47
10.00	1.26	1.28	1.17	1.56	1.51	1.55	1.62
15.00	1.31	1.33	1.23	1.59	1.57	1.60	1.80
20.00	1.33	1.35	1.24	1.69	1.62	1.64	1.86
25.00	1.37	1.39	1.27	1.75	1.64	1.66	1.98
30.00	1.46	1.44	1.29	1.80	1.73	1.75	2.12
35.00	1.50	1.50	1.34	1.86	1.79	1.86	2.40
40.00	1.61	1.53	1.35	1.96	1.89	2.04	2.63
45.00	1.67	1.53	1.34	1.99	1.92	2.17	2.78
50.00	1.72	1.57	1.39	2.11	2.02	2.24	3.01
55.00	1.84	1.61	1.41	2.24	2.16	2.37	3.15
60.00	1.93	1.69	1.49	2.29	2.24	2.46	3.25

RUN 2

Run time, min	Air scouring rates, $m^3/m^2.h$						
	1	3	5	7	10	12	0
5.00	1.39	1.35	1.34	1.49	1.44	1.46	1.54
10.00	1.41	1.40	1.38	1.52	1.51	1.59	1.58
15.00	1.45	1.41	1.40	1.62	1.61	1.67	1.66
20.00	1.46	1.43	1.41	1.65	1.62	1.74	1.74
25.00	1.48	1.45	1.42	1.74	1.72	1.86	1.94
30.00	1.58	1.47	1.42	1.80	1.79	1.92	2.18
35.00	1.59	1.50	1.46	1.87	1.93	2.11	2.32
40.00	1.65	1.51	1.47	1.96	2.12	2.25	2.43
45.00	1.66	1.55	1.48	2.09	2.17	2.34	2.58
50.00	1.70	1.57	1.50	2.16	2.34	2.55	2.81
55.00	1.71	1.59	1.53	2.30	2.51	2.69	3.12
60.00	1.73	1.62	1.53	2.35	2.57	2.74	3.29

RUN 3

Run time, min	Air scouring rates, $m^3/m^2.h$						
	1	3	5	7	10	12	0
5.00	1.40	1.35	1.27	1.38	1.42	1.39	1.45
10.00	1.43	1.42	1.28	1.49	1.45	1.51	1.61
15.00	1.45	1.44	1.32	1.53	1.52	1.59	1.79
20.00	1.49	1.46	1.33	1.61	1.57	1.66	1.83
25.00	1.53	1.48	1.36	1.69	1.59	1.68	1.96
30.00	1.61	1.50	1.36	1.74	1.69	1.75	2.13
35.00	1.64	1.52	1.39	1.75	1.76	1.84	2.36
40.00	1.70	1.54	1.39	1.85	1.86	1.96	2.51
45.00	1.70	1.59	1.42	1.93	1.90	2.07	2.67
50.00	1.76	1.59	1.43	1.99	2.01	2.11	2.87
55.00	1.83	1.62	1.44	2.11	2.14	2.21	2.93
60.00	1.87	1.68	1.50	2.16	2.22	2.29	2.94

Appendix 10. Validation of the rate of membrane resistance increase at different air scouring frequency

RATE OF MEMBRANE REISTANCE INCREASE, (x 10^{12} $m^{-1}.min^{-1}$)

Replicates	Air scouring frequency				
	100%	75%	50%	25%	0%
1	0.0078	0.0096	0.0174	0.0295	0.0336
2	0.0071	0.0089	0.0182	0.0281	0.0405

TRANSMEMBRANE PRESSURE (TMP),bars

RUN 1

Run time, min	Air scouring frequency				
	100%	75%	50%	25%	0%
5.00	0.39	0.39	0.39	0.39	0.40
10.00	0.39	0.39	0.40	0.41	0.41
15.00	0.39	0.39	0.40	0.42	0.43
20.00	0.39	0.41	0.41	0.44	0.45
25.00	0.40	0.41	0.43	0.48	0.48
30.00	0.40	0.41	0.44	0.51	0.53
35.00	0.40	0.42	0.44	0.54	0.55
40.00	0.40	0.42	0.46	0.56	0.59
45.00	0.40	0.43	0.50	0.59	0.61
50.00	0.41	0.44	0.51	0.60	0.61
55.00	0.41	0.44	0.53	0.60	0.61
60.00	0.41	0.44	0.53	0.61	0.63

RUN 2

Run time, min	Air scouring frequency				
	100%	75%	50%	25%	0%
5.00	0.39	0.39	0.39	0.39	0.40
10.00	0.39	0.39	0.40	0.41	0.41
15.00	0.39	0.39	0.40	0.42	0.43
20.00	0.39	0.41	0.41	0.44	0.45
25.00	0.40	0.41	0.43	0.48	0.48
30.00	0.40	0.41	0.44	0.51	0.53
35.00	0.40	0.42	0.44	0.54	0.55

40.00	0.40	0.42	0.46	0.56	0.59
45.00	0.40	0.43	0.50	0.59	0.61
50.00	0.41	0.44	0.51	0.60	0.61
55.00	0.41	0.44	0.53	0.60	0.61
60.00	0.41	0.44	0.53	0.61	0.63

MEMBRANE FLUX, (LMH)

RUN 1

Run time, min	Air scouring frequency				
	100%	75%	50%	25%	0%
5.00	101.10	100.30	99.25	99.10	98.60
10.00	100.41	98.77	96.30	95.10	94.80
15.00	97.92	96.66	94.84	90.30	88.50
20.00	96.70	96.34	92.73	87.40	83.30
25.00	95.50	95.08	91.32	83.90	81.30
30.00	91.50	93.25	89.85	80.90	79.60
35.00	88.95	91.30	88.95	78.41	77.10
40.00	88.70	89.54	87.65	77.98	75.80
45.00	86.50	87.20	85.65	77.83	74.40
50.00	84.90	86.14	84.62	76.33	73.60
55.00	84.80	85.06	83.24	76.37	72.50
60.00	84.70	84.03	82.56	76.06	71.30

RUN 2

Run time, min	Air scouring frequency				
	100%	75%	50%	25%	0%
5.00	98.65	98.88	98.42	99.60	99.50
10.00	98.61	95.58	95.61	94.18	97.94
15.00	96.39	92.32	93.09	92.59	94.09
20.00	93.73	91.87	92.86	91.47	89.83
25.00	92.58	89.98	91.31	88.88	85.46
30.00	92.36	89.39	89.88	87.05	80.63
35.00	89.78	87.81	87.74	84.77	76.09
40.00	88.73	87.11	85.90	83.11	71.81
45.00	87.76	85.95	84.83	81.01	70.77
50.00	86.30	84.41	82.97	79.85	69.34
55.00	84.14	84.38	81.19	78.02	67.67
60.00	83.17	83.79	80.57	77.64	65.74

MEMBRANE RESISTANCE, (x $10^{12}m^{-1}$)

RUN 1

Run time, min	Air scouring frequency				
	100%	75%	50%	25%	0%
5.00	1.37	1.40	1.41	1.41	1.46
10.00	1.38	1.42	1.50	1.55	1.56
15.00	1.42	1.45	1.52	1.67	1.75
20.00	1.46	1.53	1.59	1.81	1.94
25.00	1.50	1.55	1.70	2.06	2.13
30.00	1.56	1.58	1.76	2.27	2.40
35.00	1.61	1.66	1.78	2.48	2.57
40.00	1.62	1.69	1.89	2.59	2.80
45.00	1.67	1.78	2.10	2.73	2.95
50.00	1.73	1.84	2.17	2.83	2.98
55.00	1.74	1.86	2.29	2.83	3.03
60.00	1.75	1.88	2.31	2.89	3.18

RUN 2

Run time, min	Air scouring frequency				
	100%	75%	50%	25%	0%
5.00	1.41	1.42	1.43	1.40	1.44
10.00	1.41	1.47	1.51	1.57	1.51
15.00	1.44	1.52	1.55	1.63	1.65
20.00	1.50	1.61	1.59	1.73	1.80
25.00	1.54	1.64	1.70	1.94	2.02
30.00	1.55	1.65	1.76	2.11	2.37
35.00	1.60	1.72	1.81	2.29	2.60
40.00	1.62	1.74	1.93	2.43	2.96
45.00	1.65	1.80	2.12	2.62	3.10
50.00	1.70	1.88	2.21	2.71	3.17
55.00	1.76	1.88	2.35	2.77	3.25
60.00	1.79	1.89	2.37	2.83	3.45

Appendix 11. Effect of polymeric coagulant dosage, air scouring rate and air scouring frequency on the rate of membrane resistance increase.

Rate of membrane resistance increase, (x 10^{12} m^{-1}.min^{-1})

Air scour frequency (A)	Air scour rate (B)	Coagulant dose (C)	Labels	1	2	3	Average	Median	Stdev
-	-	-	**1**	0.0266	0.0294	0.0297	0.0286	0.0294	0.0017
+	-	-	**a**	0.0257	0.0240	0.0274	0.0257	0.0257	0.0017
-	+	-	**b**	0.0204	0.0215	0.0198	0.0206	0.0204	0.0009
+	+	-	**ab**	0.0196	0.0175	0.0172	0.0181	0.0175	0.0013
-	-	+	**c**	0.0125	0.0114	0.0139	0.0126	0.0125	0.0013
+	-	+	**ac**	0.0052	0.0055	0.0065	0.0057	0.0055	0.0007
-	+	+	**bc**	0.0120	0.0105	0.0130	0.0118	0.0120	0.0013
+	+	+	**abc**	0.0045	0.0040	0.0056	0.0047	0.0045	0.0008

TRANSMEMBRANE PRESSURE (TMP) (bars)

RUN 1

Run time, min	Treatment combinations							
	abc	ac	bc	c	ab	b	a	1
5	0.57	0.57	0.57	0.57	0.58	0.57	0.58	0.57
10	0.56	0.58	0.57	0.58	0.59	0.59	0.60	0.59
15	0.57	0.59	0.59	0.60	0.62	0.62	0.62	0.61
20	0.58	0.59	0.60	0.61	0.64	0.64	0.64	0.65
25	0.59	0.59	0.61	0.62	0.67	0.66	0.66	0.67
30	0.59	0.60	0.62	0.64	0.69	0.68	0.68	0.67
35	0.60	0.60	0.64	0.64	0.70	0.70	0.69	0.69
40	0.60	0.61	0.65	0.64	0.72	0.71	0.70	0.70
45	0.61	0.61	0.66	0.65	0.73	0.72	0.72	0.71
50	0.62	0.62	0.67	0.65	0.74	0.74	0.72	0.72
55	0.62	0.62	0.69	0.66	0.75	0.75	0.73	0.73
60	0.61	0.62	0.70	0.66	0.75	0.75	0.74	0.74

Run 2

Run time, min	Treatment combinations							
	1	a	b	ac	c	bc	ac	abc
5	0.57	0.57	0.58	0.59	0.46	0.47	0.46	0.47
10	0.65	0.57	0.60	0.63	0.47	0.48	0.51	0.47
15	0.67	0.61	0.63	0.66	0.48	0.49	0.52	0.48
20	0.70	0.64	0.65	0.70	0.50	0.49	0.52	0.48
25	0.74	0.68	0.67	0.71	0.51	0.50	0.56	0.49
30	0.77	0.70	0.69	0.74	0.52	0.50	0.58	0.50
35	0.78	0.73	0.71	0.76	0.53	0.51	0.61	0.50
40	0.78	0.75	0.72	0.77	0.55	0.51	0.61	0.50
45	0.79	0.77	0.73	0.78	0.56	0.51	0.63	0.51
50	0.79	0.78	0.74	0.79	0.57	0.52	0.64	0.51
55	0.80	0.79	0.75	0.79	0.57	0.52	0.64	0.52
60	0.80	0.79	0.75	0.79	0.58	0.53	0.64	0.52

RUN 3

Run time, min	Treatment combinations							
	1	**a**	**b**	**ac**	**c**	**bc**	**ac**	**abc**
5	0.58	0.62	0.57	0.50	0.50	0.42	0.47	0.43
10	0.61	0.64	0.61	0.52	0.52	0.45	0.48	0.44
15	0.64	0.66	0.65	0.55	0.54	0.46	0.51	0.45
20	0.67	0.68	0.68	0.57	0.55	0.47	0.53	0.46
25	0.70	0.70	0.70	0.59	0.57	0.49	0.54	0.47
30	0.73	0.71	0.73	0.61	0.58	0.50	0.56	0.48
35	0.75	0.73	0.75	0.62	0.60	0.51	0.57	0.49
40	0.77	0.73	0.74	0.63	0.60	0.52	0.59	0.50
45	0.79	0.73	0.75	0.64	0.61	0.53	0.61	0.51
50	0.78	0.74	0.75	0.64	0.63	0.54	0.62	0.51
55	0.77	0.75	0.76	0.66	0.64	0.55	0.63	0.52
60	0.77	0.74	0.76	0.66	0.65	0.55	0.64	0.52

MEMBRANE FLUX, (LMH)

RUN 1

Run time, min	Treatment combinations							
	abc	ac	bc	c	ab	b	a	1
5	115.9	115.6	115.5	114.4	113.3	112.1	109.0	106.9
10	113.7	114.8	114.2	112.2	111.8	107.9	107.7	104.9
15	113.9	114.5	113.3	111.3	109.8	107.8	104.7	103.6
20	113.4	113.4	113.0	109.9	106.5	103.6	101.9	101.7
25	113.3	113.1	111.4	108.6	104.6	102.0	101.2	99.0
30	113.4	111.7	109.5	108.0	103.7	100.3	98.8	98.5
35	113.0	110.5	109.1	105.6	102.0	99.0	97.0	94.6
40	112.6	110.7	108.3	104.4	100.2	98.3	94.7	93.2
45	111.9	109.8	106.8	102.1	99.4	95.1	93.9	90.6
50	111.4	109.3	106.1	100.1	98.5	93.4	91.0	88.1
55	111.1	108.6	106.0	98.9	97.0	93.3	89.1	86.4
60	110.1	108.5	103.8	98.2	95.3	92.4	87.9	83.7

RUN 2

Run time, min	Treatment combinations							
	1	a	b	ac	c	bc	ac	abc
5	111.9	111.9	111.4	110.8	118.8	118.8	117.6	119.9
10	110.8	110.8	109.7	109.7	117.6	117.6	115.4	118.8
15	108.5	107.4	108.5	108.5	117.6	117.1	110.8	118.2
20	106.2	105.1	103.9	107.9	116.5	116.5	109.7	117.6
25	102.8	103.9	101.7	107.4	115.4	116.5	108.5	117.1
30	101.7	102.8	99.4	106.8	114.2	115.9	107.9	116.5
35	99.4	101.7	98.2	106.2	114.2	115.9	107.4	115.9
40	96.5	101.7	94.8	105.7	113.1	113.1	106.8	115.9
45	94.2	98.2	93.7	105.1	111.9	113.1	106.2	115.9
50	90.8	93.7	91.4	103.9	109.7	110.8	105.7	115.9
55	87.9	91.4	90.2	101.7	108.5	108.5	103.9	115.4
60	85.1	89.1	89.1	100.5	107.4	108.5	102.8	115.4

RUN 3

Run time, min	Treatment combinations							
	1	**a**	**b**	**ac**	**c**	**bc**	**ac**	**abc**
5	108.3	115.4	112.5	110.7	115.4	121.3	122.5	121.3
10	106.0	114.2	110.7	110.7	114.2	120.1	121.3	121.3
15	102.5	111.3	108.3	109.5	111.3	118.4	120.1	120.1
20	100.7	108.3	106.0	106.0	110.7	116.6	118.9	118.9
25	97.7	106.0	103.6	103.6	109.5	114.2	118.4	117.8
30	95.4	103.6	102.5	101.3	108.3	113.6	116.0	117.8
35	93.0	101.3	100.1	100.1	107.2	111.9	114.2	116.6
40	91.9	98.9	91.9	98.3	106.0	111.3	113.6	116.6
45	89.5	96.6	90.7	96.6	105.4	110.7	111.9	116.6
50	86.0	94.2	88.3	95.4	104.8	108.9	110.7	116.6
55	80.1	91.9	83.6	94.2	103.6	108.3	109.5	116.6
60	78.9	89.5	82.4	93.0	102.5	107.2	108.3	116.6

MEMBRANE RESISTANCE(x 10^{12} m^{-1})

RUN 1

Run time, min	Treatment combinations							
	abc	ac	bc	c	ab	b	a	1
5	1.78	1.79	1.77	1.80	1.85	1.84	1.92	1.93
10	1.79	1.80	1.81	1.86	1.91	1.96	2.01	2.03
15	1.81	1.84	1.87	1.93	2.04	2.07	2.15	2.14
20	1.84	1.88	1.92	2.00	2.17	2.23	2.27	2.29
25	1.86	1.89	1.97	2.06	2.31	2.34	2.34	2.43
30	1.88	1.94	2.05	2.12	2.38	2.45	2.48	2.46
35	1.90	1.95	2.11	2.17	2.47	2.54	2.58	2.61
40	1.93	1.97	2.17	2.20	2.57	2.60	2.67	2.71
45	1.95	2.00	2.23	2.28	2.63	2.73	2.75	2.82
50	1.99	2.03	2.28	2.35	2.70	2.86	2.87	2.95
55	1.99	2.05	2.34	2.42	2.78	2.88	2.96	3.06
60	2.01	2.06	2.43	2.43	2.85	2.93	3.04	3.18

RUN 2

Run time, min	Treatment combinations							
	1	a	b	ac	c	bc	ac	abc
5	1.85	1.84	1.86	1.93	1.38	1.44	1.41	1.40
10	2.10	1.85	1.97	2.08	1.44	1.48	1.59	1.42
15	2.24	2.04	2.10	2.20	1.47	1.52	1.69	1.45
20	2.36	2.19	2.24	2.32	1.54	1.52	1.72	1.47
25	2.60	2.34	2.37	2.40	1.59	1.55	1.85	1.49
30	2.72	2.47	2.50	2.49	1.64	1.57	1.93	1.53
35	2.83	2.59	2.61	2.57	1.68	1.57	2.05	1.55
40	2.91	2.64	2.73	2.62	1.76	1.64	2.07	1.55
45	3.00	2.82	2.81	2.66	1.79	1.64	2.14	1.58
50	3.14	2.98	2.93	2.74	1.86	1.70	2.18	1.58
55	3.26	3.10	2.99	2.81	1.89	1.73	2.21	1.61
60	3.40	3.18	3.04	2.83	1.96	1.75	2.25	1.61

RUN 3

Run time, min	Treatment combinations							
	1	**a**	**b**	**ac**	**c**	**bc**	**ac**	**abc**
5	1.93	1.93	1.83	1.64	1.55	1.26	1.38	1.29
10	2.07	2.01	1.99	1.70	1.63	1.34	1.42	1.32
15	2.26	2.14	2.15	1.82	1.73	1.41	1.53	1.34
20	2.41	2.27	2.29	1.94	1.79	1.46	1.60	1.40
25	2.57	2.36	2.45	2.06	1.86	1.56	1.64	1.43
30	2.74	2.48	2.57	2.16	1.91	1.59	1.74	1.47
35	2.90	2.58	2.71	2.23	2.00	1.63	1.80	1.50
40	3.01	2.65	2.91	2.32	2.05	1.68	1.88	1.55
45	3.17	2.72	2.96	2.38	2.10	1.73	1.96	1.56
50	3.27	2.84	3.07	2.43	2.16	1.78	2.02	1.59
55	3.47	2.95	3.26	2.50	2.23	1.82	2.06	1.60
60	3.53	2.99	3.32	2.55	2.29	1.85	2.12	1.61

Appendix 12. Final Water quality, Tubidity (NTU)

RUN 1: TURBIDITY (NTU)

Run time, min	Treatment combinations							
	1	a	b	ac	c	bc	ac	abc
5	0.12	0.15	0.16	0.12	0.14	0.12	0.1	0.18
10	0.12	0.15	0.16	0.12	0.14	0.12	0.1	0.18
15	0.15	0.16	0.12	0.11	0.12	0.11	0.14	0.12
20	0.15	0.16	0.12	0.11	0.12	0.11	0.14	0.12
25	0.13	0.16	0.11	0.11	0.12	0.13	0.11	0.12
30	0.13	0.16	0.11	0.11	0.12	0.13	0.11	0.12
35	0.13	0.18	0.13	0.13	0.13	0.1	0.12	0.12
40	0.13	0.18	0.13	0.13	0.13	0.1	0.12	0.12
45	0.14	0.14	0.14	0.1	0.11	0.13	0.12	0.11
50	0.14	0.14	0.14	0.1	0.11	0.13	0.12	0.11
55	0.14	0.13	0.1	0.12	0.11	0.12	0.12	0.12
60	0.14	0.13	0.1	0.12	0.11	0.12	0.12	0.12

RUN 2: TURBIDITY (NTU)

Run time, min	Treatment combinations							
	1	a	b	ac	c	bc	ac	abc
5	0.11	0.2	0.11	0.14	0.13	0.16	0.12	0.1
10	0.11	0.2	0.11	0.14	0.13	0.16	0.12	0.1
15	0.12	0.17	0.12	0.11	0.13	0.17	0.13	0.13
20	0.12	0.17	0.12	0.11	0.13	0.17	0.13	0.13
25	0.13	0.12	0.1	0.12	0.11	0.17	0.13	0.1
30	0.13	0.12	0.1	0.12	0.11	0.17	0.13	0.1
35	0.14	0.13	0.15	0.12	0.11	0.15	0.14	0.13
40	0.14	0.13	0.15	0.12	0.11	0.15	0.14	0.13
45	0.16	0.12	0.14	0.12	0.14	0.12	0.11	0.17
50	0.16	0.12	0.14	0.12	0.14	0.12	0.11	0.17
55	0.12	0.13	0.13	0.12	0.11	0.17	0.13	0.12
60	0.12	0.13	0.13	0.12	0.11	0.17	0.13	0.12

RUN 3: TURBIDITY (NTU)

Run time, min	Treatment combinations							
	1	**a**	**b**	**ac**	**c**	**bc**	**ac**	**abc**
5	0.16	0.14	0.14	0.14	0.19	0.11	0.1	0.16
10	0.16	0.14	0.14	0.14	0.19	0.11	0.1	0.16
15	0.15	0.15	0.13	0.13	0.18	0.12	0.12	0.13
20	0.15	0.15	0.13	0.13	0.18	0.12	0.12	0.13
25	0.16	0.14	0.13	0.15	0.16	0.12	0.13	0.14
30	0.16	0.14	0.13	0.15	0.16	0.12	0.13	0.14
35	0.15	0.18	0.16	0.14	0.15	0.17	0.13	0.16
40	0.15	0.18	0.16	0.14	0.15	0.17	0.13	0.16
45	0.14	0.18	0.16	0.13	0.16	0.14	0.16	0.18
50	0.14	0.18	0.16	0.13	0.16	0.14	0.16	0.18
55	0.14	0.17	0.17	0.14	0.11	0.15	0.17	0.15
60	0.14	0.17	0.17	0.14	0.11	0.15	0.17	0.15

Appendix 13. Log turbidity removal

RUN 1

Run time, min	Treatment combinations							
	1	a	b	ac	c	bc	ac	abc
5	2.10	2.07	2.12	2.22	2.07	1.98	2.22	2.26
10	2.10	2.07	2.12	2.22	2.07	1.98	2.22	2.26
15	2.10	2.02	2.07	2.12	2.07	2.15	2.07	2.26
20	2.10	2.02	2.07	2.12	2.07	2.15	2.07	2.26
25	2.10	2.15	2.12	2.07	2.15	2.02	2.10	2.07
30	2.10	2.15	2.12	2.07	2.15	2.02	2.10	2.07
35	2.15	2.22	2.19	2.12	2.10	2.19	1.94	2.15
40	2.15	2.22	2.19	2.12	2.10	2.19	1.94	2.15
45	2.19	2.10	2.26	2.07	2.22	2.15	2.12	2.15
50	2.19	2.10	2.26	2.07	2.22	2.15	2.12	2.15
55	2.10	2.02	2.07	2.22	2.12	2.02	2.15	2.10
60	2.10	2.02	2.07	2.22	2.12	2.02	2.15	2.10

RUN 2

Run time, min	Treatment combinations							
	1	a	b	ac	c	bc	ac	abc
5	2.22	2.12	2.10	2.22	2.15	2.22	2.30	2.05
10	2.22	2.12	2.10	2.22	2.15	2.22	2.30	2.05
15	2.12	2.10	2.22	2.26	2.22	2.26	2.15	2.22
20	2.12	2.10	2.22	2.26	2.22	2.26	2.15	2.22
25	2.19	2.10	2.26	2.26	2.22	2.19	2.26	2.22
30	2.19	2.10	2.26	2.26	2.22	2.19	2.26	2.22
35	2.19	2.05	2.19	2.19	2.19	2.30	2.22	2.22
40	2.19	2.05	2.19	2.19	2.19	2.30	2.22	2.22
45	2.15	2.15	2.15	2.30	2.26	2.19	2.22	2.26
50	2.15	2.15	2.15	2.30	2.26	2.19	2.22	2.26
55	2.15	2.19	2.30	2.22	2.26	2.22	2.22	2.22
60	2.15	2.19	2.30	2.22	2.26	2.22	2.22	2.22

RUN 3

Run time, min	Treatment combinations							
	1	**a**	**b**	**ac**	**c**	**bc**	**ac**	**abc**
5	2.26	2.00	2.26	2.15	2.19	2.10	2.22	2.30
10	2.26	2.00	2.26	2.15	2.19	2.10	2.22	2.30
15	2.22	2.07	2.22	2.26	2.19	2.07	2.19	2.19
20	2.22	2.07	2.22	2.26	2.19	2.07	2.19	2.19
25	2.19	2.22	2.30	2.22	2.26	2.07	2.19	2.30
30	2.19	2.22	2.30	2.22	2.26	2.07	2.19	2.30
35	2.15	2.19	2.12	2.22	2.26	2.12	2.15	2.19
40	2.15	2.19	2.12	2.22	2.26	2.12	2.15	2.19
45	2.10	2.22	2.15	2.22	2.15	2.22	2.26	2.07
50	2.10	2.22	2.15	2.22	2.15	2.22	2.26	2.07
55	2.22	2.19	2.19	2.22	2.26	2.07	2.19	2.22
60	2.22	2.19	2.19	2.22	2.26	2.07	2.19	2.22

Appendix 14. Raw water Quality

Chlorophyl a	Humic Acids	TOC	DOC	UV254 cm^{-1}	SUVA	EC	TC	HPC	Conductivity
µg/l	mg/l	mg/l as C	mg/l as C	cm^{-1}	mg/l.m	MPN/100ml	MPN/100ml	cfu/ml	(mS/m)
<2		7.6	6.2	0.246	3.97	0			18.98
2.8	9	10	8.6	0.383	4.45	10	1396	1700	20.26
<2	8.7	9	5.8	0.312	5.38	29	126	268	20.63
<2	5.3	7.4	6.1	0.395	6.48	29	411	560	20.34
2.7	7	8.1	6.3	0.314	4.98	44	310	298	21.75
8.9	8.8	8.1	5.5	0.341	6.20	82	465	1970	23.7
2.9	8.2	8.2	7.4	0.436	5.89	26	260	540	20.26
<2	10	7.1	5.5	0.3878	7.05	23	25	203	18.88
2.2		5.7	6.6	0.2959	4.48	3	1553	284	18.88
<2	7.1	6.6	5.7	0.2576	4.52	22	687	300	20.25
<2		5.7	5.7	0.3147	5.52	26	579	870	21.95
<2	8.2	5.9	5.1	0.2923	5.73	18	1690	2880	19.81
<2	12	6.4	4.9	0.2796	5.71	0	1300	730	19.01

Appendix 15. Final Water Quality

Chlorophyl a	Humic Acids	TOC	DOC	UV254 cm^{-1}	SUVA	EC	TC	HPC	Conductivity
µg/l	mg/l	mg/l as C	mg/l as C	cm^{-1}	mg/l.m	MPN/100ml	MPN/100ml	cfu/ml	(mS/m)
<2		5	4.3	0.117	2.72	0	0		20.62
<2	3.3	6.4	4.3	0.114	2.65	0	0	22	21.26
<2	2.7	7.1	4.4	0.122	2.77	0	0	5	22.3
<2	3.2	5.8	5.9	0.102	1.73	0	0	2	19.89
<2	3.9	6.4	4.5	0.093	2.07	0	0	0	18.88
<2	3.3	5	4.2	0.113	2.69	0	0	53	18.73
<2	4.3	4.8	4	0.118	2.95	0	0	0	20.14
<2	<2.0	4.2	4.3	0.1222	2.84	0	0	1	23.05
<2	3.5	4.9	3.7	0.0883	2.39	0	0	0	20.37
<2	5.6	3.9	4.2	0.1218	2.90	0	0	31	18.9
<2		4.1	4	0.107	2.68	0	0	2	19.45
<2	6.5	4.3	3.6	0.1014	2.82	0	0	5400	18.81
<2	4.3	4.6	4.6	0.1197	2.60	0	0	9	20.06

Appendix 16. The ANOVA results obtained when the effect of sparger pore size on the rate of membrane resistance was analyzed.

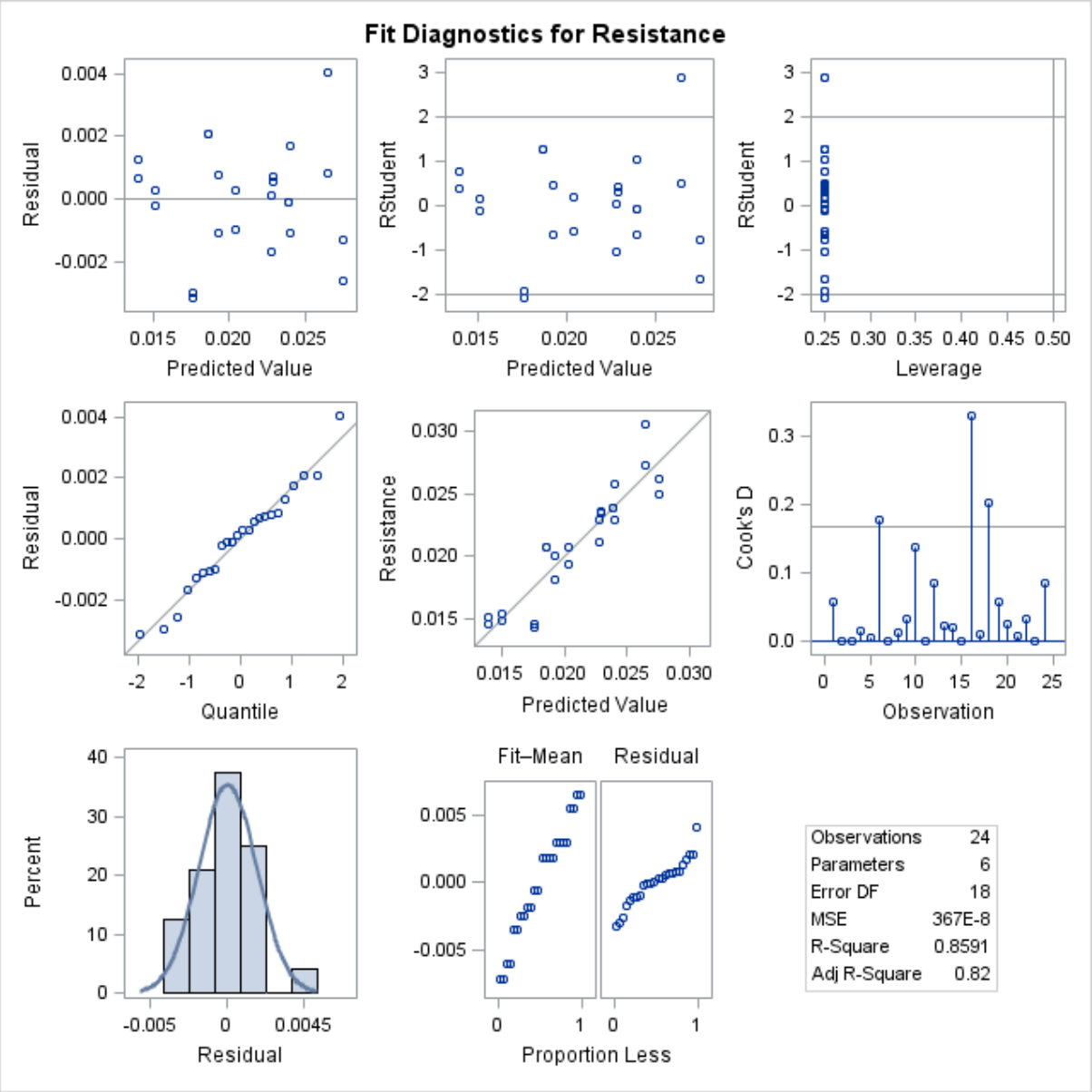

Table 0-1: ANOVA for Air scour rate

Levene's Test for Homogeneity of Resistance Variance					
ANOVA of Squared Deviations from Group Means					
Source	DF	Sum of Squares	Mean square	F Value	Pr > F
PoreSize	3	3.57E-09	1.19E-09	3.96	0.0229
Error	20	6.01E-09	3.01E-10		

Least Squares Means for effect Air Rate			
Pr> |t| for H0: LSMean(i)=LSMean(j)			
Dependent Variable: Resistance			
Air scour rate	1	3	5
1		0.004	<.0001
3	0.004		<.0001
5	<.0001	<.0001	

Levene's Test for Homogeneity of Resistance Variance					
ANOVA of Squared Deviations from Group Means					
Source	DF	Sum of Squares	Mean square	F Value	Pr > F
AirRate	2	3.62E-11	1.81E-11	0.32	0.7322
Error	21	1.20E-09	5.72E-11		

Least Squares Means for effect PoreSize				
Pr> |t| for H0: LSMean(i)=LSMean(j)				
Dependent Variable: Resistance				
Sparger pore size	1	2	3	4
1		0.1532	0.712	0.0245
2	0.1532		0.019	0.7794
3	0.712	0.019		0.0025
4	0.0245	0.7794	0.0025	

Appendix 17. Calculation of the main effects for the 2^3 fractional design equations: $\mathbf{A} = \frac{\mathbf{1}}{\mathbf{4n}}[\mathbf{a} - (\mathbf{1}) + \mathbf{ab} - \mathbf{b} + \mathbf{ac} - \mathbf{c} + \mathbf{abc} - \mathbf{bc}]$ Equation (0-1)

$$\mathbf{B} = \frac{\mathbf{1}}{\mathbf{4n}}[\mathbf{b} + \mathbf{ab} + \mathbf{bc} + \mathbf{abc} - (\mathbf{1}) - \mathbf{a} - \mathbf{c} - \mathbf{ac}] \quad \text{Equation (0-2)}$$

$$\mathbf{C} = \frac{\mathbf{1}}{\mathbf{4n}}[\mathbf{c} + \mathbf{ac} + \mathbf{bc} + \mathbf{abc} - (\mathbf{1}) - \mathbf{a} - \mathbf{b} - \mathbf{ab}] \quad \text{Equation (0-3)}$$

The two-parameters interactionsmain effect is calculated using the equations below:

$$\mathbf{AB} = \frac{[\mathbf{abc}-\mathbf{bc}+\mathbf{ab}-\mathbf{ac}+\mathbf{c}-\mathbf{a}+(\mathbf{1})]}{\mathbf{4n}} \quad \text{Equation (0-4)}$$

$$\mathbf{AC} = \frac{[(\mathbf{1})-\mathbf{a}+\mathbf{b}-\mathbf{ab}-\mathbf{c}+\mathbf{ac}-\mathbf{bc}+\mathbf{abc}]}{\mathbf{4n}} \quad \text{Equation (0-5)}$$

$$\mathbf{BC} = \frac{[(\mathbf{1})-\mathbf{a}-\mathbf{b}-\mathbf{ab}-\mathbf{c}-\mathbf{ac}+\mathbf{bc}+\mathbf{abc}]}{\mathbf{4n}} \quad \text{Equation (0-6)}$$

The three-parameters interactions main effect is calculated using the equation below:

$$\mathbf{ABC} = \frac{[\mathbf{abc}-\mathbf{bc}-\mathbf{ac}+\mathbf{c}-\mathbf{ab}+\mathbf{b}+\mathbf{a}-(\mathbf{1})]}{\mathbf{4n}} \quad \text{Equation (0-7)}$$

The numeration on equations (3-1 to 3-7) is called contrast. The sum of squares (SS) was calculated as follows:

$$\mathbf{SS}= \frac{(\text{contrast})^2}{8n} \quad \text{Equation (0-8)}$$

The parameter main effects and parameters interactions main effects calculated using equations (3-1 to 3-7) were used to develop the empirical regression model below.

$$\mathbf{y} = \boldsymbol{\beta_0} + \boldsymbol{\beta_1} * \mathbf{x_1} + \boldsymbol{\beta_2} * \mathbf{x_2} + \boldsymbol{\beta_{12}} * \mathbf{x_1 x_2} \ldots. \quad \text{Equation (0-9)}$$

The regression model was used to draw the response surface plot. The constant factors (β) were calculated. The β_0 is the average value of all responses obtained from the experiments The other effects estimates β_1, β_2, β_{12} etc. were calculated by one-half the value of the corresponding main effect.

Appendix 18. Bench scale UF membrane operating methodology

The methodology describes step-by-step instructions of the operation of the bench-scale submerged ultrafiltration system.

XXII. CYCLES was set to 60 to give a filtration of 60 min (Figure 4-4)

XXIII. For the periodic air scouring, the CYCLE DURATION was set to 20 min, AIR SCOUR DURATION was set to 60 (Figure 5-4).

XXIV. The STIRRER TIME was set to mix for 90 s (Figure 4-4).

XXV. The PUMP speed was set at 12 to achieve an initial flux of 120 LMH (Figure 4-4).

XXVI. The deionized water used to soak the membrane module tank was drained out (Figure 5-2).

XXVII. The raw water was filled into the raw water tank (Figure 4-2).

XXVIII. The FILLING button (see Figure 4-5) was initiated and the stirrer started to rotate and mix raw water.

XXIX. The coagulant was added after the first 30 s had elapsed. The coagulant and raw water mixed for 60 s.

XXX. The powered actuated valve opened when the 90 s lapsed, the coagulated water gravitated into the empty membrane tank.

XXXI. When the membrane tank was full, (see Figure 4-5) the filtration process was activated by pressing the START button.

XXXII. The needle next to the airflow meter was manually adjusted to the required airflow rate (see Table 4-5).

XXXIII. The permeate flow rates, pressure readings (in bars), permeate turbidity and water temperature (in ^{o}C) were recorded every 5 min for the duration of the filtration cycle (60 min)

XXXIV. The remaining coagulated water in the membrane tank was drained out.

XXXV. The membrane tank was filled with deionized water

XXXVI. Membrane hydraulic backwash was initiated by pressing the BACKWASHING and START buttons (Figure 4-5). The backwashing was performed at the pressure of 1 bar for 1 min. The peristaltic pump served both purposes of filtration and backwashing.

XXXVII. The membrane module was then ready for the next experimental run.

XXXVIII. The recorded permeate flow rates were converted into flux (in LMH) as follows: Flux $= \frac{\text{Permeate flow rate } (\frac{\text{mL}}{\text{min}})}{\text{membrane surface area}} \text{ x } \frac{1\text{l}}{1000\text{mL}} \text{ x } \frac{60 \text{ min}}{1\text{h}}$ (membrane area = 0.051m^2)

XXXIX. The membrane flux was normalised to 20 ^oC using equation (2-7).

XL. The membrane resistance was calculated using equation 2-10. The pressure units were converted from bars to $kg.m^{-1}. s^{-2}$ and the dynamic viscosity units were converted from centipoise (cP) to $kg.m^{-1}. s^{-1}$ The flux units were converted from LMH to $m^3.m^{-2}. s^{-1}$

XLI. The graph of time and the membrane resistance are drawn. The linear trend line was fitted. The results were accepted when the graph correlation coefficient (r^2) was greater than 0.95

XLII. The slope of the graph represented the rate of membrane resistance increase.

Appendix 19. Absorption in different regions of the Infrared spectrum (Bradley, 2015)

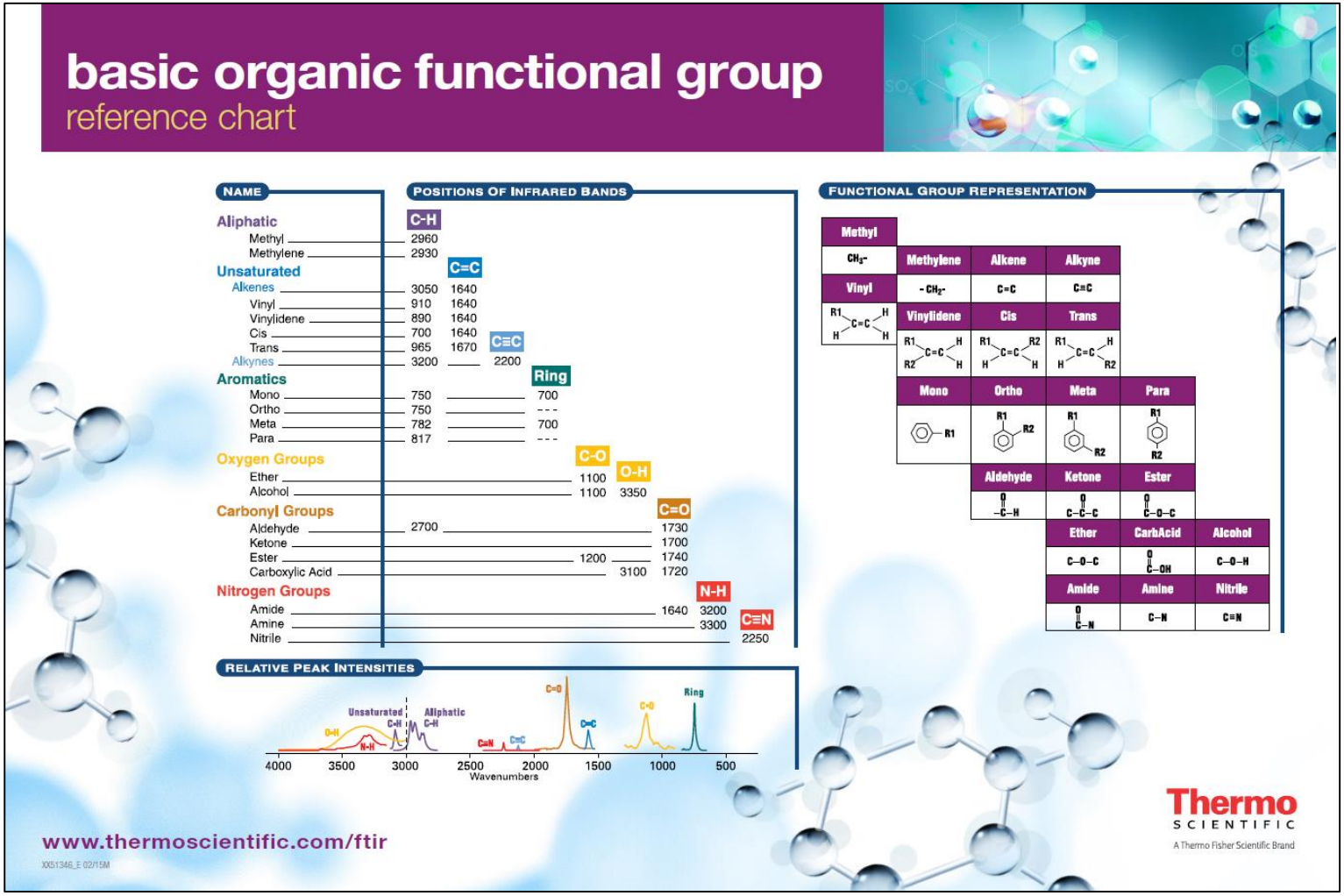

Appendix 20. Absorption in different regions of the Infrared spectrum, PerkinElmer FTIR instrument, UNISA

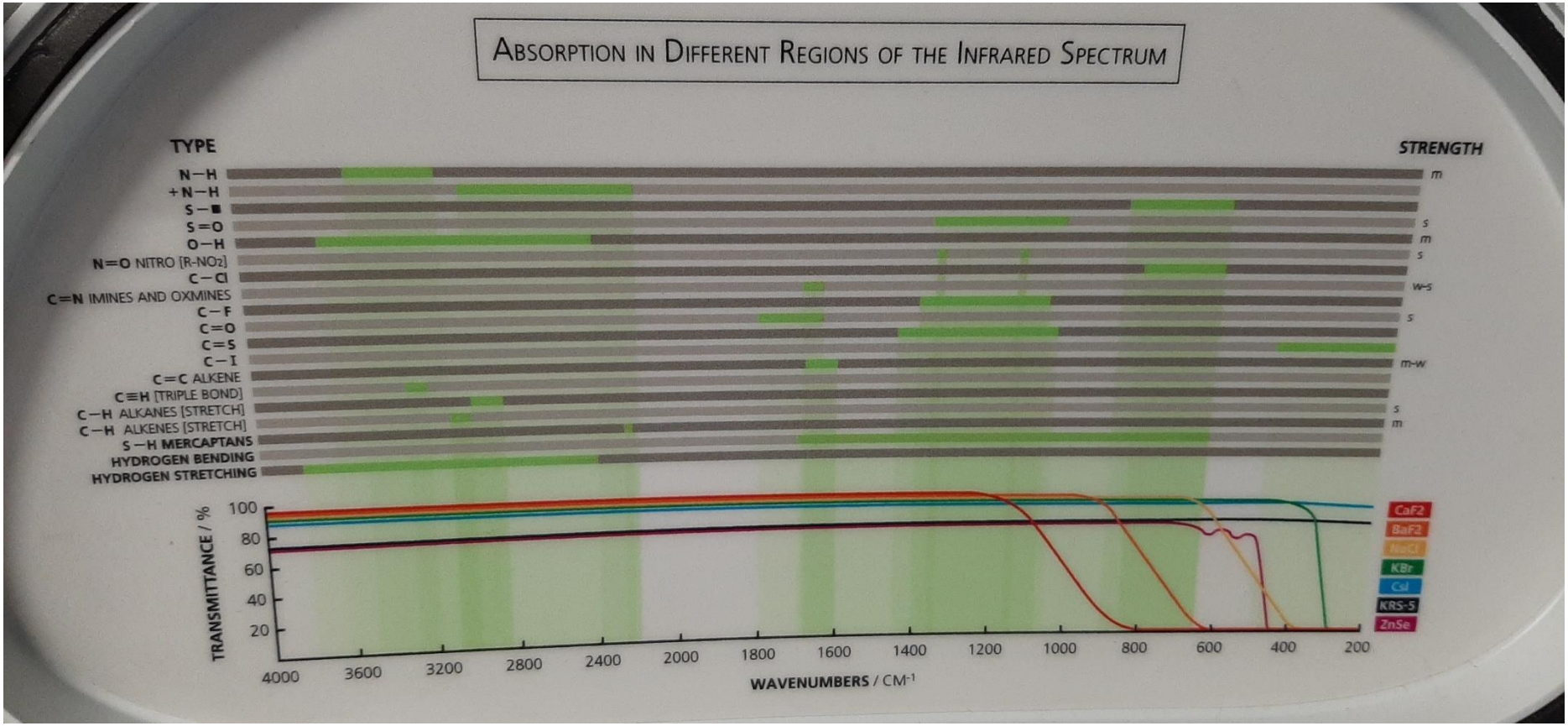

Appendix 21. Summary list of mechanisms, effects, and application of the major pre-treatment for low-pressure membrane filtration system (Huang et al., 2009).

	Pre-treatment			
	Coagulation	**Adsorption**	**Oxidation**	**Filtration**
Chemical applied	Coagulant at a pre-determined dosage to form pin flocs	Powdered or granular adsorbent (slurry or fixed contactor)	Gaseous or liquid	Granular media
Dose-effect	(the purpose of coagulant e.g. enhanced coagulation) under, optimal, or overdose	Added as a slurry	Minimal effective dose	None
Physical mechanism	Increases the particle size of impurities in the water to a filterable level.	Binds small impurities to the absorbents much larger than the membrane pore	May cause dissociation of organic colloids into smaller size or release of Extracellular Polysaccharides (EPS) by aquatic organisms	Removes coarse material that may have caused cake/gel layer formation on the membrane surface
Chemical mechanism	Destabilized impurities agglomerates, adsorption of the	Provides a new interface to adsorb/accumulate substances	Oxidized and partially decomposes NOM and mineral precipitation	Selectively removes other impurities that

	Pre-treatment			
	Coagulation	**Adsorption**	**Oxidation**	**Filtration**
	agglomerates into the membrane surface or pores	detrimental to the membrane performance		are sticky to the membrane surface
Biological mechanism	Partially removes NOM and hinder bacterial growth in source water or membrane	May adsorb organic contaminants relevant to the biofouling	Suppresses microbial growth	Partially removes microorganisms that can cause biofouling
Target impurities	Viruses, humic/fulvic acids, proteins, polysaccharides with acid groups, colloids smaller than membrane pores	Humic/fulvic acids, small natural organic acids, some DBPs, pesticides, and other synthetic organic compounds	Viruses, metals and organic contaminants	Particulate and colloidal organic and inorganic substances, microorganisms
Effect on membrane fouling	Reduces fouling caused by colloidal and NOM matter	May increase or decrease membrane fouling	May reduce biofouling and NOM fouling	May reduce fouling to a certain extent
Advantages	Significantly reduces fouling and increase membrane performance	Increase the removal of disinfection by-products (DBPs) and precursors of DBPs	Reduces the occurrence of biofouling; increases organic removal	May reduce biofouling, colloidal fouling, and solids loading

	Pre-treatment			
	Coagulation	**Adsorption**	**Oxidation**	**Filtration**
Disadvantages	1. The required proper dose that may be difficult to meet when sources water is continuously varying 2. May exacerbate fouling 3. Produce solid water 4. Ineffective in mitigating the fouling by hydrophilic natural organics	1. Possible exacerbation of membrane fouling 2. Difficulty in removing PAC powder for the treatment facilities	1. Formation of DBPs 2. May damage the membrane due to incompatibility with the oxidant 3. Maybe ineffective in suppressing microorganisms that are resistant to the oxidant	1. Performance may deteriorate and be difficult to recover 2. May require pre-treatment (coagulation or oxidant) to enhance the efficacy